Fine-tuning of Supramolecular Selectivity in Metal–salophen-based Receptors
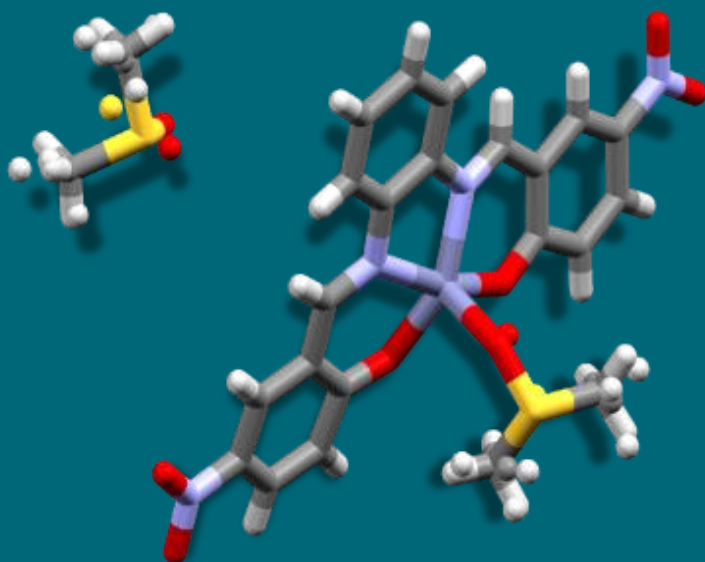

Luca Leoni

Supervisor:

Antonella Dalla Cort

PhD IN CHEMICAL SCIENCES

XXXI CYCLE

2019

Fine-tuning of Supramolecular Selectivity in Metal–salophen-based Receptors

Supervisor

Antonella Dalla Cort

Candidate

Luca Leoni

Coordinator

Osvaldo Lanzalunga

SAPIENZA
UNIVERSITÀ DI ROMA

Acknowledgements

A Luca

"Miei cari,

io vi amo con tutto il cuore,

e basta che siate giovani perché io vi ami assai"

(San Giovanni Bosco)

«Se vogliamo che tutto rimanga come è,

bisogna che tutto cambi»

(Giuseppe Tomasi di Lampedusa -Il Gattopardo)

I'm a fucking genius

I'm a fucking failure

Table of contents

General introduction

Supramolecular chemistry

Supramolecular chemistry can be defined as *"the chemistry beyond the molecule"*.[1] This discipline focuses on *"The study of organized entities of higher complexity that result from the association of two or more species held together by intermolecular forces"*. There are four main types of established non-covalent bonds, namely the hydrogen bond,[2] ionic interactions,[3] van der Waals interactions[4] and hydrophobic bonds.[5]

Nature offers amazing example of how non-covalent and highly specific molecular interactions are involved in the successful execution of vital processes, *i.e.* the crucial rule of the hydrogen bonding between adjacent complementary residuals in the association of the two polynucleotidic strands of DNA. Taking inspiration from Nature, supramolecular chemistry includes not only molecular recognition processes and catalysis,[6] but is actively exploring systems undergoing self-organization[7] and continuous change in constitution by reorganization and exchange in building blocks[8] (Constitutional Dynamic Chemistry); also includes the development of functional devices such as molecular machines[9] and the development of nanoscience and nanotechnology.[10]

Molecular recognition

Nature is the major source of inspiration for supramolecular chemists. Enzyme-substrate complex for example is a preliminary step in enzymatic catalysis and highly specific non-covalent molecular interactions are formed.[11] When the enzyme binds the substrate it exploits only weak interactions so that complexation is reversible and the product can be easily removed.

Moving from biological to artificial systems, since the pioneering work of Lehn,[12] Cram[13] and Pedersen[14] (Nobel Prize for Chemistry in 1987) on complexation of charged and neutral molecules, supramolecular chemists have devoted considerable effort to develop a great number of synthetic molecules that share with molecular enzymes the ability to recognize specific substrates by means of the same interactions involved in biochemical recognition (an example in Figure 1).[15]
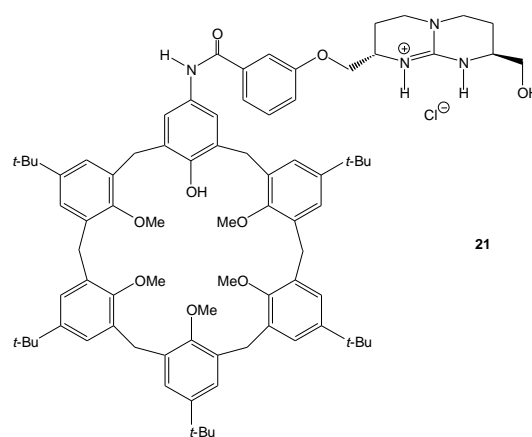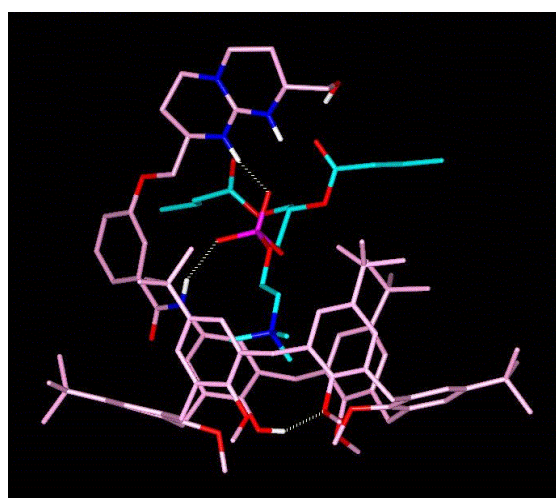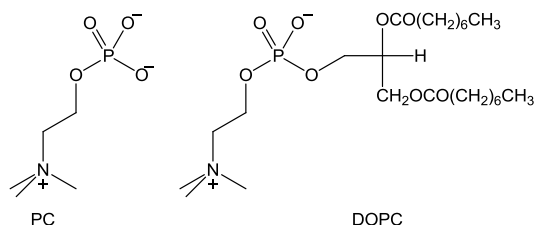

Figure 1. A designed non-peptidic receptor that mimics the phosphocholine (PC) binding site of the mcPC603 antibody. This receptor binds dioctanoyl-L-α-phosphatidylcholine (DOPC) by making use of the same key interactions found in the crystal structure of the Fab domain of the McPC603 antibody complexed with PC. [15c]

In supramolecular chemistry we deal with systems in which a molecule (receptor) endowed with a suitable recognition site (called *host*) is able to form a complex (supermolecule) with a substrate (called *guest*) (Figure 2).
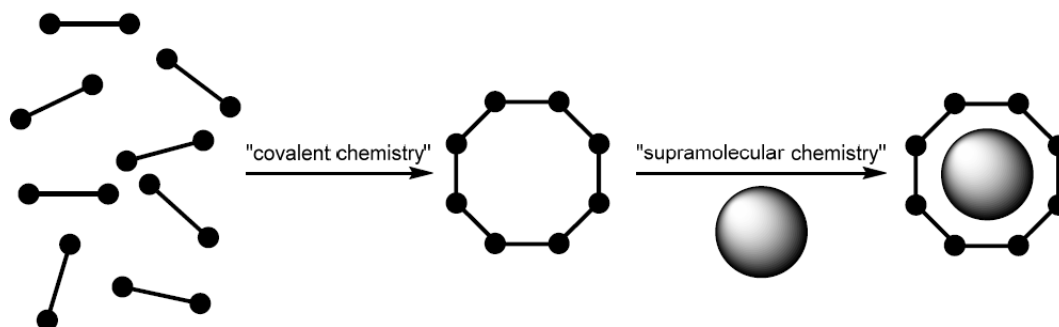
Figure 2. Schematic representation for the covalent and supramolecular chemistry.

The receptor-substrate interaction can be considered a recognition event that necessitate sterical and geometrical requirements between the two partners. To obtain this specificity in the recognition of a substrate a high degree of synthetic design is required for the receptor.

One of the fundamental issues in supramolecular chemistry has always been the quantitative analysis of the intermolecular interactions of interest. The substrate (*guest*) is gradually added to the *host* while monitoring a physical property such as specific chemical resonance in the case of NMR spectroscopy or absorption band (UV) that is sensitive to the supramolecular interaction of interest. The resulting information is then compared and fitted to binding model to obtain information about the association constant K_a, (in a simple 1:1 equilibria $K_a = [HG]/[H][G]$) energetics (ΔG, ΔH and ΔS) and stoichiometry (1:1, 1:2 etc.). The more the binding constant is high the more the specificity in the recognition has been obtained. Moreover, through the analysis and interpretation of non-covalent bonding patterns in organic solids we can obtain, whenever possible, the evidence of the supramolecular interactions involved in the binding event. Indeed, crystals might be regarded as the top examples of supramolecular assemblies or supermolecules. Dunitz (widely known chemical crystallographer) referred to organic crystals as "supermolecule(s) *par excellence*".[16]

Therefore, solid-state crystal structure analysis is an integral part and an added value in supramolecular chemistry.

Metal-salophen complexes

Metal-salophen complexes are an old[17] and popular class of compounds in supramolecular chemistry. They can be obtained from the condensation reaction of a salicylaldehyde and a *o*-phenylenediamine in the presence of a metal salt (Scheme 1).[18]

M = Nickel(II), Copper(II), Platinum(II), Vanadium(IV), Zinc(II), etc
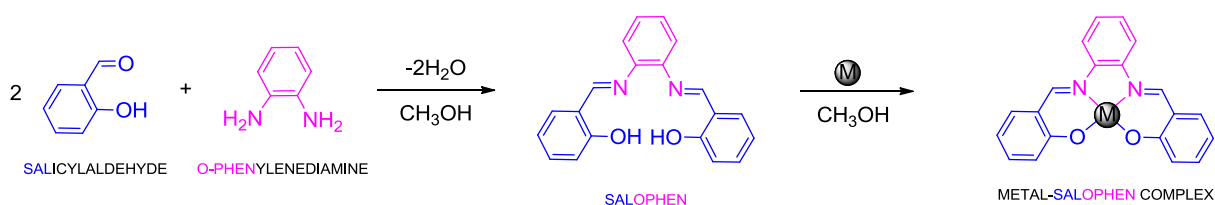
Scheme 1. General scheme for the synthesis of a metal-salophen complex.

The geometry of these complexes is largely defined by the metal center as highlighted in Figure 3 which shows the molecular structure of several metal–salophen complexes. As examples, in the case of nickel(II),[19] copper(II)[20] and platinum(II),[21] the coordination geometry around the metal cation is square planar.
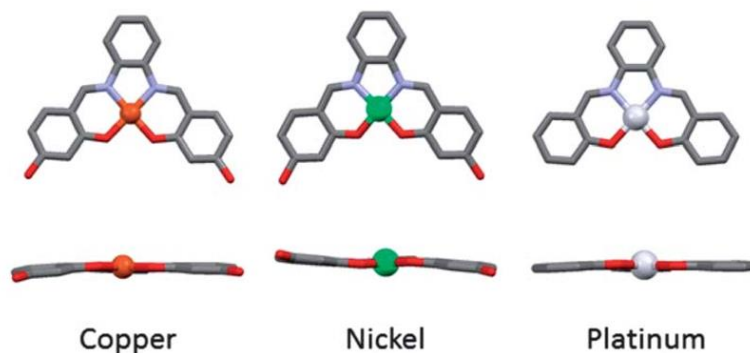
Figure 3. X-ray structures of a series of analogous metal salophens.[19, 20, 21]

In contrast (see Figure 4), in case of zinc(II) salophen complexes[22] and more significantly in uranyl-salophen complexes,[23] the phenyl rings of the ligand are clearly not coplanar.
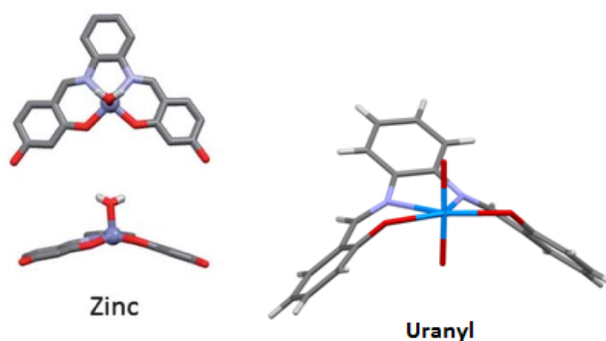
Figure 4. X-ray structures of Zn/uranyl- salophens.[22,23]

Zinc and uranyl-salophens are Lewis acids able to coordinate Lewis bases by accommodating them in the apical positions or in the equatorial ones.

In the Zn-salophen complexes, the Zn atom is in a five coordinate square pyramidal geometry in which the ligand occupies the basal plane and the guest occupies the apical position. [18]

Differently, uranyl-salophen complexes display a well defined preference for a pentagonal bipyramidal coordination geometry. In this arrangement, the donor atoms of the ligand occupy

four of the five equatorial coordination sites of the metal, while the two oxygen atoms of the uranyl ion occupy the apical positions. The fifth equatorial coordination site generally accommodates a solvent molecules with a donor group such as methanol or water, in absence of other guests.[18] From the structural point of view, these uranyl-complexes display a characteristic "bird-like" shape as in Figure 4, in which the ligand structure is particularly distorted from the classical planar conformation when any metal is coordinated.

Uranyl-salophen compounds are efficient receptors for anions and suitable supramolecular systems to be studied both in solution and in the solid state for many supramolecular applications spreading from recognition to catalysis.[24] They can be used as good receptors because we can take advantage from the predictable directionality of coordinative interaction and from their well-defined structural preorganization. The introduction of additional groups, able to interact in a favourable manner with the guest, provides a second binding site that can help not only the affinity but also the selectivity of the process giving an additional supramolecular effect. In Figure 5 are showed a series of uranyl-salophen complexes. In such compounds, by keeping the same uranyl-sal(oph)en skeleton and introducing different additional groups, we can obtain efficient receptors for different guests. Compound **A** is a good receptor for phosphate anion through H-bond interaction.[25] Compound **B** was able to interact selectively with fluoride anion because of the short size of the macrocycle structure.[26] Compound **C** displays appended aromatic arms with a suitable spacer to interact selectively with contact ion pair in lipophilic solvents through cation-π interactions and Lewis acid-base interactions.[27] Since the lengths and electronic features of the pendant aromatic arms attached on the salophen skeleton are quite easy to tune, the introduction of pendant electron-deficient arene units allowed us to catch elusive anion-π interaction through the derivative similar to compound **D**.[28] Therefore, the supramolecular attitude of such derivatives is straightforward.

A   **B**   **C**   **D**
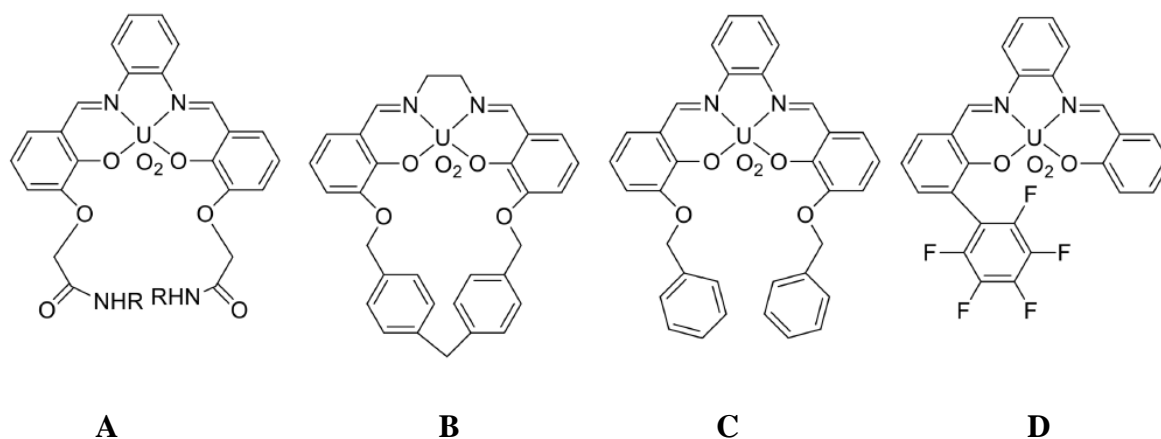
Figure 5. Series of uranyl-salophen complexes.[25, 26, 27, 28]

As receptors, Zn(II)-salophen complexes are able to bind tertiary amines.[29] and alkaloids.[30] The steric hindrance of the guests effects the binding. Only when the steric hindrance around the N atom is minimal, they estimated a binding constant higher than 10^6 M^{-1} in chloroform solution.[29] Zinc-salophens have also a high affinity for oxygenated anions such as phosphates and acetates. Hence, Dalla Cort and co-workers designed a receptors for inorganic phosphates and nucleotide anions. Better results were obtained with nucleotides showing the following binding order: $ADP^{3-} > ATP^{4-} > AMP^{2-}$. The naphthalene moiety on the receptor structure serves as a second binding site through π-π stacking interaction. [31a] Very interesting results were obtained by Dalla Cort and co-workers by a water soluble zinc-salophen complex **E** (Figure 6) that was able to bind carboxylate anions in water with a binding constant greater than 10^6 M^{-1}. In such work, an unexpected enantioselectivity was found towards α-aminoacids in the case of phenylalanine.[31b]

Moreover, metal–salphen complexes can be very good G-quadruplex DNA binders and are used for biomedical applications.[32] In particoular compound **F** in Figure 7, presents biological properties and its biological activity has been analyzed. In vitro studies show that there is a strong interaction with free plasmid DNA and cellular uptake and cytotoxicity studies show that they enter the cells but are not cytotoxic.[33]
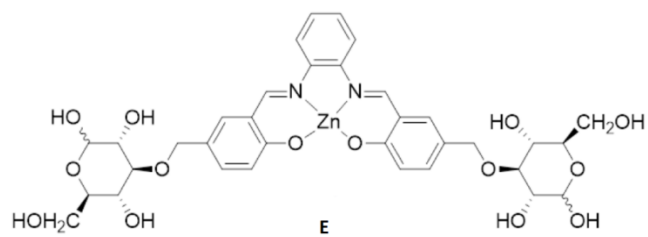
Figure 6. Structure of compound **E**.[31b]
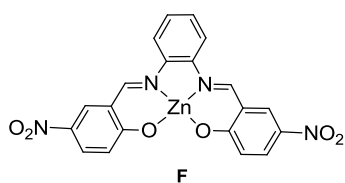
Figure 7. Structure of compound **F**.[33]

Bibliography

1. J. M. Lehn (Nobel Lecture), *Angew. Chem. Int. Engl. Ed.,* **1988**, 27, 89.

2. E. Arunan, G. R. Desiraju, R. A. Klein, J. Sadlej, S. Scheiner, I. Alkorta, D. C. Clary, R. H. Crabtree, J. J. Dannenberg, P. Hobza, H. G. Kjaergaard, A. C. Legon, B. Mennucci and D. J. Nesbitt, Pure *Appl. Chem.,* **2011**, 83, 1619.

3. Ionic interactions in natural and synthetic macromolecules, ed. Alberto Ciferri and Angelo Perico, John Wiley & Sons, Inc., Hoboken, New Jersey, **2012**.

4. J. N. Israelachvili, Intermolecular and Surface Forces, Academic Press, Waltham, San Diego, Oxford, Amsterdam, 3rd edn, **2011**.

5. D. Chandler, *Nature*, **2005**, 437, 640.

6. J.-M. Lehn (**1995**) Supramolecular Chemistry: Concepts and Perspectives (New York: VCH).

7. B. Hasenknopf, J.-M. Lehn, N. Boumediene, E. Leize and A. Van Dorsselaer, *Angew. Chem. Int. Ed.,* **1998**, 37, 3265.

8. (a) M. Ciaccia, R. Cacciapaglia, P. Mencarelli, L. Mandolini and S. Di Stefano, *Chem. Sci.,* **2013**, 4, 2253. (b) P. A. Brady, R. P. Bonar-Law, S. J. Rowan, C. J. Suckling and J. K. M. Sanders, *Chem. Commun.,* **1996**, 319.

9. (a) J. D. Badijch, C. M. Ronconi, F. J. Stoddart, V. Balzani, S. Silvi, A. Credi, *J. Am. Chem. Soc.,* **2006**, 128, 1489. (b) C. J Bruns, J. F. Stoddart, et al, *Angew. Chem. Int. Ed.* **2014**, 53, 1953. (c) V. Balzani, M. Clemente-Leon, A. Credi, B. Ferrer, M. Venturi, A. H. Flood, F. Stoddart, *J. Proc. Natl. Acad. Sci. U.S.A.* **2006**, 103, 1178. (d) M. R. Wilson, J. Solà, A. Carlone, S. M. Goldup, N. Lebrasseur, D. Leigh , *Nature,* **2016**, 534, 235.

10. (a) A. J. Bard (**1994**) Integrated Chemical Systems: A Chemical Approach to Nanotechnology (New York: Wiley). (b) E. A. Chandross and R. D. Miller (eds), **1999**, *Chem. Rev.,* 99, 1641.

11. E. Fischer, Ber. *Dt. Chem. Ges.,* **1984**, 27, 2985.

12. J. M. Lehn (Nobel Lecture), *Angew. Chem. Int. Engl. Ed.,* **1988**, 27, 89.

13. D. J. Cram (Nobel Lecture), *Angew. Chem. Int. Ed. Engl.,* **1988**, 27, 1009.

14. (a) C. J. Pedersen, *J. Am. Chem. Soc.,* **1967**, 89, 2495. (b) C. J. Pedersen, *J. Org. Chem.*, **1971**, 36, 1690. (c) C. J. Pedersen (Nobel Lecture), *Angew. Chem. Int. Ed. Engl.,* **1988**, 27, 1021.

15. Some remarkable examples: (a) G. Illuminati, L. Mandolini, B. Masci, *J. Am. Chem. Soc.*, **1983**, 105, 555. (b) D. J. Cram, M. A. Turner, M. Thomas, *Angew. Chem. Int. Eng. Ed.* **1991**, 30, 1024. (c) J. O. Magrans, A. R. Ortiz, M. A. Molins, P. H. P. Lebouille, J. Sanchez Quesada, P. Prados, M. Pons, F. Gago, J. de Mendoza, *Angew. Chem Int. Ed. Engl.,* **1996**, 35, 1712. (d) F. Cramer, W. Saenger and H. –Ch. Spatz, *J. Am. Chem. Soc.,* **1967**, 89, 14. (e) R. Behrend, E. Meyer, F. Rusche, Liebigs *Ann. Chem.,* **1905**, 339, 1. (f) W. A. Freeman, W. L. Mock, N.-Y. Shih, *J. Am. Chem. Soc.*, **1981**, 103, 7367. (g) T. J. Shepodd, M. A. Petti, A. D. Dougherty, *J. Am. Chem. Soc.*, **1986**, 108, 6085. (h) J. Canceill, L. Lacombe, A. Collet, *Chem. Comm.,* **1987**, 219. (i) L. Garel, B. Lozach, J. P. Dutasta, A. Collet, *J. Am. Chem. Soc.,* **1993**, 115, 11652.

16. (a) J. D. Dunitz, *Pure Appl. Chem.,* **1991**, 63, 177. (b) J. D. Dunitz, Perspectives in Supramolecular Chemistry; *G. R. Desiraju, Ed.; Wiley: New York*, **1996**; Vol. 2.

17. P. Pfeiffer, E. Breith, E. Lubbe, T. Tsumaki, Tricyclische orthokondensierte Nebenvalenzringe, *Eur. J. Org. Chem.* **1933**, 503, 84–130.

18. A. Dalla Cort, P. De Bernardin, G. Forte, F. Y. Mihan, *Chem. Soc. Rev.* **2010**, 39, 3863-3874.

19. H.-K. Fun, R. Kia, V. Mirkhani and H. Zargoshi, *Acta Crystallogr., Sect. E: Struct. Rep. Online*, **2008**, 64, m1181.

20. M. Niu, S. Fan, K. Liu, Z. Cao and D. Wang, *Acta Crystallogr., Sect. E: Struct. Rep. Online,* **2010**, 66, m77.

21. C.-M. Che, C.-C. Kwok, S.-W. Lai, A. F. Rausch, W. J. Finkenzeller, N. Zhu and H. Yersin, *Chem.–Eur. J.,* **2010**, 16, 233.

22. N. E. Eltayeb, S. G. Teoh, S. Chantrapromma, H.-K. Fun and K. Ibrahim, *Acta Crystallogr., Sect. E: Struct. Rep. Online,* **2007**, 63, m2838.

23. K. Takao and Y. Ikeda, *Inorg. Chem.,* **2007**, 46 , 1550.

24. L. Leoni, A. Dalla Cort, *Inorganics* **2018**, 6, 42.

25. D.M. Rudkevich, W. Verboom, Z. Brzozka, M.J. Palys, W.P.R.V. Stauthamer, G.J. van Humme, S.M. Franken, S. Harkema, J.F.J. Engbersen, D.N. Reinhoudt, *J. Am. Chem. Soc.* **1994**, 116, 4341–4351.

26. M. Cametti, A. Dalla Cort, L. Mandolini, M. Nissinen and K. Rissanen, *New J. Chem.,* **2008**, 32, 1113–1116.

27. M. Cametti, M. Nissinen, A. Dalla Cort, L. Mandolini, K. Rissanen, *J. Am. Chem. Soc.* **2007**, *129*, 3641–3648.

28. L. Leoni, R. Puttreddy, O. Jurcêk, A. Mele, I. Giannicchi, F. Yafteh Mihan, K. Rissanen, A. Dalla Cort, *Chem. Eur. J.* **2016**, *22*, 18714–18717.

29. A. Dalla Cort, L. Mandolini, C. Pasquini, K. Rissanen, L. Russo, L. Schiaffino, *New J. Chem.* **2007**, *31*, 1633-1638.

30. E. C. Escudero-Adan, J. Benet-Buchholz, A. W. Kleij, *Inorg. Chem.* **2008**, 47, 4256-4263.

31. (a) M. Cano, L. Rodriguez, J. C. Lima, F. Pina, A. D. Cort, C. Pasquini, L. Schiaffino, *Inorg. Chem.* **2009**, 48, 6229-6235. (b) A. Dalla Cort, P. De Bernardin, L. Schiaffino, *CHIRALITY,* **2009,** *21*, 104–109.

32. Nurul H. Abd Karim, Oscar Mendoza, Arun Shivalingam, Alexander J. Thompson, Sushobhan Ghosh, Marina K. Kuimovaa and Ramon Vilar, *RSC Adv.,* **2014**, 4, 3355–3363.

33. I. Giannicchi, R. Brissos, D. Ramos, J. de Lapuente, J. C. Lima, A. Dalla Cort, L. Rodríguez, *Inorg. Chem.* **2013**, 52, 9245.

Chapter 1. Halides recognition

1.1 Anion-π interactions

Anions play a crucial rule in biological and chemical systems. A large number of enzymes and enzymatic cofactors are negatively charged [1] and diseases such as cystic fibrosis are caused by a malfunction of anion channels.[2] This shows the high relevance in designing anion receptors to understand the biological processes and to design systems for environmental monitoring.[3]

Common anion receptors are based on electrostatics attractions, hydrogen bond or hydrophobic effects.[4] The design of anion receptors is particularly challenging:

- Anions are larger than isoelectronic cations (Table 1.1) [5] and therefore have a lower charge to radius ratio. Thus, electrostatic binding interactions are less effective than the smaller cation.

Cation	r[Å]	Anion	r[Å]
Na^+	1.16	F^-	1.19
K^+	1.52	Cl^-	1.67
Rb^+	1.66	Br^-	1.82
Cs^+	1.81	I^-	2.06

Table 1.1. A comparison of the radii r of isoelectronic cations and anions in octahedral environments.

- Anions may be sensitive to pH
- Anionic species have a wide range of geometries (Figure 1.1) and therefore a higher degree of design may be required to make receptors complementary to their anionic guest.
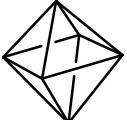
⬭ (circle)	spherical	F^-, Cl^-, Br^-, I^-
(ellipse)	linear	N_3^-, CN^-, SCN^-, OH^-
(trigonal)	trigonal planar	CO_3^{2-}, NO_3^-
(tetrahedron)	tetrahedral	PO_4^{3-}, VO_4^{3-}, SO_4^{2-}, MoO_4^{2-}, SeO_4^{2-}, MnO_4^-
(octahedron)	octahedral	$[Fe(CN)_6]^{4-}$, $[Co(CN)_6]^{3-}$

Figure 1.1. The structural variety of anions.

- Solvent effects also play a crucial role in controlling anion binding strength and selectivity. A potential anion receptor must therefore effectively compete with the solvent environment in which the anion recognition event takes place.

In recent year, a new type of non-covalent interaction is attracting considerable attention in the field of anion recognition, namely the anion-π interaction.[6] Such interaction appears to be an appealing non-covalent tool with interesting applications for the design of highly selective anion receptors,[7] channels,[8] in catalysis[9] and its relevance in biological systems is increasingly considered.[10]

The cation-π interaction, a peculiar type of van der Waals interactions dominated by electrostatic and polarization effects, is a peculiar supramolecular bond extensively studied by the chemistry community and the importance of which in biology, chemistry and materials science is fully demonstrated.[11]

Anion-π interaction, i.e. the interaction of an anion with the positive electrostatic potential on the ring edge of an electron-deficient aromatic group, can be considered as the related inverse of cation-π interaction.

Electrostatic forces and ion-induced polarization effects are the main contributors to the bonding energy of the anion–π contact. The electrostatic term is associated with the quadrupole moment, i.e. Q_{zz}, of the aromatic host (Figure 1.2). The Q_{zz} value for benzene is −8.45 B (B = Buckingham); therefore, benzene is able to interact with a positively charged entity, such as a cation (cation–π interaction). When the hydrogen atoms of benzene are replaced by electron-withdrawing fluorine atoms, the Q_{zz} value of the resulting hexafluorobenzene molecule amounts to +9.50 B; hence, hexafluorobenzene can favorably interact with anions.
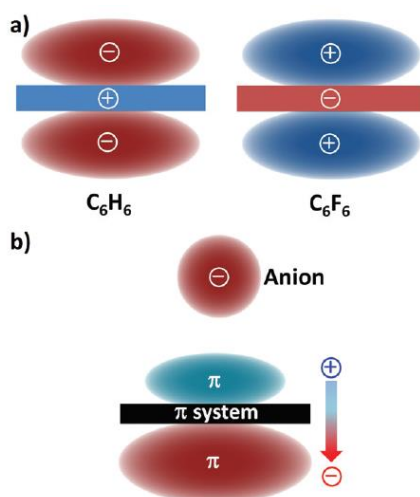
Figure 1.2. Schematic representation of the quadrupole moments of benzene (C_6H_6; Q_{zz} = −8.45 B) and hexafluorobenzene (C_6F_6; Q_{zz} =+9.50 B) [12] and (b) the ion-induced dipole (the molecular polarizabilities parallel to the main symmetry axis are α‖ = 41.5 and 37.7 a.u. (a.u. stands for atomic units), for benzene and hexafluorobenzene, respectively).[13]

Pentafluorophenyl derivatives are suitable receptors to investigate anion-π interactions due to the opposite charge distribution compared to corresponding phenyl derivatives; moreover, an advantage of these fluorinated compounds is that they are readily accessible from cheap precursor commercially available. Through these derivatives, anion-π interaction has been underscored in many crystal structures, in the gas phase and in solution.[14]

1.2 Catching Elusive Halide-π Interactions in Solution and in the Solid State using Differently Substituted Uranyl-Salophen Receptors.

In the field of halide recognition, among the receptors that have been recently used there are the strongly Lewis acidic uranyl-salophen complexes. These receptors have the fifth equatorial binding site available for coordination with halides after the coordination of the UO_2^{2+} ion to the salophen ligand.[15] In absence of a guest they form stable complexes with solvent molecules endowed with donor groups (Figure 1.3a) or form dimeric supramolecular assemblies [16] both in solution and in the solid state in which two receptor units assemble into dimers, as in Figure 1.3b).

a)   b)
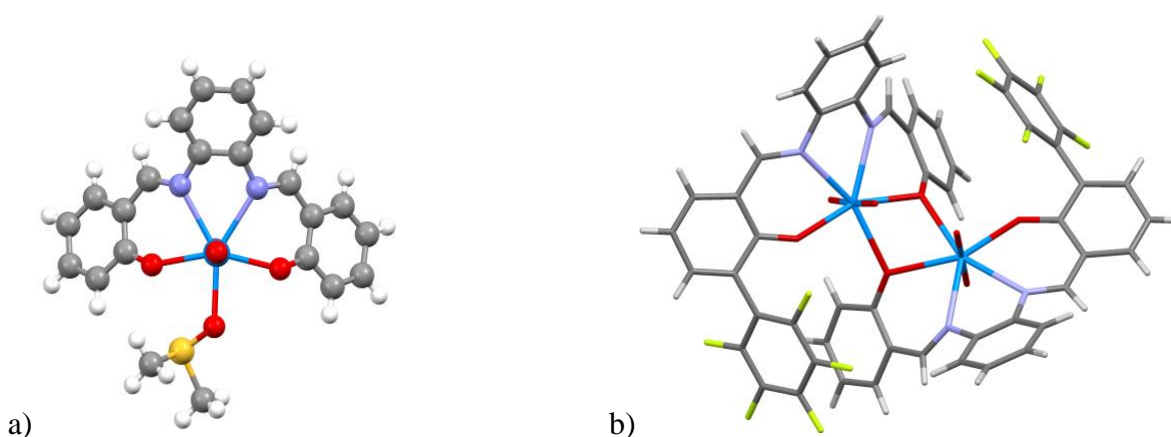
Figure 1.3. X-ray crystal structures of a) DMSO@uranyl-salophen complex. b) Dimeric structure of the perfluorophenyl substituted uranyl-salophen complex **1d** (Scheme 1.1).[16]

In solution, coordinative interactions of a Lewis-acidic receptor and an anion are very efficients because of their covalent but dynamic nature.[17] In presence of tetrabutylammonium halide salts (TBAX, X = F-, Cl-, Br-, I-), coordination of halides with the hard uranyl center supplies a major driving force for complexation.

The "free" complexes present a dark orange coloration indicative of a metal-to-ligand charge-transfer LMCT excitations between uranyl and the double Schiff bases ligand environment.[18]

Upon addition of a halide in organic solvents, the anion binds the hard Lewis acidic uranyl center giving rise to a strong absorption change in the UV/Vis spectrum since the binding process effects exactly where the absorption of chromophore occurs. Therefore, for the precise estimate of the binding constants values (K_a, M^{-1}) towards halides, we relied on UV/Vis titration. An example of a typical UV/Vis spectral change and the relative fit plot of such receptors upon addition of tetrabutylammonium halide salts, is reported in Figure 1.4. All the titration curve of such compounds showed excellent fits for the theoretical binding isotherm following a 1:1 binding model. The strong 1:1 complexes are motivated also by the present of the two isosbestic points that indicate two state systems during the titration experiments.[19]
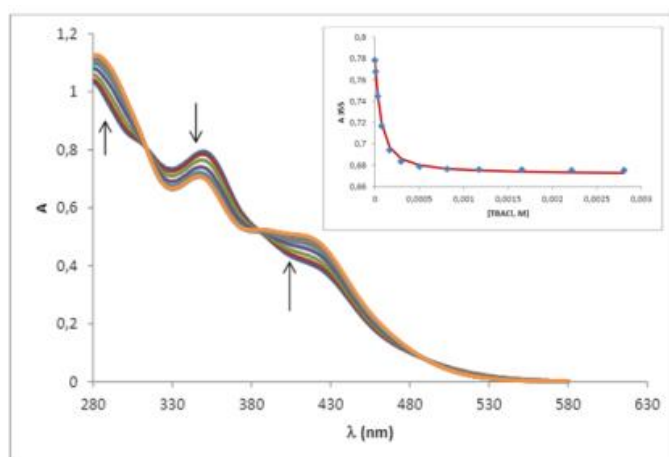
Figure 1.4. UV-vis spectral changes of a 4.96×10^{-5} M solution of **1a** (Scheme 1.1) $CHCl_3$, 25°C upon addition of TBACl. The inset shows the spectral changes at 355 nm; points are experimental and the full line is the fitted curve relative to the formation of a 1:1 complex.

1.2.1 *ortho*-mono-substituted aromatic uranyl-salophen complexes and binding studies in chloroform

We are aware of the directionality of the coordinative interaction and of the well-defined structural preorganization of these immobilized Lewis acids. The presence of additional groups such as electron-deficient aromatic pendants on the main skeleton of the salophen structure, beside the metal center, could increase the affinity and the selectivity of the recognition of halides through an additional supramolecular interaction, i.e., halide-π interaction. In the perfluoro derivative showed below, the distance between the electron-deficient perfluorophenyl pendant arm and the metal binding site is short enough to favor the interaction with the anion coordinated to the uranyl center. Fluorine is the most electronegative element, and it is known that, when present as a substituent in hexafluorobenzene, it induces a large positive quadrupole moment $(Q_{zz}(C_6F_6)=+9.50$ B).[12] For this reason, electron-deficient fluorinated arenes are known to act as π-acceptors.[20]
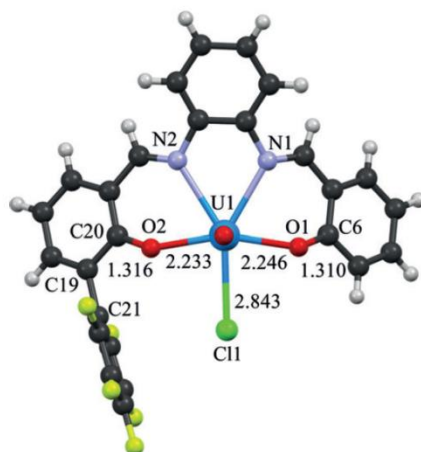
To elucidate the contribution of this quite elusive interaction, a series of uranyl-salophen complexes with one properly substituted aromatic pendant arm, Scheme 1.1, have been synthesized.

1a, R = Ph   R' = H

1b, R = [structure]   R' = H

1c, R = [structure]   R' = H

1d, R = [structure]   R' = H
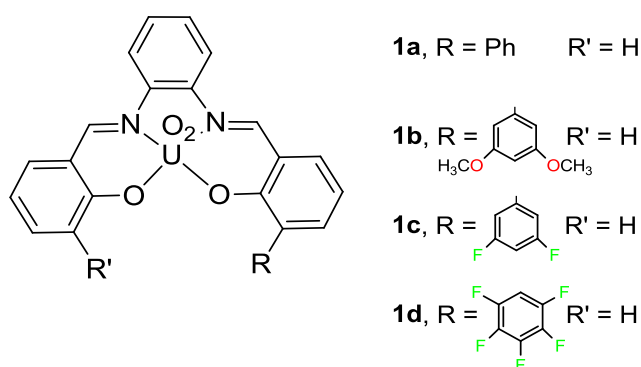
Scheme 1.1. Chemical formulae of uranyl-salophen receptors **1a-d.**

Herein, we report a systematic study of the binding of halides (TBAX, X = F⁻, Cl⁻, Br⁻ I⁻) to the series of uranyl-salophen receptors **1a-d** with subtle electronic variations on the receptor structure. These compounds are used as model systems to obtain quantitative data on the strength of halide-π interaction both in solution and in the solid state and to understand the effect of the aromatic substituents on the halide binding. The data here reported represent the first example of the occurrence of anion-π interactions in systems in which the main driving force for recognition is controlled by Lewis acid-base interactions instead of hydrogen bonding.

As Showed in Scheme 1.2, we synthesized the properly functionalized salicylaldehyde derivatives by a palladium-catalyzed cross-coupling reaction[21] (Suzuki coupling) of penta/(3,5-di)fluorophenyl boronic acid and 2-bromoanisole or 3,5-dimethoxyphenylboronic acid and 1-benzyloxy-2-iodobenzene, followed by the deprotection of the phenolic groups and *ortho*-formylation. The obtained aldehyde derivatives were then reacted with the monoimine prepared from *o*-phenylenediamine and salicylaldehyde in the presence of uranyl acetate. For the uranyl-salophen complex **1a**, the *ortho*-formylation of 1,1'-biphenyl-2-ol leads to the corresponding salicylaldehyde, which was reacted with the monoimine.[22]
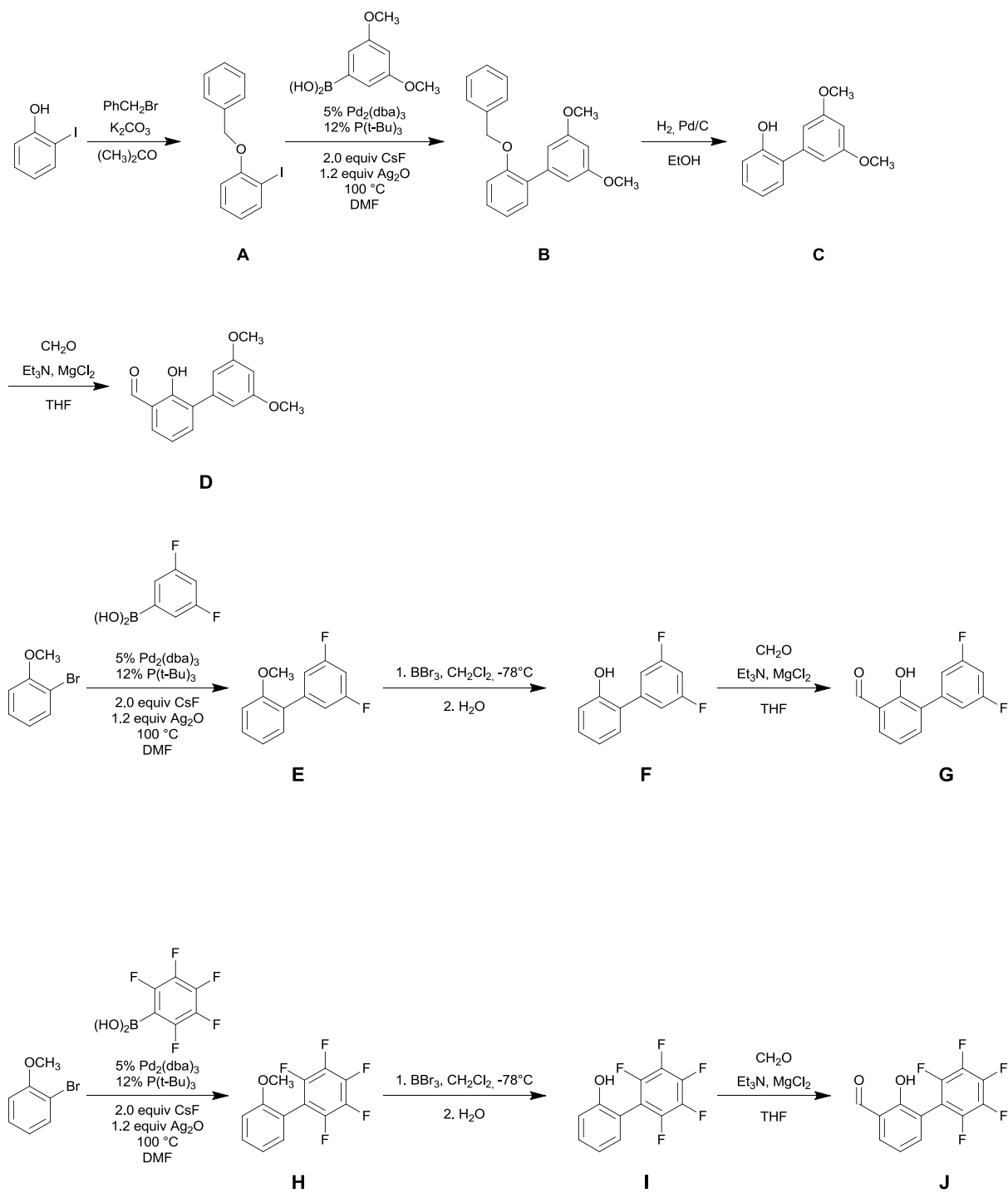
Scheme 1.2. Synthesis of the *ortho*-substituted aromatic aldehydes **D, G** and **J**. Yields: **A** 100%; **B** 89%; **C** 70%; **D** 72%; **E** 47%; **F** 57%; **G** 48%; **H** 37%; **I** 87%; **J** 50 %.
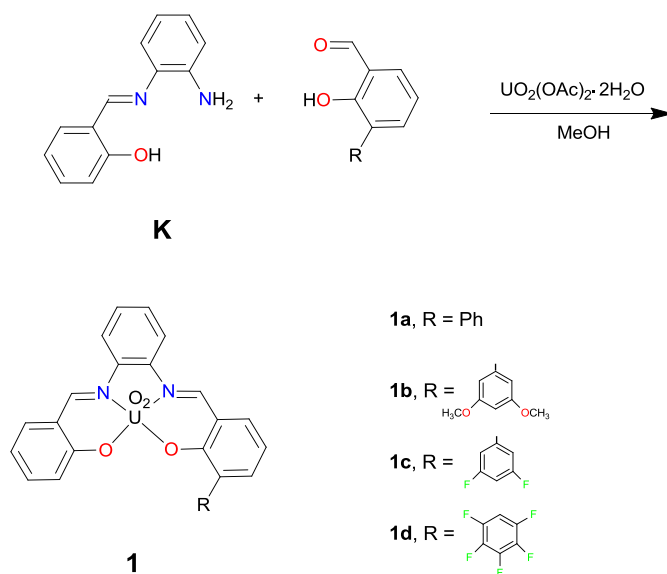
Scheme 1.3. Synthesis of the *ortho*-mono-substituted aromatic uranyl-salophen complexes. Yields: **1a** 40%; **1b** 20%; **1c** 48%; **1d** 52%.

Binding constants for the 1:1 complexes of TBAX (X = F⁻, Cl⁻, Br⁻, I⁻) with the uranyl–salophen complexes **1a-d** were obtained in CHCl₃ at 25°C, from UV/Vis titrations. Binding constants K_a [M^{-1}] are listed in Table 1.2. To evaluate the binding constant with iodine we had to undertake ^{1}H-NMR titrations.

Table 1.2. Association constant values, K_a (M^{-1}), for the complexation of TBAX (X = F^-, Cl^-, Br^-, I^-) with receptors **1a-d** obtained by UV-vis titrations in $CHCl_3$ at 298 K. (Concentration of the hosts of 10^{-5} M and successive addition of TBAX)

X^-	1a	1b	1c	1d
F^-	$>10^6$	$>10^6$	$>10^6$	$>10^6$
Cl^-	24000 ± 200	11000 ± 1200	51000 ± 3400	140000 ± 10000
Br^-	650 ± 65	100 ± 5	466 ± 9	2090 ± 15
I^-	$<20^a$	$<20^a$	$<20^a$	$<20^a$

[a] Obtained by H NMR titrations in $CDCl_3$.

Inspection of the results shows that the binding order of the complexes with the TBA salts, namely, $F^- > Cl^- > Br^- > I^-$, is in good agreement with the hard Lewis acidic character of the uranyl center. The strong affinity of the TBA fluoride salt is dominated by the interaction of the hard fluoride anion with the metal center. Such binding is so high for all the receptors ($K_a > 10^6$) that it prevents the observation of any difference, if present, caused by the nature of the substituents on the aromatic appended arm. Instead, lower binding affinities in the case of chloride allow for interesting considerations: the highest stabilization of the **host**@chloride complex was found with receptor **1d**, decorated with a perfluorophenyl unit. The measured binding affinities towards chloride shown by the other receptors either displaying two methoxy groups, **1b**, or no substituents, **1a**, or two fluorine atoms, **1c**, are definitely lower. They behave quite similarly, although **1a** is slightly more efficient for chloride binding than **1b**. **1c** is the second best receptor in the series with slightly further stabilization with respect to **1a** because of the two strong electronegative fluorine atoms.

The choice to synthesize the receptor **1c** with substitution of hydrogen atoms (with respect of **1a**) by fluorine in 3', 5' positions on the biphenyl units, was inspired by the work of Giese and

coworkers,[23] in which it is reported that, upon subsequent substitution of fluorine with hydrogen atoms, the more electron rich units do not allow anion-π contacts and the interaction becomes repulsive in the solid state. From our investigation seems that, also in this case, with receptors **1c** bearing a difluorophenyl moiety, no substantial anion-π interaction takes place and almost no significant increase of binding affinities with respect to receptor **1a**, taken as reference. Thus, the straightforward further stabilization through anion–π interactions takes place only with receptor **1d**, which displays a π-acceptor character that enhances halide binding in solution.[24]

The same behavior is observed with bromide, whereas the association with iodine is too weak to be measured.

We can claim from our results that the directionality of the complexation, in which the halide is hosted in the fifth equatorial site of the uranyl, provides a suitable geometrical orientation to establish intramolecular contacts with the π-cloud of the pendant arm.

The potential electronic effect of the substituents on the Lewis acidity of the uranyl center can be easily ruled out because a direct interaction between the sidearm and the uranyl center is prevented by the marked curvature imposed to the coordinated salophen ligand by the large atomic radius of uranium. This is clearly highlighted by the solid state crystal structures and also easily reproduced by molecular mechanics calculations.[25]

Slight variations in the resonances of the TBA salt during titrations seem to indicate that the uranyl complexes do not behave as ditopic receptor as in Figure 1.6. Of course in chloroform the resultant complex is tightly ion-paired,[26] but the aromatic pendant arm affects exclusively the anion in the contact ion pair, Figure 1.5.
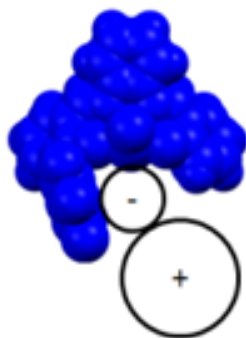
Figure 1.5. Schematic representation of the tightly ion-paired complexes in chloroform solution.
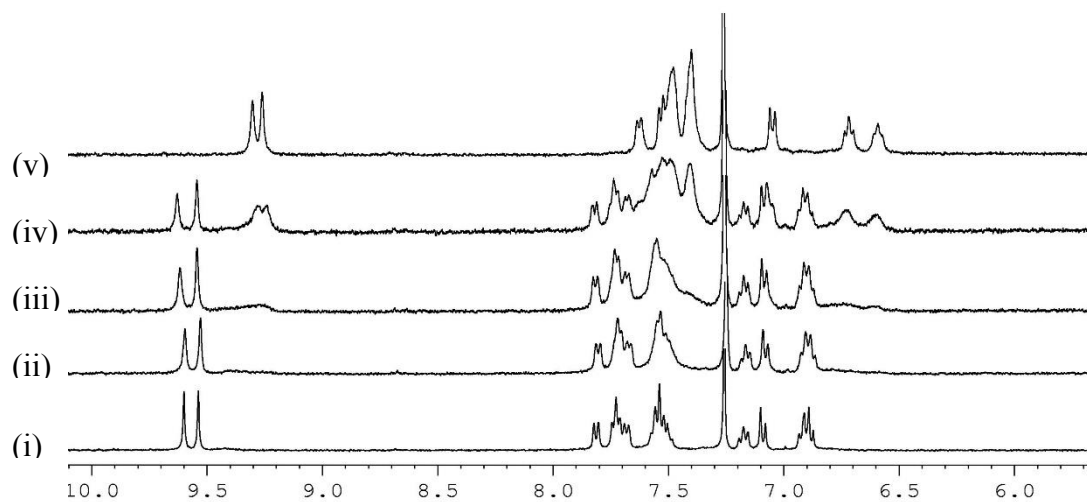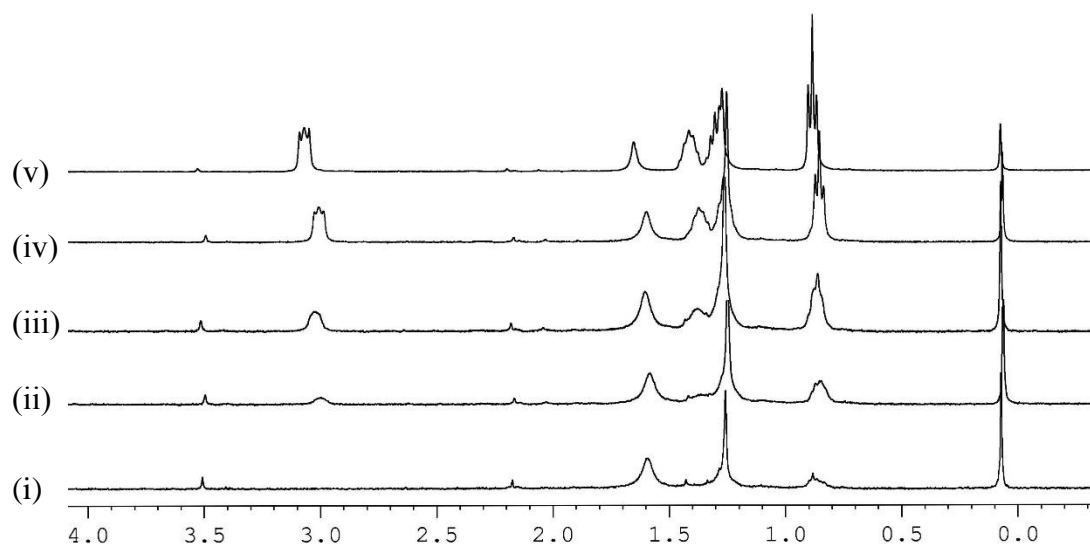
Figure 1.6. Portions of the ^{1}H NMR (0-4 and 6-10 ppm) spectra (400 MHz, 25°C in CDCl$_3$): (i) **1d**, C = 7.97x 10^{-3}M; (ii) after addition of 0.5 mol equiv. of TBACl; (iii) after addition of 1.2 mol equiv. of TBACl, (iv) after addition of 3.0 mol equiv. of TBACl, (v) after addition of 8.0 mol equiv. of TBACl. The system is under slow exchange condition.[27]

The choice of **1a** bearing a simple unsubstituted phenyl as control receptor is motivated by the negligible interaction between halides and benzene even if is intuitively expected to be repulsive: its unfavorable quadrupole moment (Q_{zz} = -8.45 B) and favorable polarizability cancels each other ($\alpha\parallel$ = 41.5 a.u.; the molecular polarizabilities parallel to the main symmetry axis are $\alpha\parallel$ = 41.5 and 37.7 a.u. (a.u. stands for atomic units), for benzene and hexafluorobenzene, respectively). Indeed, the interaction energy of the benzene–chloride pair is negligible.[28] The same phenomenon is observed for the interaction of hexafluorobenzene (Q_{zz} = +9.50 B and $\alpha\parallel$ = 37.7 a.u.) with sodium.[28]

To quantify the contribution in solution of the anion–π interaction for these systems, we calculated $\Delta\Delta G$ values, where $\Delta\Delta G = \Delta G_{X\text{-}@\textbf{Host}} - \Delta G_{X\text{-}@\textbf{1a}}$,[29] with respect to the control receptor **1a**, in which the appended phenyl ring does not have any substituent. The free energies relative to anion binding are obviously the sum of two different types of intermolecular interactions: Lewis acid–base interaction with the metal center and anion–π interaction with the pendant aromatic wall that are treated as addictive. We estimated for receptor **1d** an

attractive free energy of -1.0 kcal mol^{-1} for chloride binding and -0.7 kcal mol^{-1} for bromide, whereas for receptor **1b**, a repulsive free energy of 0.5 kcal mol^{-1} for chloride and 1.1 kcal mol^{-1} for bromide was calculated. Finally, we estimated for receptor **1c** an attractive free energy of -0.4 kcal mol^{-1} for chloride binding and a negligible repulsive 0.2 kcal mol^{-1} for bromide. All the values are reported in Table 1.3. The observed trend is in agreement with the existence of a weak non-covalent stabilizing interaction for the perfluorinated derivative, whose magnitude is in accordance with the values reported by Ballester and co-workers[30] for a series of "two-wall" calix[4]pyrrole receptors bearing two sixmembered electronically different aromatic rings.

Table 1.3. Differences of Free Binding Energies ($\Delta\Delta G$, kcal mol^{-1}) for the complexation of TBAX (Cl$^-$ and Br$^-$) with receptors **1b-d** with respect to receptor **1a**, taken as reference, i.e. $\Delta\Delta G = \Delta G_{X\text{-}@\mathbf{1b}} - \Delta G_{X\text{-}@\mathbf{1a}}$ etc, in chloroform solution.

X$^-$	1b	1c	1d
Cl$^-$	0.5	-0.4	-1.0
Br$^-$	1.1	0.2	-0.7

1.2.2 *ortho*-di-substituted aromatic uranyl-salophen complexes and binding studies in chloroform and acetonitrile.

As for receptors **1a-d**, we synthesized and investigated the association constant (K_a, M^{-1}) values for the 1:1 complexes of TBAX ($X^- = F^-$, Cl^-, Br^-, I^-) with the symmetrical disubstituted uranyl-salophen complexes **2a-d** in CHCl$_3$ solution at 25°C, from UV/Vis titration. The synthesis of such compounds was quite simple: 2 equiv. of the properly functionalized salicylaldehyde derivatives were reacted with the o-phenylenediamine in the presence of uranyl acetate to give the disubstituted compound **2a-d** without any chromatographic treatment. See Scheme 1.4.

D

2b   55%

G

2c   97%

J

2d   24%
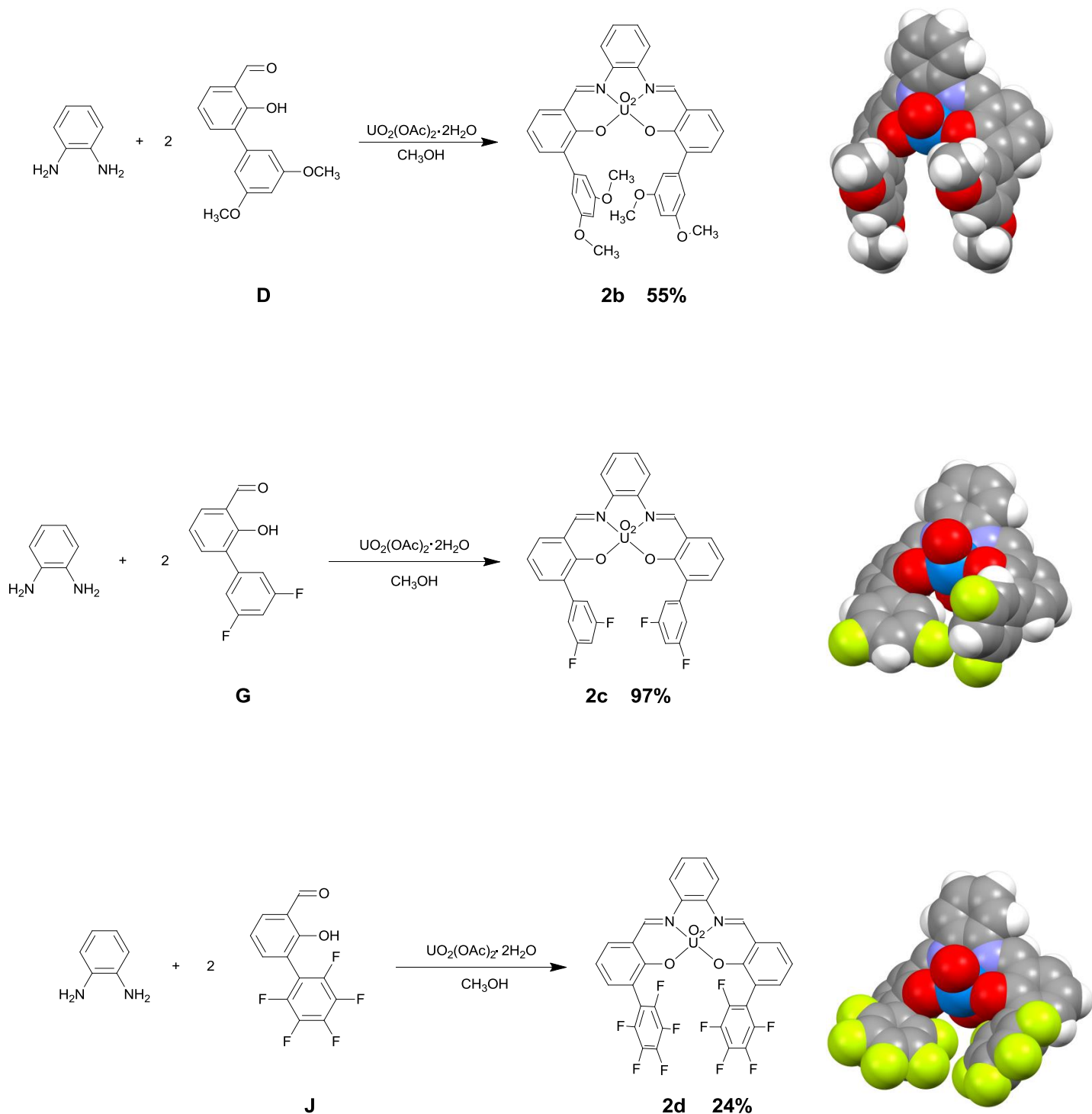
Scheme 1.4. Synthesis of the *ortho*-di-substituted aromatic uranyl-salophen complexes and the X-ray crystal structures of the free complexes that highlight the spatial conformation of such receptors.

The thermodynamic data for TBAX (Cl⁻ and Br⁻) are summarized in Table 1.4.

Table 1.4. Association constant values, K_a (M^{-1}), for the complexation of TBAX (Cl⁻ and Br⁻) with receptors **2a-d** obtained by UV-vis titrations in $CHCl_3$ at 298 K. (Concentration of the hosts of 10^{-5} M and successive addition of TBAX)

X⁻	2a	2b	2c	2d
Cl⁻	2200 ± 100	160 ± 2	15600 ± 1300	56000 ± 1600
Br⁻	48 ± 1	[a]	540 ± 10	1400 ± 50

[a] No change in absorption during titration experiments.

In such a lipophilic solvent, the tetrabutylammonium salts are highly ion-paired and the resultant complexes are formed by trimolecular neutral ion-paired complexes upon titration with the receptors; as shown in the schematic representation (a) and (b), Figure 1.7.

In the "two wall" uranyl-salophen receptors **2a-d**, the increased steric bulkiness, with respect to the mono substituted receptors **1a-d,** effects the binding of TBAX salts, especially in the presence of bulky substituents, as in the case of the four methoxy groups **2b** (see Scheme 1.4). In accordance with this, we can appreciate the steric hindrance during the binding process that leads to a marked decrease of the binding affinities because of the rule played by the big coutercation (TBA⁺).

a)
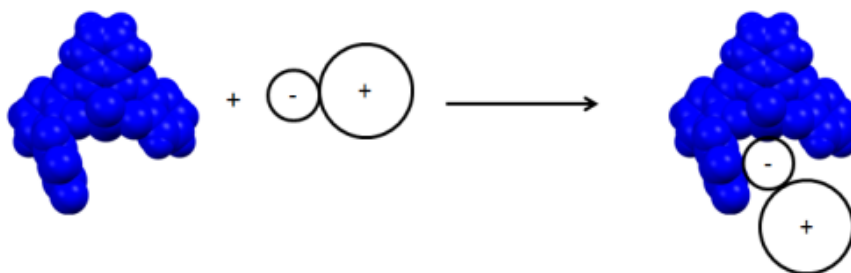
b)
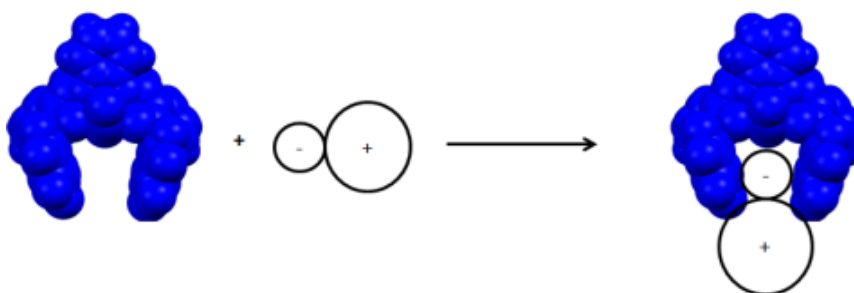
Figure 1.7. Schematic representation of trimolecular neutral ion-paired complexes of side-armed receptors **1a-d** (a) and **2a-d** (b).

In particular, in chloroform solution, the large affinity of the investigated TBAF due to the strong interaction with the hard fluoride with the uranyl center, didn't allow us to observe any difference, if present, toward all the different substituted receptors, due to strong binding ($K_a > 10^6 M^{-1}$). However, for the worst binder **2b** bearing four methoxy groups, it was possible to estimate the association constant toward fluoride (**$K_a = 93500 \pm 6700 M^{-1}$**). The slight affinity showed by all receptors toward iodide (TBAI) did not permit to measure any binding constant. The binding affinities in the case of chloride and bromide lead to interesting considerations. We observed a clear enhancement of the halide binding with the highest stabilization, in the case of receptor **2d** bearing two perfluorophenyl units. So, we can claim that the intramolecular contact with the π-cloud of the pendant arms in solution is taking place. This unambiguous proof of the occurrence of anion-π interactions in solution is one of rare evidences reported in the literature[31]. Definitely lower binding was observed for receptors **2a-c**, bearing aromatic pendant units substituted with dimethoxy, difluoro or without substituents, toward TBACl and TBABr, with a marked steric effect for receptor **2b.** With bromide, no change in absorption

spectra was observed during titration experiments and this can be ascribed to the bulkiness of TBA$^+$ as well as to the bulkiness of the four methoxy groups that prevent the anion approaching the metal center.

Differently from **1c** with one difluorophenyl ring**,** receptor **2c** with two difluorophenyl moiety seems to bind chloride and bromide better than the reference **2a** (reference for the disubstituted compounds) (see Table 1.2 and 1.4). Probably the "two wall" uranyl-salophen **2c** assumes in solution a spatial conformation that enhance the stability of the resultant complex through anion-π interaction differently with respect of **1c**.

Due to the role acted by TBA$^+$ in chloroform, we changed the solvent and measured the binding constants (K_a, M^{-1}) in acetonitrile, CH$_3$CN. In such a polar solvent, the free and complexed salts are in their ionic form[32] and an equation (eq.1) representative of the binding, can be formulated in dipolar aprotic solvents (s = CH$_3$CN) for the interaction of all receptors studied and the halide anions (X$^-$ = F$^-$, Cl$^-$, Br$^-$, I$^-$).

$$\textbf{Receptor}_{(s)} + \textbf{X}^-_{(s)} \rightleftarrows \textbf{[Receptor@X]}^-_{(s)} \qquad \text{(eq.1)}$$

The thermodynamic data for receptors **1a-d** and **2a-d** towards TBAX (Cl$^-$ and Br$^-$) in CH$_3$CN solution are summarized in Table 1.5 and 1.6.

Table 1.5. Association constant values, K_a (M^{-1}), for the complexation of TBAX (Cl^- and Br^-) with receptors **1a-d** obtained by UV-vis titrations in CH_3CN at 298 K. (Concentration of the hosts of 10^{-5} M and successive addition of TBAX)

X^-	1a	1b	1c	1d
Cl^-	30700 ± 1200	11400 ± 1100	67500 ± 7700	$>10^6$
Br^-	220 ± 6	83 ± 1	310 ± 40	1700 ± 200

Table 1.6. Association constant values, K_a (M^{-1}), for the complexation of TBAX (Cl^- and Br^-) with receptors **2a-d** obtained by UV-vis titrations in CH_3CN at 298 K. (Concentration of the hosts of 10^{-5} M and successive addition of TBAX)

X^-	2a	2b	2c	2d
Cl^-	8800 ± 1100	[a]	120000 ± 20000	$>10^6$
Br^-	43 ± 1	[a]	540 ± 60	5900 ± 400

[a] Compound **2b** is not soluble in CH_3CN.

Again, we noticed the large affinity of TBAF with the uranyl center for all receptors. It didn't allow us to observe any differences in binding constants, if present ($K_a > 10^6$ M^{-1}).

The different substituted receptors toward TBAI behave quite similarly to what observed in chloroform solution, i.e. we couldn't observe any binding because of the soft Lewis base character of I⁻. Except for the best binder and π-acceptor **2d**, bearing a pentafluorophenyl moiety, it was possible to measure the association constant toward Iodide (**$K_a = 42 \pm 2$ M^{-1}**).

For receptor **2b**, since it was not soluble in acetonitrile solution, no binding constants were measured. Again, we had a clear enhancement of the halide binding with the highest stabilization for the **host**@chloride/bromide complexes in case of **1d** and for **host**@chloride/bromide/iodide complexes **2d** bearing one or two perfluorophenyl units. Actually, we couldn't estimate the binding constants of receptors **1d** and **2d** toward chloride too, because it is so high to be measured ($K_a > 10^6$ M^{-1}). Lower binding was found for receptors **1a-c** and **2a-c**.

Surprisingly, despite the possibility of acetonitrile molecules to be hosted in the fifth vacant equatorial binding site of the uranyl[33] being in this way a competitor for the guest, we measured an enhancement of the halides binding for almost all receptors, especially for **1d** and **2b** able to establish anion-π contacts with the halides. This quite strange behavior can be explained by thermodynamic considerations and by the schematic representation in Figure 1.8.
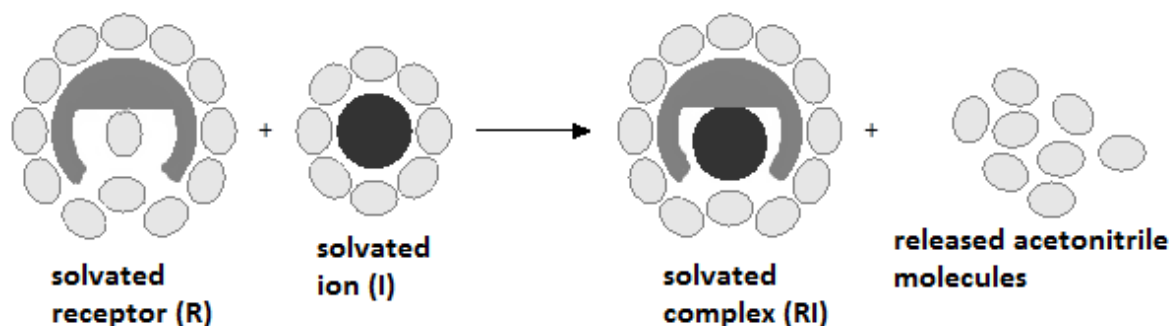
Figure 1.8. Schematic representation of the steps associated with the binding of halides by our receptors in acetonitrile solution.

The energy paid to replace the acetonitrile molecules with the anions during the binding process is overcompensated by the desolvation effects that entail a gain in entropy and enhances the halide binding despite the presence of the coordinating solvent. Going deeper, during the binding process, the constrained acetonitrile molecules solvating the receptor and anion will be released in the bulk solution with a gain in entropy. The overall more negative ΔG can result if the entropically favorable desolvation of the binding partners overcompensates the desolvation enthalpy leading to an overall entropically driven host-guest complex formation.

Nevertheless, by changing the solvent from a lipophilic to a polar one, the binding affinity trend is almost the same. This can be explained considering that the nature of solvent doesn't affect the anion-π interaction *per se*.

We calculated the free energies of binding for the complexes with TBAX ($X^- = Cl^-$, Br^-) considering them as the sum of two different and independent types of supramolecular interactions, i.e. Lewis acid-base interaction and anion-π interaction.

To estimate the contribution of a single anion-π interaction from the set of ΔG values calculated in chloroform and acetonitrile, we needed to compare these with the free energies of suitable control receptors, i.e. **1a** for the monosubstituted ones and **2a** for the two side arms receptors, bearing simple aromatic rings. The control receptors can help us to understand the electronic effects of the substituents on the binding.

Thus, to quantify the contribution in solution of the anion-π interaction in our systems, we calculated the $\Delta\Delta G$ values ($\Delta\Delta G = \Delta G_{X^-@\textbf{Host}} - \Delta G_{X^-@\textbf{1a}}$; $\Delta\Delta G = [\Delta G_{X^-@\textbf{Host}} - \Delta G_{X^-@\textbf{2a}}]/2$) with respect to the two control receptors (Table 1.7, 1.8 and 1.9).

Table 1.7. Differences of Free Binding Energies ($\Delta\Delta G/2$, kcal mol^{-1}) for the complexation of TBAX (Cl$^-$ and Br$^-$) with receptors **2b-d** with respect to receptor **2a**, taken as reference, i.e. $\Delta\Delta G/2 = [(\Delta G_{X@\textbf{2b}} - \Delta G_{X@\textbf{2a}})/2]$ etc, in **chloroform** solution.

X$^-$	2b	2c	2d
Cl$^-$	0.8	-0.6	-1.0
Br$^-$		-0.7	-1.0

Table 1.8. Differences of Free Binding Energies ($\Delta\Delta G$, kcal mol^{-1}) for the complexation of TBAX (Cl$^-$ and Br$^-$) with receptors **1b-d** with respect to receptor **1a**, taken as reference, i.e. $\Delta\Delta G = \Delta G_{X@\textbf{1b}} - \Delta G_{X@\textbf{1a}}$ etc, in **acetonitrile.**

X$^-$	1b	1c	1d
Cl$^-$	0.6	-0.5	
Br$^-$	0.6	-0.2	-1.2

Table 1.9. Differences of Free Binding Energies ($\Delta\Delta G/2$, kcal mol^{-1}) for the complexation of TBAX (Cl$^-$ and Br$^-$) with receptors **2b-d** with respect to receptor **2a**, taken as reference, i.e. $\Delta\Delta G/2 = [(\Delta G_{X@2b} - \Delta G_{X@2a})/2]$ etc, in **acetonitrile.**

X$^-$	2b	2c	2d
Cl$^-$		-0.8	
Br$^-$		-0.8	-1.5

We estimated in chloroform solution, energy values from attractive free energies of -1.0 kcal mol^{-1} for receptor **2d**@Cl$^-$/Br$^-$, to a repulsive free energy of 0.8 kcal mol^{-1} for the worst binder **2b**. Estimates of energy values for receptor **1b-d** with respect to **1a** are reported in Table 1.3.

In acetonitrile solution we calculated energy values from an attractive free energy of -1.5 kcal mol^{-1} for the best binder **2d**, to a repulsive free energy of 0.6 kcal mol^{-1} for **1b**.

In view of the above, we have shown that these systems can be used to quantify anion-π interactions in solution similarly to what done by Ballester and co-workers[29]where the main driving force for complexation is hydrogen bonding (their $\Delta\Delta G$ energies are in accordance with our work).

1.2.3 *Electrostatic potential (ESP)*

To have a full picture of this elusive interactions in solution by means of these anion receptors we calculated the ESP (electrostatic potential) values at the ring centroid of the respective aromatic rings. ESP values correlate very well with the ΔG (ΔG = -RTln (K_a)) values both in chloroform and acetonitrile. Correlation lines, ΔG vs ESP (CH_3CN) and ΔG vs ESP ($CHCl_3$) calculated at 2 Å from the ring centroid are reported in the Figures 1.9$_{1)-4)}$ below.

We claim that in general, halide-π contacts are dominated by electrostatic effects.

The slope of the correlation lines for bromide and chloride are similar [34]

The dot **2b** in the plot number 4 (see the arrow in violet) is way off to the side of the general trend-line of the points; in particular, it is quite a little bit higher than the trend indicated by the rest of the plotted data points. A likely explanation is that the steric bulk, of the four methoxy groups in the symmetric receptor **2b,** effects the binding of TBAX salts. This steric effect is strongly stability decreasing.

ΔG $_{Cl/Br@Host}$ *(kcal mol^{-1})*= **-** RTln (**K_a**)

ESP *(kcal mol^{-1})* = -19.97(**1a**); -20.23(**1b**); -8.94(**1c**); 6.13(**1d**); -21.18(**2a**); -21.44(**2b**); -8.84 (**2c**); 7.81(**2d**)

1)

ΔG (CH₃CN) *vs* **ESP (at 2Å)**

2)
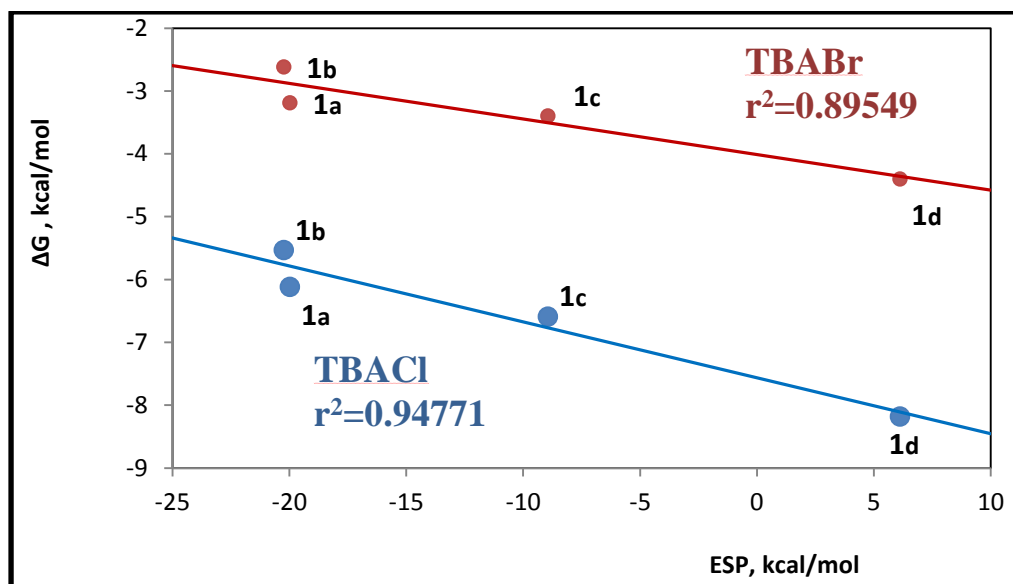
ΔG (CH₃CN) vs ESP (at 2Å)

3)
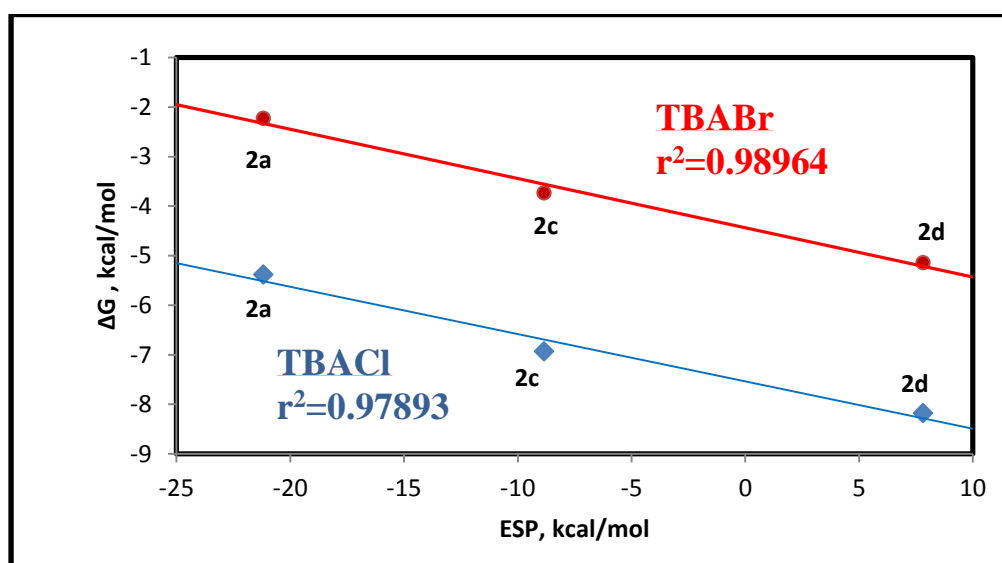
ΔG (CHCl₃) *vs* ESP (at 2Å)

4)
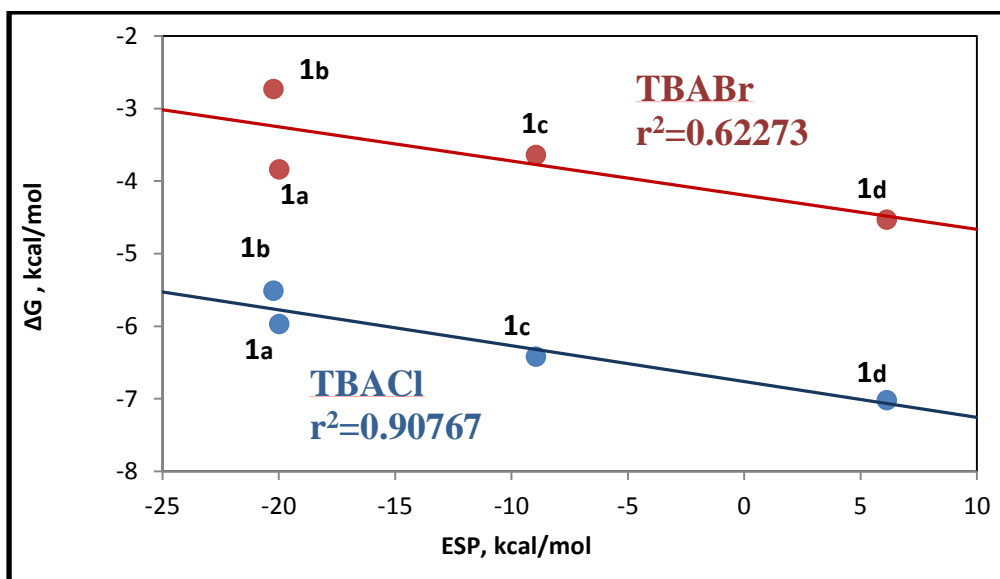
ΔG (CHCl₃) *vs* ESP (at 2Å)
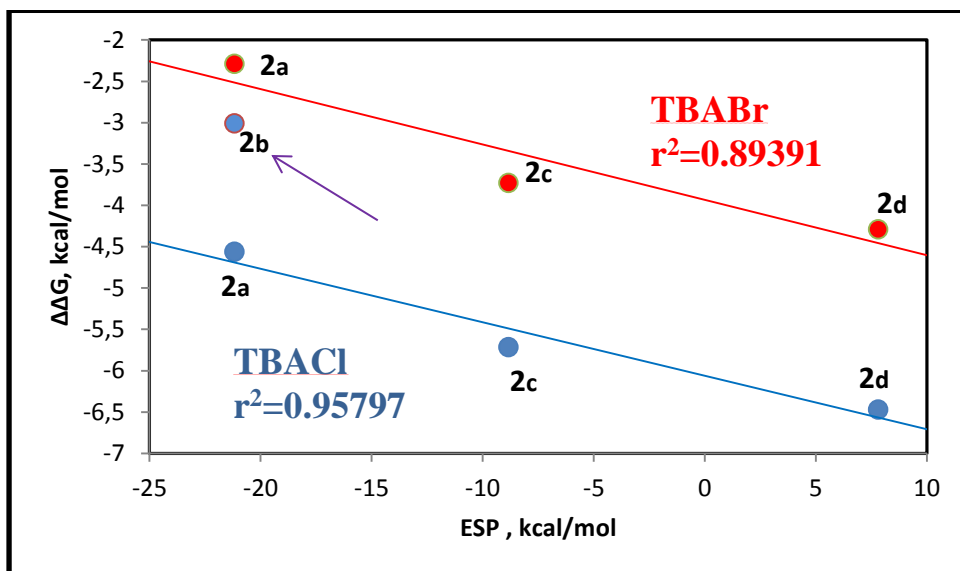
Figures 1.9[1)-4)] Plot of the experimental ΔG values derived from the binding of chloride (blue), bromide (red) *vs* the ESP values calculated at the centroid of the aromatic walls.

1.2.4 *Solid state*

Crystals of the complexes [TBA][Cl⁻@**1d**] and [TBA][Br⁻@**1d**] were obtained by slow evaporation of CHCl$_3$ and CHCl$_3$:CCl$_4$, 50:50 solutions, respectively. The crystal structures are isomorphous and crystallize in the monoclinic space group P21/c, Figure 1.10.
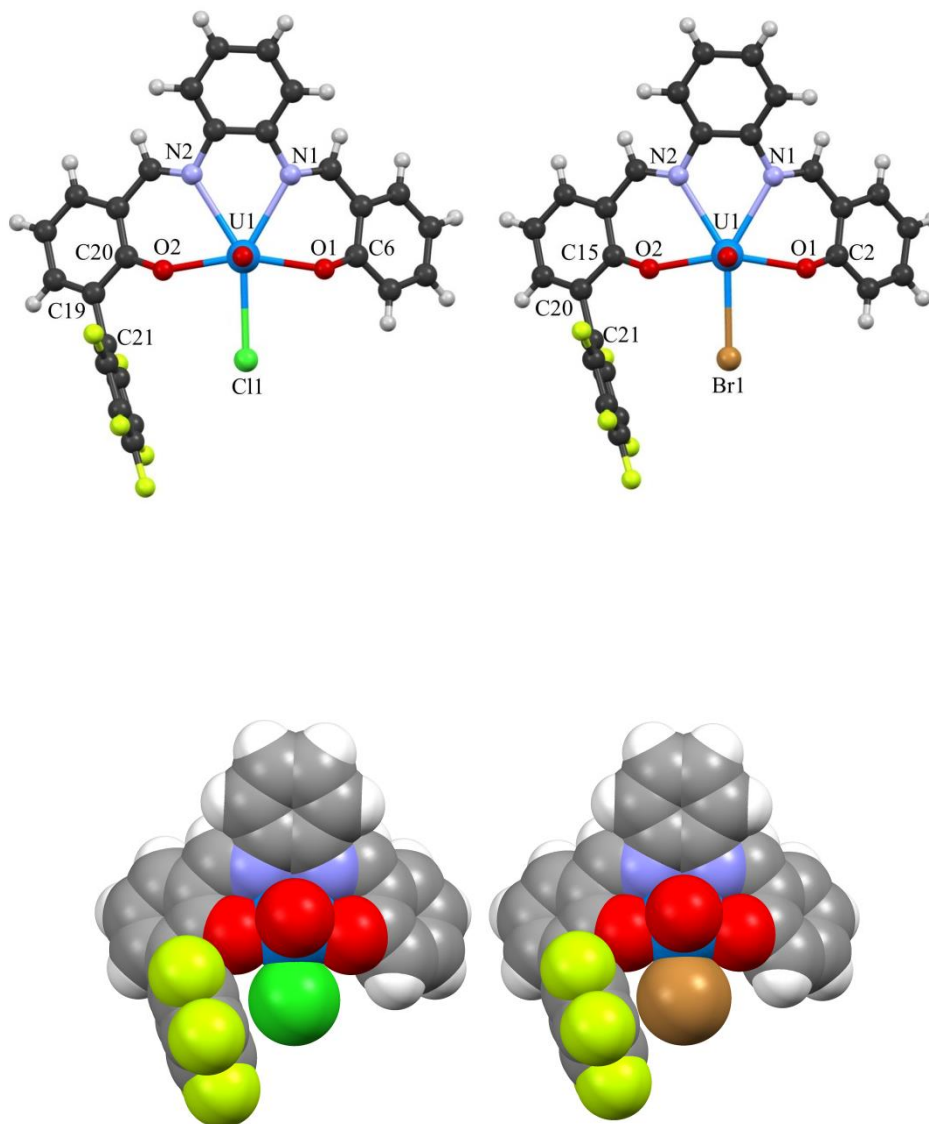
Figure 1.10. X-Ray crystal structures of [TBA][Cl⁻@**1d**] (a) and (b) [TBA][Br⁻@**1d**] in (top) ball and stick and CPK (bottom) presentations.

The biphenyl unit formed by the salicylaldehyde and the pendant perfluoro arene ring displays a very similar twist angle, 63.3(8)° and 64.8(8)°, in the chloride complex and the bromide one, respectively. The wide twist angles we found can be ascribed to the presence in the equatorial coordination plane of the bound anion, close to the pentafluoro phenyl ring, with which it establishes stabilizing anion-π interactions. The C_{ring}···X (X = Cl^- and Br^-) distances range between 3.82 – 3.94 Å in [TBA][Cl^-@**1d**] and 3.77 – 3.94 Å in [TBA][Br^-@**1d**]. However, remarkably, the π(centroid)···X, [X = Cl^- and Br^-] has the shortest distances of 3.63 and 3.60 Å, respectively, indicating clear η^6 anion-π interactions.[35] The normal U-Cl bond distances in similar uranyl salophen complexes varies between 2.713 – 2.760 Å, the same distance in [TBA][Cl^-@**1d**] 2.843(2) Å is markedly longer (0.083 - 0.130 Å) and statistically significantly different. Thus the distance becomes longer to have the further stabilization with the perfluorophenyl unit. For the bigger Br^- the distance in already good enough to interact with the centroid. On the other hand, there are no observed short contacts between the aromatic ring and TBA cations, like cation-π interactions. The X-ray structures provide additional proof that the perfluoro group, though having five highly electron-withdrawing fluorine substituents, does not influence the Lewis acidity of the uranyl center. The C-O and O-U bond distances are equal in [TBA][Cl^-@**1d**] and [TBA][Br^-@**1d**], and are close for example to the unsubstituted uranyl salophen@tetraethylammonium chloride (TEACl) complex,[36] in Figure 1.11:
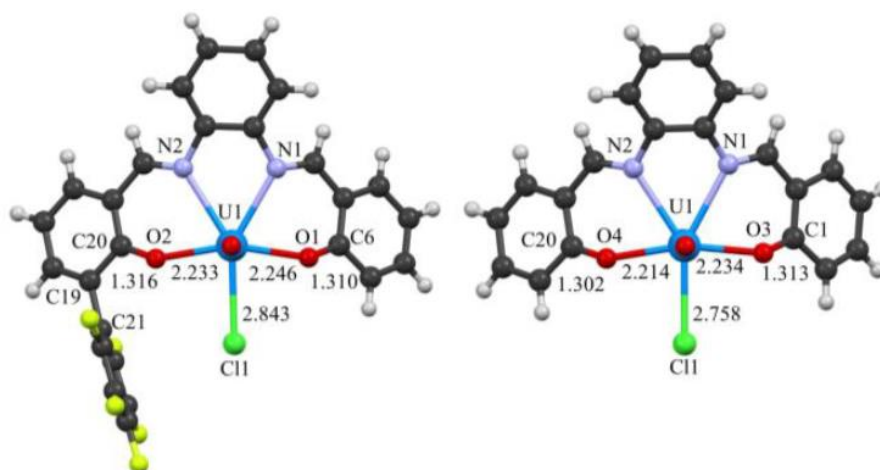

Figure 1.11. Comparison of C-O and O-U bond distances in **[TBA][Cl^-@1d]** (left), and in UO_2-Salophen@TEACl (CCDC code LADCUO).[36b)] The TBA cations are omitted for clarity.

In addition due to the η^6 (η = apticity) anion-π interactions, the perfluorobenzene group is "leaning" towards the uranyl bound halide, manifesting reduced biphenylic C20-C19-C21 bond angle. In [TBA][Cl⁻@**1d**] and [TBA][Br⁻@**1d**] the angle is 117.1° and 115.1°, markedly smaller than the typical 120° trigonal planar systems.

In addition, we obtained X-ray crystal structures of the symmetrical disubstituted uranyl-salophen complexes **2a-d** with TBAX, X = F⁻, Cl⁻, Br⁻ I⁻. These structures provide an unbiased view for the existence of anion-π interactions also in these systems and support the data and considerations obtained in solution state.

X-ray crystal structure, apticity, crystallization conditions, twist angles, space groups and solvents, are reported in the Figure 1.12-20 below.

In particular, crystal structures in which our uranyl-salophen receptors are coordinated with TBAI in the solid state, as far as we know, are never been obtained before and are important structures because they prove the existence of a the further stabilization (iodide-π interactions) besides the main, but anyway weak in case of iodide, driving force for complexation (Lewis acid-base interactions) that stabilize the iodide. In fact, ion-induced polarization effects in the case of iodide are very important because I⁻ possess a high polarizability and the binding of iodide is enhanced because of iodide-π interaction despite the low Lewis-base character of such anion.

[2c@F⁻]

Figure 1.12. Symmetric salophen difluoro in (a) Ball&Stick and (b) model CPK. The dotted lines show anion-π interactions and twisting angles. The cation tetrabutylammonium (TBA) and the solvent Acetone-CH_2Cl_2 was omitted for clarity.

Monoclinic, *P21/c* space group.

[2c@Cl⁻]

Figure 1.13. Symmetric salophen difluoro in (a) Ball&Stick and (b) model CPK. The dotted lines show anion-π interactions and twisting angles. The cation dimetylammonium (DMA) and the solvent CH_2Cl_2 was omitted for clarity.

Triclinic, P⁻1 space group.

[2c@Br⁻]

Figure 1.14. Symmetric salophen difluoro in (a) Ball&Stick and (b) model CPK. The dotted lines show anion-π interactions and twisting angles. The cation tetrabutylammonium (TBA) and the solvent CH_2Cl_2 were omitted for clarity.
Monoclinic, *P21/c* space group. Crystal structure is isomorphous with the next structure [2c@I⁻]

[2c@I⁻]

Figure 1.15. Symmetric salophen difluoro in (a) Ball&Stick and (b) model CPK. The dotted lines show anion-π interactions and twisting angles. The cation tetrabutylammonium (TBA) and the solvent $CHCl_3$:CCl_4 were omitted for clarity. Monoclinic, *P2₁/c* space group.

[2d@F⁻]

Figure 1.16. Symmetric salophen perfluoro in (a) Ball&Stick and (b) model CPK. The dotted lines show anion-π interactions and twisting angles. The cation tetrabutylammonium (TBA) and the solvent $CHCl_3:CCl_4$ were omitted for clarity.

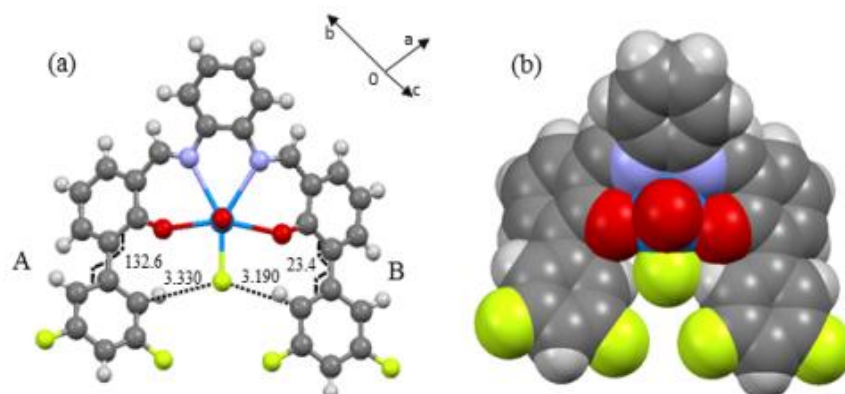Triclinic, P$\bar{1}$ space group.

[2d@Cl⁻]
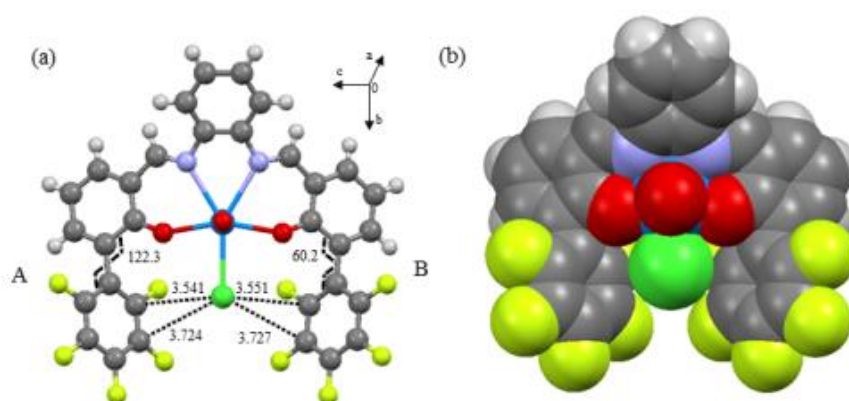
Figure 1.17. Symmetric salophen perfluoro in (a) Ball&Stick and (b) model CPK. The dotted lines show anion-π interactions and twisting angles. The cation diethylammonium (DEA) and the solvent CH_2Cl_2 were omitted for clarity.

Monoclinic, P21/n space group.

[2d@Br⁻]
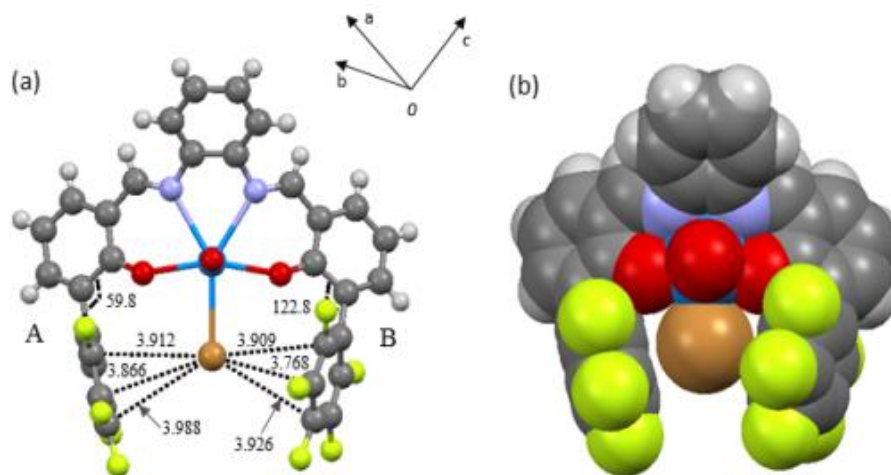
Figure 1.18. Symmetric salophen perfluoro in (a) Ball&Stick and (b) model CPK. The dotted lines show anion-π interactions and twisting angles. The cation tetrabutylammonium (TBA) and the solvent $CH_2Cl_2:CCl_4$ was omitted for clarity.

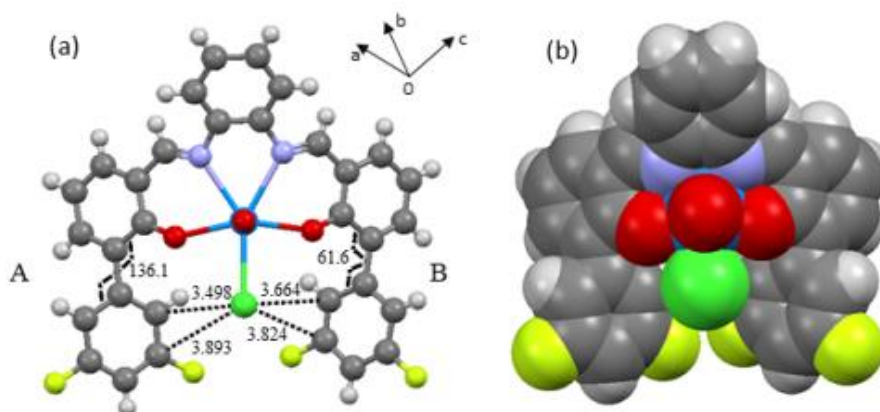Triclinic, P‾1 space group.

[2d@I⁻]
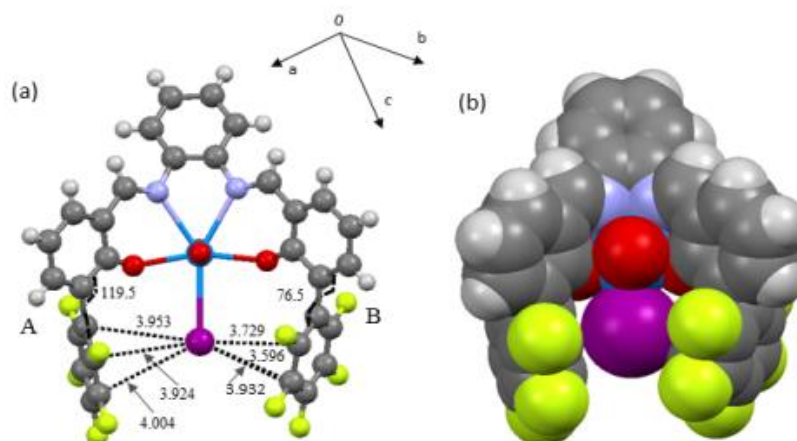
Figure 1.19. Symmetric salophen perfluoro in (a) Ball&Stick and (b) model CPK. The dotted lines show anion-π interactions and twisting angles. The cation tetrabutylammonium (TBA) and the solvent CH_2Cl_2/hexane were omitted for clarity.
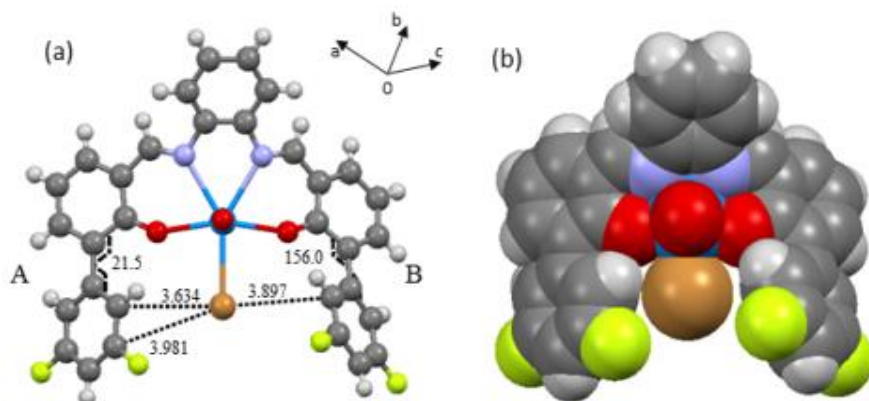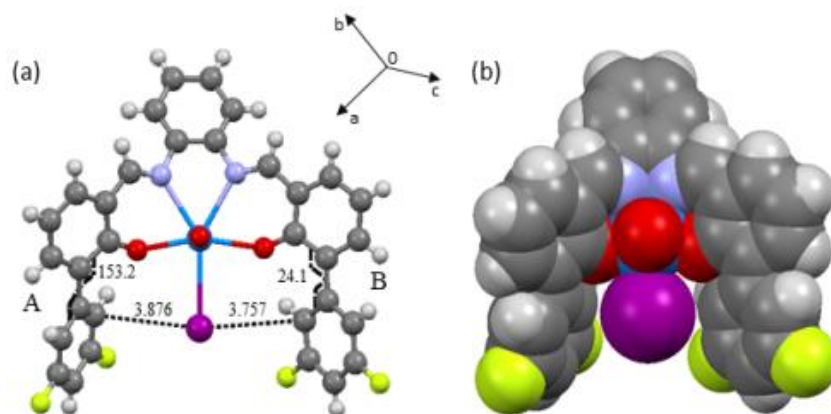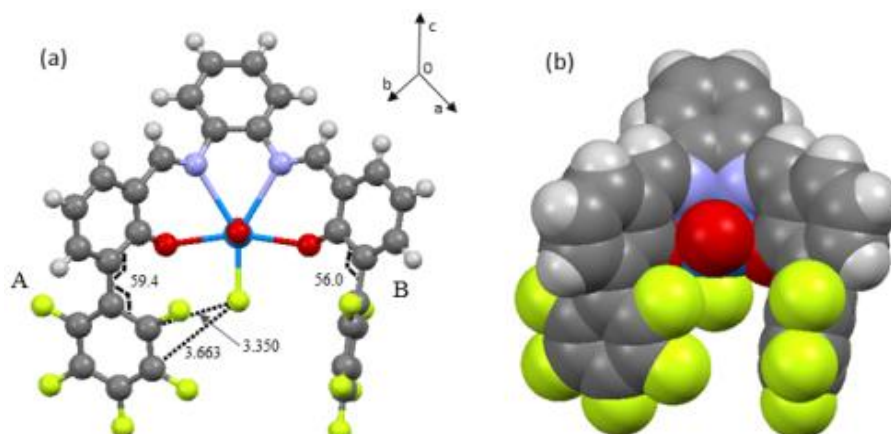
Triclinic, P‾1 space group.

[2d@Br⁻]
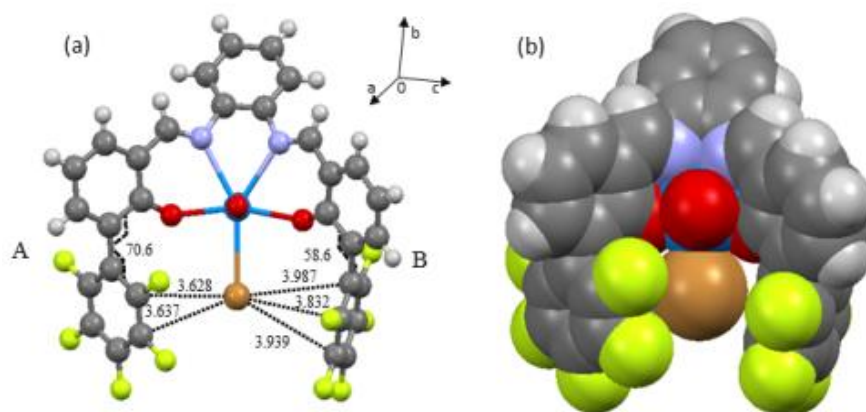
Figure 1.20. Symmetric salophen perfluoro in (a) Ball&Stick and (b) model CPK. The dotted lines show anion-π interactions and twisting angles. The cation Benzyltriethylammonium (BzTEA) and the solvent CH_2Cl_2:CCl_4 was omitted for clarity.

Monoclinic, *P21/n* space group.

1.3 Substituent Effects in Chloride-π Interactions.
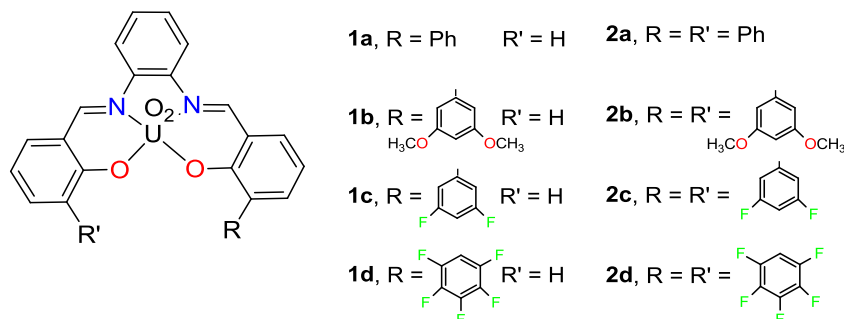
Scheme 1.5. Chemical formulae of uranyl-salophen receptors **1a-d** and **2a-d** studied in the previous investigation.

Encouraged by the results obtained with receptors **1a-d** and **2a-d**, (Scheme 1.4, see chapter 1.2) in this study, we explored the influence of substituents upon chloride-π interaction by measuring the binding affinity of tetrabutylammonium (TBA) chloride to nonsymmetric uranyl-salophen receptors decorated with X-substituted aromatic pendants (X = $N(CH_3)_2$, OCH_3, Br, NO_2) as in Scheme 1.5.
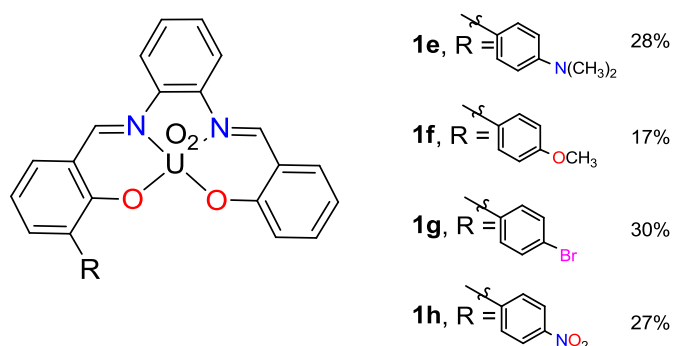
Scheme 1.6. Synthesized monosubstituted uranyl-salophen receptors **1e-h**.The yields are referred to the final step (see Scheme 1.7)

Different *para* substituents are used to modify the charge distribution of the aromatic ring.

We decided not to use the symmetric disubstituted uranyl-salophen type receptors **2** to avoid any steric effect around the metal center. As solvent, instead of chloroform,[37] we chose a polar aprotic solvent (acetonitrile [38]), where the free and complexed salts are in their ionic form and neutral ternary ion-paired complexes are not present in solution.[32] Thus, the big tetrabutylammonium cation (TBA+) is solvated by the acetonitrile molecules and does not influence the binding. The halide used as tetrabutylammonium salt was chloride for the reason that the high affinity of fluoride and the relative low affinity of bromide and iodide with the uranyl center, couldn't allow us to appreciate any difference in binding constants and thus we couldn't perform a meaningful Hammett-type analysis. The receptor used as model system was the monosubstituted receptor **1a** bearing a simple aromatic ring.

Receptors **1e-h** were synthesized according to the general Scheme 1.6 that involves a Suzuki cross-coupling reaction between aryl-boronic acids differently substituted in *para* position (X = N(CH$_3$)$_2$, OCH$_3$, Br, NO$_2$) and 2-iodophenol in presence of a catalytic amount of Pd(II)acetate and of a base in a mixture of DMF and water as solvent.[39]
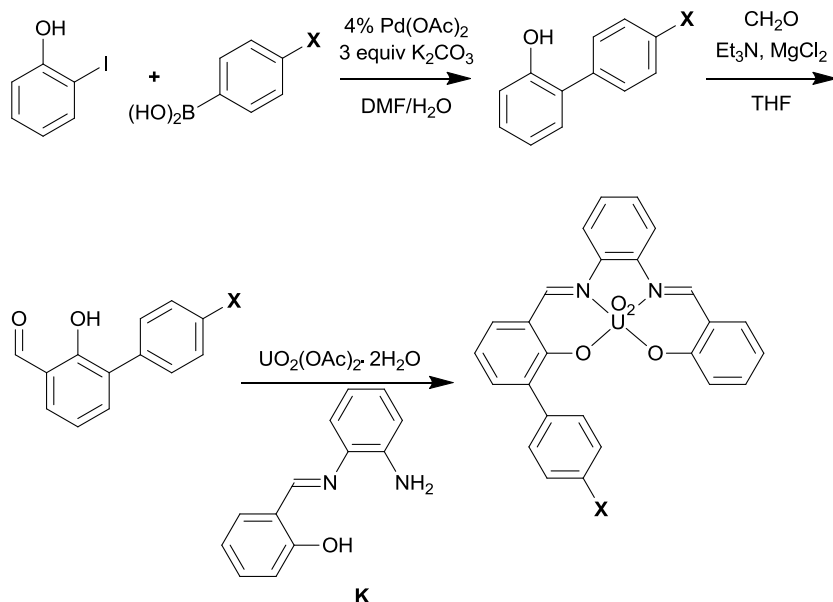
X= N(CH$_3$)$_2$, OCH$_3$, Br, NO$_2$

Scheme 1.7. General scheme for the synthesis of monosubstituted uranyl-salophens **1e-h** used in this study. For the yields of the single steps see Scheme 1.6 and 1.8.

Through this procedure, the use of phosphines is avoided and the reaction is conducted under mild conditions. From the resultant *ortho*-substituted phenol we obtained the corresponding *ortho*-salcylaldehyde by selective *ortho*-formylation.[40] The obtained salycilaldehyde derivatives were then reacted with the monoimine prepared from o-phenylenediamine and salycilaldehyde in the presence of uranyl acetate in methanol to obtain the receptors **1e-h** after chromatographic treatment of the raw material.

The synthetic route followed for every compound to obtain aldehydes **L**, **N**, **P** and **R** is reported in Scheme 1.8ₐ₋d.
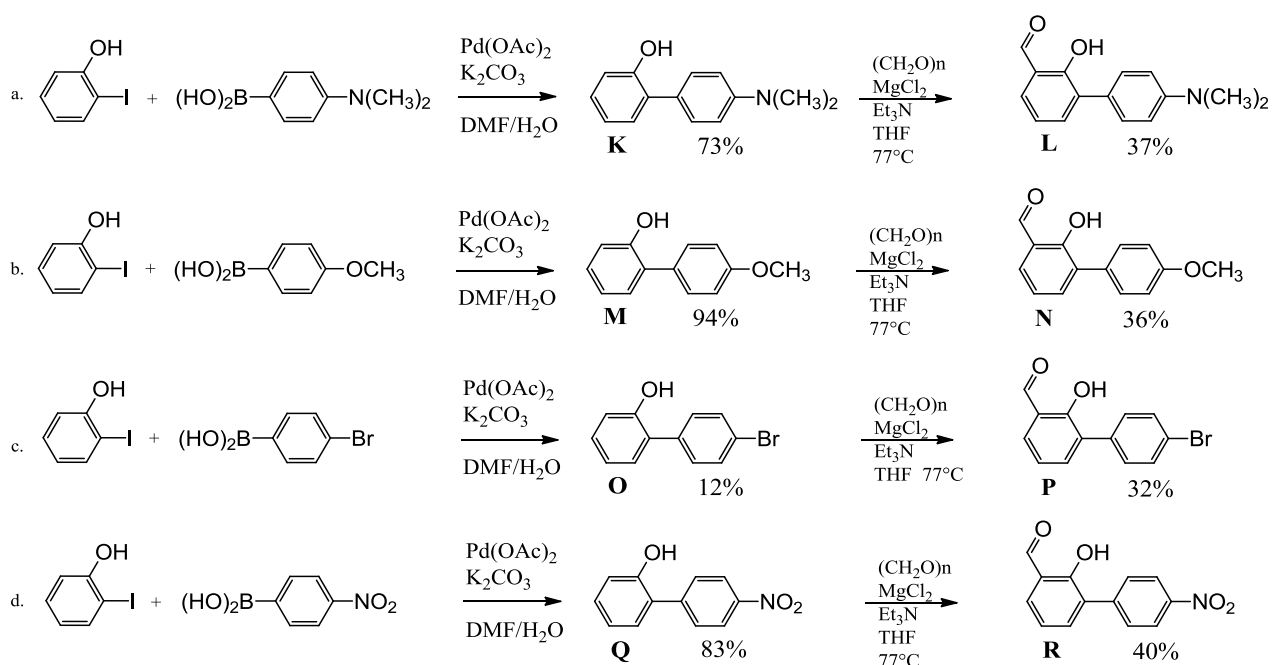
Scheme 1.8ₐ₋d. Scheme for the synthesis of phenols **K**, **M**, **O** and **Q** and aldehydes **L**, **N**, **P** and **R**.

The yield of the phenol **O** is definitely lower. Indeed, both the starting aryl-boronic acid $(R_1B(OH)_2, R_1 = Br$-Aryl) and the product **P** (Scheme 1.7c.) are, consecutively, aryl-halides. Therefore, quite a number of side Suzuki cross-coupling reactions occur that lead prevalently to the formation of the biphenyl and terphenyl derivatives as proved by GC-MS analysis. These

compounds together with the molecular ion peaks and their relative intensities are reported below:
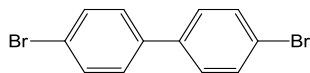
m/z: 310:312:314
relative intensity 1:2:1
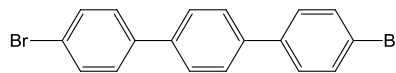
m/z: 386:388:390
relative intensity 1:2:1
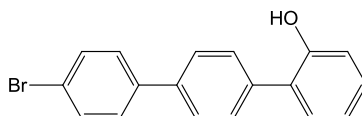
m/z: 324:326
relative intensity 1:1

This data justify, together with the isolation of a consistent amount of the unreacted 2-iodophenol, the lower yield of compound **O**.

Binding constant for 1:1 complexes of (TBA)Cl with uranyl-salophen receptors **1e-h** were obtained in CH_3CN at 25°C from UV-vis titrations. Binding constants K_a [M^{-1}] are listed in Table 1.10.

Table 1.10. Association constant values, K_a [M^{-1}], for the complexation of TBACl with receptors **1a** and **1e-h** obtained by UV-vis titrations in CH_3CN at 298 K. Free energy values $\Delta\Delta G$ [kcal mol^{-1}] calculated for the chloride-π interaction. $\Delta\Delta G = \Delta G_{Cl\text{-@1e-h}} - \Delta G_{Cl\text{-@1a}}$. (Concentration of the hosts of 10^{-5} M and successive addition of TBACl)

Receptor	K_a [M^{-1}]	$\Delta\Delta G$, [kcal mol^{-1}]
1a (H)	30700 (1200)	0
1e N(CH$_3$)$_2$	13600 (200)	0.5
1f (OCH$_3$)	21000 (700)	0.2
1g (Br)	46600 (3200)	-0.2
1h (NO$_2$)	79200 (9900)	-0.6

We can notice that the association constant values for Cl⁻@**1** complexes increase with the electron-withdrawing character of the X substituent. The evidence the halide hosted in the fifth equatorial site of the uranyl center establishes intramolecular contact with the π-cloud perturbed by the X-substituent is straightforward.

A good linear correlation with Hammett's **σp** [41] ($R^2 = 0.98$, $\rho = 0.49$) is reported in Figure 1.21: it shows how resonance effects act on the interaction of Cl⁻ with receptors **1** and that in general, chloride-π contact is dominated by electrostatic effects and all depend on the interaction involving the anion and the electrostatic potential of the aromatic ring (see chapter 1.2.3).

To provide a direct measurement of the relative interaction energy of chloride, we calculated the chloride-π free energy values $\Delta\Delta G$ between different aromatic π systems and with respect to the control receptor **1a** ($\Delta\Delta G = \Delta G_{Cl\text{-}@\mathbf{1e\text{-}h}} - \Delta G_{Cl\text{-}@\mathbf{1a}}$). The maximum contribution of the chloride-π interactions to the overall free energy of binding in the receptor series **1e-h** can be estimated as 1.0 kcal mol⁻¹ ($\Delta\Delta G = \Delta G_{Cl\text{-}@\mathbf{1e}} - \Delta G_{Cl\text{-}@\mathbf{1h}}$) between **1e** and **1h**. To better quantify the free energy values for chloride-π interaction in solution we used the model system **1a** and the $\Delta\Delta G$ values are reported in Table 1.10. The electron-withdrawing nitro and bromo substituents are stability enhancing with respect of the control receptor **1a** and the nitro compound **1h** is the best receptor in the lot. Indeed, we estimated attractive free energies of -0.6 kcal mol⁻¹ for **1h** and -0.2 kcal mol⁻¹ for **1g**. On the other hand, the electron-donating methoxy and dimethylamino groups are stability decreasing and the dimethylamino compound is the worst receptor. We noticed that $\Delta\Delta G$ of the worst and the best receptor **1e** and **1h** (0.5 and -0.6 kcal mol⁻¹ respectively) and $\Delta\Delta G$ of **1f** and **1g** (0.2 and -0.2 kcal mol⁻¹ respectively) are diametrically opposed, symmetrically with respect of **1a** that is the midpoint in the plot.
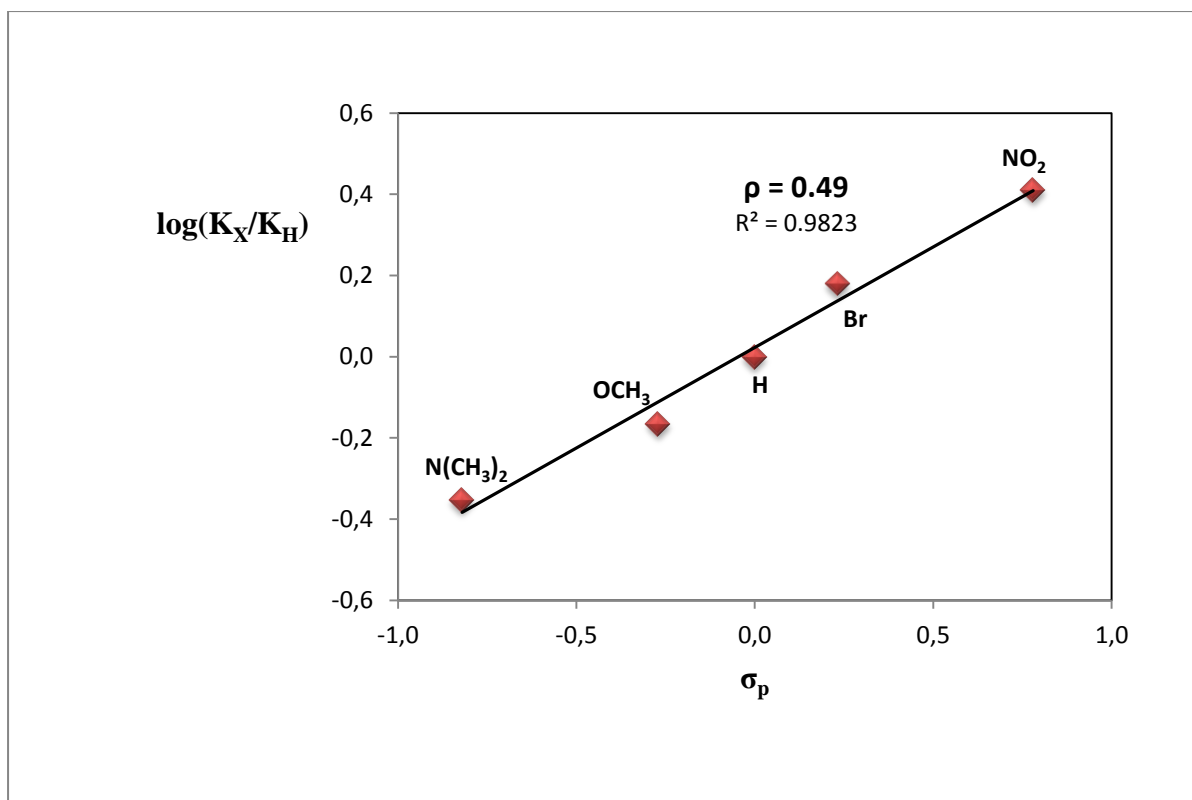
Figure 1.21. Experimental chloride-π interaction binding constant values plotted against σ_P ($R^2 = 0.98$, $\rho = 0.49$).

This measure reflects the behavior of the substituents that are all electron-withdrawing via induction (-I) and, except for the nitro group (a powerful, in any case, electron-withdrawing group), gradually electron-releasing through resonance effects.

In conclusion, we have shown that these systems can be used to quantify chloride-π interaction in solution similarly to what done by Ballester and co-workers [42] with the series of meso-tetraaryl calix[4]pyrrole where the main driving force for complexation is hydrogen bonding.

1.4 Experimental section

TBAX (X = F, Cl, Br and I) reagents were purchased from Sigma-Aldrich. All the solvents used for reactions, titrations and crystallizations were reagent grade and used as received. NMR Spectra, UV-vis titrations were performed using $CHCl_3$ and $CDCl_3$ by eluting through an aluminum oxide activated basic (56 Å) column. Flash column chromatography was performed with Silica gel 40 – 63 μm. NMR spectra were recorded on a Bruker AC300P spectrometer. GC–MS analyses were performed on a HP5890 GC (OV 1 capillary column, 12 m × 0.2 mm) coupled with a HP5970 MSD. HRMS Spectra were recorded by a MICROMASS Q-Tof micromass spectrometer or a LABSCIEX API4000 Q-TRAP spectrometer in enhanced resolution mode. UV–vis measurements were performed on a Perkin Elmer Lambda 18 spectrophotometer. Association constants obtained by UV-vis titrations were calculated using ReactLabTM EQUILIBRIA. The association constants (K_a) for the binding processes were determined by averaging the values from at least two titrations using a simple 1:1 binding model. Single crystal X-ray data are reported in literature [43].

Salophen-UO_2 complex **1a** and **2a** [22] and mono-imine **K**[22] were available from previous investigations. 1-(benzyloxy)-2-iodobenzene (**A**) [44], 2',3',4',5',6'-pentafluoro-[1,1'-biphenyl]-2-ol (**I**), [45] 2',3',4',5',6'-pentafluoro-2-hydroxy-[1,1'-biphenyl]-3-carbaldehyde [45] (**J**) were prepared according to previously reported procedures.

2-(benzyloxy)-3',5'-dimethoxy-1,1'-biphenyl (**B**). (89% yield) To a solution of 1-(benzyloxy)-2-iodobenzene, **A**, (1.49 g, 4.81 mmol) dissolved in 48 mL of dried dimethylformamide, was added 3,5-dimethoxyphenylboronic acid (0.86 g, 4.75 mmol), tris(dibenzylideneacetone)dipalladium (0.22 g, 0.240 mmol), cesium fluoride (1.43 g, 9.43 mmol), silver oxide (1.32 g, 5.71 mmol), tri-tert-butylphosphine (0.13 mL, 0.56 mmol). The solution was stirred overnight at 100 °C under Ar atmosphere. The mixture was diluted with ethyl acetate and washed with water to remove DMF and metal impurities; washed with brine, dried over $NaSO_4$ and concentrated to obtain a clear oil. The residue was purified by silica column chromatography, using hexane/dichloromethane (8/2) as eluent, to yield **B** as clear oil(1.36 g). ^{1}H NMR δH (300 MHz, $CDCl_3$), 7.37-7.28 (7 H, m, CH), 7.05-7.02 (2 H, m, CH), 6.76 (2 H, d, J = 2.1 Hz, CH), 6.46 (1 H, t, J = 2.1 Hz, CH), 5.09 (2 H, s, CH_2), 3.77 (6 H, s, OCH_3). ^{13}C NMR δc (75 MHz, $CDCl_3$), 160.2, 155.6, 140.4, 137.1, 130.9, 130.83, 130.82,

130.78, 130.1, 121.3, 113.4, 107.7, 99.6, 70.5, 55.3. TOF MS ES+ m/z: calc for $C_{21}H_{20}O_3Na$ 343.1310 found 343.1319.

3',5'-dimethoxy-[1,1'-biphenyl]-2-ol (C). (70% yield) 9 mL of ethanol were degassed by bubbling Ar for 30 min. A large excess of gaseous hydrogen was bubbled into the solution containing Pd/C 10% (0.05 g) and **B** (0.51 g, 1.57 mmol).The solution was stirred overnight at 70°C under hydrogen atmosphere. The warm reaction mixture was filtered through Celite, and the solution was evaporated under reduced pressure to obtain **C** as a clear oil[46] (0.25 g, 70%). ^{1}H NMR δH (300 MHz, CDCl₃), 7.26-7.24 (2 H, m, CH), 7.00-6.98 (2 H, m, CH), 6.59 (2 H, d, J = 2,1 Hz, CH), 6.50 (1 H, t, J = 2,1 Hz, CH), 5.42 (1 H , br s, OH), 3.82 (6 H, s, CH₃). ^{13}C NMR δc (75 MHz in CDCl₃), 161.5, 152.3, 139.0, 129.7, 129.2, 128.0, 120.6, 115.6, 106.8, 99.9, 55.4. TOF MS ES+ m/z: calc for $C_{14}H_{14}O_3Na$ 253.0841 found 253.0838.

2-hydroxy-3',5'-dimethoxy-[1,1'-biphenyl]-3-carbaldehyde (D). (72 % yield) Compound **C** (0.25 g, 1.10 mmol), triethylamine (0.92 mL, 6.61 mmol) and magnesium chloride $MgCl_2$ (0.63 g, 6.62 mmol) were added to 25 mL of freshly distilled dry THF. After 20 min solid paraformaldehyde (0.49 g, 16.5 mmol) was added. The reaction was stirred overnight at 77°C under Ar atmosphere. The reaction mixture was diluted with ethyl acetate and washed with HCl 1M solution, water, and with brine, dried over $NaSO_4$. The crude product was purified by silica column chromatography, using hexane/dichloromethane (6/4) as eluent to yield **D** as a clear oil (0.20 g, 72 %). ^{1}H NMR δH (300 MHz, CDCl₃), 11.52 (1 H, s, OH), 9.96 (1 H, s, CHO), 7.64 (1 H, dd, J₁=7,5 Hz, J₂=1,5 Hz, CH), 7.57 (1 H, dd, J₁=7,5 Hz, J₂=1,5 Hz, CH), 7.10 (1 H, t, J = 7,5 Hz, CH), 6.73 (2 H, d; J = 2,4 Hz, CH), 6.5 (1 H, t, J = 2,1 Hz, CH), 3.83 (6 H, s, OCH₃). ^{13}C NMR δc (75 MHz, CDCl₃), 196.8, 160.5, 158.8, 138.2, 137.6, 133.3, 130.3, 120.8, 119.8, 107.5, 99.8, 55.4. TOF MS ES+ m/z: calc for $C_{15}H_{15}O_4$ 258.0981 found 258.0970.

Uranyl-salophen complex 1b. (20% yield) Monoimine **K** (0.074 g, 0.348 mmol) was added to a solution of **D** (0.090 g, 0.348 mmol) in methanol, 2 mL. After 10 min, uranyl acetate dihydrate $UO_2(OAc)_2 \cdot 2H_2O$ (0.177 g, 0.418 mmol) was added at room temperature and the solution was stirred overnight. The crude was purified over silica column chromatography using cyclohexane/ethyl acetate (7/3) as eluent, to yield **1b** (0.05 g, yield 20%). ^{1}H NMR δH (300 MHz, acetone-d6), 9.72 (1 H, s, CHNR), 9.64 (1 H, s, CHNR), 7.82-7.73 (5 H, m, CH), 7.60-7.56 (3 H, m, CH), 7.07 (2 H, d, J=2.1 Hz, CH), 6.92 (1 H, d, J = 8.4 Hz, CH), 6.83 (1 H, t, J = 7.8 Hz, CH), 6.71 (1 H, t, J = 7.8 Hz, CH), 6.56 (1 H, t, J=2.1 Hz, CH), 3.78 (6 H, s, OCH₃). ^{13}C NMR δc (75 MHz, acetone-d6), 170.5, 166.9, 166.3, 160.5, 147.1, 141.7, 136.5,

136.0, 135.8, 135.7, 132.3, 128.9, 128.8, 125.2, 124.3, 120.0, 117.1, 116.9, 107.8, 98.7, 54.7. TOF MS ES+ m/z: calc for $C_{28}H_{23}N_2O_6U$ 721.2058 found 721.2060.

3',5'-difluoro-2-methoxy-1,1'-biphenyl (E). (47% yield) This compound was prepared following the same procedure previously described for **B**. 1-bromo-2-methoxybenzene (1 mL, 8.04 mmol), (3,5-difluorophenyl)boronic acid (1.27 g, 8.04 mmol), tris(dibenzylideneacetone)dipalladium (0.37 g, 0.40 mmol), cesium fluoride (2.44 g, 16.08 mmol), silver oxide (2.23 g, 9.65 mmol) and tri-tert-butylphosphine (0.23 mL, 0.96 mmol) were put in 50 mL of dried dimethylformamide DMF. The residue was purified by column chromatography on silica gel, using hexane:CH_2Cl_2 95:5 as eluent, to yield **E** as a grey oil (0.83 g). ^1H NMR (300 MHz in $CDCl_3$, 25°C), δ (ppm) 3.84 (s, 3H, OCH_3); 6.77 (tt, 1H, CH, J_1 = 9.0 Hz, J_2 = 2.4 Hz); 7.09-6.98 (m, 4H, CH,); 7.37-7.26 (m, 2H, CH). ^{13}C NMR (75 MHz in $CDCl_3$, 25°C), δ (ppm) 55.5, 102.2 (t, J_{CF} = 25.0 Hz), 111.3, 112.4 (d, J_{CF} = 8.0 Hz), 120.9, 128.3 (t, J_{CF} = 2.5 Hz), 129.7, 130.5, 141.7 (t, J_{CF} = 10.0), 156.2, 162.6 (dd, J_{1CF} = 244.1, J_{2CF} =13.1 Hz).

3',5'-difluoro-[1,1'-biphenyl]-2-ol (F). (57% yield) Compound **F** was prepared following a literature procedure[45].To a solution of **E** (0.83 g, 3.75 mmol) in 15 mL CH_2Cl_2 was added dropwise a solution of BBr_3 (10 mL, 10 mmol, in CH_2Cl_2) at -80°C. The resultant solution was allowed to stir 3h at room temperature. Afterwards, the resultant brown solution was poured into ice water, extracted with CH_2Cl_2, washed with brine, dried over Na_2SO_4 and concentrated to obtain a grey oil (0.44 g). ^1H NMR (300 MHz in $CDCl_3$, 25°C), δ (ppm) 5.08 (s, 1H, OH); 6.83 (tt, 1H, CH, J_1 = 8.7 Hz, J_2 = 2.1 Hz); 7.09-6.94 (m, 4H, CH); 7.31-7.23 (m, 2H, CH). ^{13}C NMR (75 MHz in $CDCl_3$, 25°C), δ (ppm) 102.9 (t, J_{CF} = 25.1 Hz), 112.1 (d, J_{CF} = 25 Hz), 116.3, 121.2, 126.1 (t, J_{CF} = 2.3 Hz), 129.9, 130.2, 140.7 (t, J_{CF} = 9.7 Hz), 152.2, 163.2 (dd, J_{CF} = 247.4, J_{CF} =13.0 Hz). TOF MS ES- m/z: calc for $C_{12}H_7OF_2$ 205.0465 found 205.0473.

3',5'-difluoro-2-hydroxy-[1,1'-biphenyl]-3-carbaldehyde (G). (48% yield) Compound **F** (0.44 g, 2.13 mmol), freshly distilled triethylamine (0.59 mL, 4.27 mmol) and magnesium chloride $MgCl_2$ (0.41 g, 4.30 mmol) were added to 10 mL of freshly distilled dry THF. After 20 min solid paraformaldehyde (0.32 g, 10.70 mmol) was added. The reaction was stirred overnight at 77°C under Ar atmosphere. The bright yellow reaction mixture was diluted with ethyl acetate and washed with HCl 1M solution, water, and with brine; dried over Na_2SO_4. The crude product was purified by silica column chromatography, using hexane:dichloromethane (6:4) as eluent to yield **G** (0.24 g). ^1H NMR (300 MHz in $CDCl_3$, 25°C), δ (ppm) 6.82 (tt, 1H,

CH, J_1 = 8.7 Hz, J_2 = 2.1 Hz); 7.18-7.11 (m, 3H, CH); 7.63-7.60 (m, 2H, CH); 9.97 (s, 1H, CHO); 11.63 (s, 1H, OH). ^{13}C NMR (75 MHz in CDCl$_3$, 25°C), δ (ppm) 102.8 (t, J_{CF} = 25.1 Hz), 112.2 (d, J_{CF} = 25.5 Hz), 120.0, 121.0, 126.1 (t, J_{CF} = 2.3 Hz), 134.1, 137.4, 140.7 (t, J_{CF} = 9.7 Hz), 158.7, 163.2 (dd, J_{CF} = 245.0, J_{2CF} =13.0 Hz), 196.8. TOF MS ES+ m/z: calc for $C_{13}H_8F_2NaO_2$ 257.0385 found 257.0390.

Uranyl-salophen 1c. (48% yield) Salicylaldehyde **G** (0.21 mmol, 1 equiv), monoimine **K** (0.21 mmol, 1 equiv.) and UO$_2$(OAc)$_2$·2H$_2$O (0.25 mmol, 1.2 equiv.) were solubilized in methanol (2.5 mL). The red solid obtained at the end of the reaction was purified by silica column chromatography using dichloromethane:acetone (9:1) as eluent, to yield **1c** (0.07 g). ^{1}H NMR (300 MHz in CDCl$_3$, 25°C), δ (ppm) 6.70 (t, 1H, CH, J = 7.2 Hz), 6.95-6.75 (m, 2H, CH), 7.06 (tt, 1H, CH, J_1 = 9 Hz, J_2 = 2.1 Hz), 7.61-7.59 (m, 5H, CH), 7.91-7.81 (m, 5H, CH), 9.66 (s, 1H, CHNR), 9.73 (s, 1H, CHNR). ^{13}C NMR (75 MHz in CDCl3, 25°C), δ (ppm) 102.5 (t, J_{CF} = 25.7 Hz), 112.6 (d, J_{CF} = 7.8 Hz), 117.1, 117.2, 120.0,120.1, 121.0, 124.4, 125.5, 128.9, 129.0, 129.8, 135.7, 136.0, 136.4, 137.0, 143.1 (t, J_{CF} = 9.9 Hz), 146.9, 147.1, 162.1 (dd, J_{CF} = 245.0, J_{2CF} =13.0 Hz), 166.4, 166.8, 167.5. TOF MS ES+ m/z: calc for $C_{26}H_{16}F_2N_2O_4U$ 696.1586 found 696.1616.

Uranyl-salophen 2c. (97% yield) Salicylaldehyde **G** (0.42 mmol, 2 equiv.), o-phenylenediamine (0.21 mmol, 1 equiv.) and UO$_2$(OAc)$_2$·2H$_2$O (0.25 mmol, 1.2 equiv.) were solubilized in methanol (2.5 mL) at room temperature and the solution was stirred overnight. The red solid obtained at the end of the reaction was filtered off, washed with methanol and left sever hours under high vacuum (0.164 g). ^{1}H NMR (300 MHz in acetone-d6, 25°C) δ (ppm) 6.90 (t, 2H, CH, J = 7.8 Hz), 7.06 (t, 2H, CH, J = 9.3 Hz), 7.64-7.54 (m, 6H, CH), 7.80 (dd, 2H, CH, J_1 = 7.5 Hz, J_2 = 1.8 Hz), 7.90-7.94 (m, 6H, CH), 9.77 (s, 2H, CHNR). ^{13}C NMR (75 MHz in CDCl$_3$, 25°C), δ (ppm) 102.1 (t, J_{CF} = 25.4 Hz), 112.6 (d, J_{CF} = 16.9 Hz), 112.8, 118.1, 119.7, 124.8, 129.2, 130.5, 136.2, 136.6, 146.5, 162.7 (dd, J_{CF} = 245.7, J_{2CF} =13.5 Hz), 165.8, 166.82. TOF MS ES+ m/z: calc for $C_{32}H_{18}F_4N_2NaO_4U$ 831.1603 found 831.1581.

2,3,4,5,6-pentafluoro-2'-methoxy-1,1'-biphenyl (H). (37% yield) This compound was prepared following the same procedure previously described for **B**. 1-bromo-2-methoxybenzene (0.3 mL, 2.36 mmol), perfluorophenyl)boronic acid (0.5 g, 2.36 mmol), tris(dibenzylideneacetone)dipalladium (0.11 g, 0.118 mmol), cesium fluoride (0.70 g, 4.48 mmol), silver oxide (0.60 g, 2.70 mmol) and tri-tert-butylphosphine (0.07 mL, 0.269 mmol) were put in 20 mL of dried dimethylformamide DMF. The residue was purified by column

chromatography on silica gel, using hexane as eluent, to yield **H** as clear a oil (0.24 g, yield 37%). ^{1}H NMR δH (300 MHz, CDCl$_3$), 7.45-7.42 (1 H, m, CH), 7.24-7.21 (1 H, m, CH), 7.08-7.01 (2 H, m, CH), 3.81 (3 H, s, OCH$_3$). ^{13}C NMR δc (75 MHz, CDCl$_3$), 157.0, 146.4, 139.3, 136.3, 131.6, 131.0, 120.5, 115.4, 113.0, 111.2, 55.6.

Uranyl-salophen complex 1d. (yield 52%) This compound was prepared applying a procedure similar to that already described for **1b**. Compound **J** (0.29 g, 0.694 mmol), monoimine **K** (0.15 g, 0.694 mmol) and UO$_2$(OAc)$_2$·2H$_2$O (0.353 g, 0.833 mmol) were solubilized in methanol (10 mL). The red solid obtained at the end of the reaction was purified by silica column chromatography using dichloromethane /acetone (9/1) as eluent, to yield **1d** (0.27 g, 52% yield). ^{1}H NMR δH (300 MHz, DMSO-d6), 9.68 (1 H, s, CHNR), 9.61 (1 H, s, CHNR), 7.95 (1 H, dd, J$_1$ = 7.8 Hz, J$_2$ = 1.8 Hz, CH), 7.83-7.73 (3 H, m, CH), 7.65-7.51 (4 H, m, CH), 6.99 (1 H, d, J = 8.1 Hz, CH), 6.83 (1 H, t, J = 7.8 Hz, CH), 6.71 (1 H, t, J = 8.1 Hz, CH). ^{13}C NMR δc (75 MHz, acetone-d6), 170.3, 166.5, 147.02, 147.00, 137.9, 137.6, 136.0, 135.7, 129.1, 128.8, 125.0, 124.4, 120.9, 120.1, 120.0, 117.1, 116.5. ^{19}F NMR δf (282 MHz, CDCl$_3$; KF in CDCl$_3$), -135.0 (1 F, dd, J$_1$ = 22.6 Hz, J$_2$ = 5.6 Hz, CF), -146.3 (1 F, dd, J$_1$ = 25.4 Hz, J$_2$ = 8.5 Hz, CF), -158.8 (1 F, t, J = 22.6 Hz, CF), -163.7 (1 F, td, J$_1$ = 22.6 Hz, J$_2$ = 8.5 Hz, CF), -167.9 (1 F, td, J$_1$ = 22.6 Hz, J$_2$ = 8.6 Hz, CF). TOF MS ES+ m/z: calc for C$_{26}$H$_{13}$N$_2$O$_4$F$_5$NaU 773.1201 found 773.1164.

General synthesis of uranyl-salophen complexes 2d and 2b. The proper salicylaldehyde (0.62 mmol, 2 equiv.), o-phenylenediamine (0.31 mmol, 1 equiv.) and UO$_2$(OAc)$_2$·2H$_2$O (0.37 mmol, 1.2 equiv.) were solubilized in methanol (2.5 mL) at room temperature and the solution was stirred overnight. The red solid obtained at the end of the reaction was filtered off, washed with methanol and left sever hours under hight vacuum.

Uranyl-salophen 2d. (90% yield) ^{1}H NMR (300 MHz, acetone-d6, 25°C), δ (ppm) 6.89 (t, 2H, CH, J = 9.0 Hz), 7.63-7.60 (m, 2H, CH), 7.71 (d, 2H, CH, J = 6.0 Hz), 7.93-7.90 (m, 2H, CH), 8.01 (dd, 2H, J$_1$ = 6, J$_2$ =1.8 Hz), 9.76 (s, 2H, CHNR). ^{13}C NMR (100 MHz, acetone-d6, 25°C), δ (ppm) 111.7, 116.0, 116.1, 118.6, 119.7, 122.0, 130.9, 138.2, 138.3, 139.5, 139.6, 140.2, 140.3, 140.9, 142.9, 145.7, 147.7, 148.6, 168.4, 169.3. TOF MS ES+ m/z: calc for C$_{32}$H$_{12}$F$_{10}$N$_2$O$_4$U 916.1145 found 916.1188.

Uranyl-salophen 2b. (55% yield) ^{1}H NMR (300 MHz, acetone-d6, 25°C), δ (ppm) 3.83 (s, 12H, OCH$_3$), 6.52 (t, 2H, CH, J = 2.4 Hz), 6.81 (t, 2H, CH, J = 7.5 Hz), 7.01 (d, 4H, CH, J = 2.4 Hz), 7.62-7.58 (m, 2H, CH), 7.72 (dd, 2H, J$_1$ = 7.5, J$_2$ =1.8 Hz), 7.91-7.81 (m, 4H, CH),

9.72 (s, 2H, CHNR). ^{13}C NMR (100 MHz, acetone-d6, 25°C), δ (ppm) 55.5, 99.1, 108.3, 117.9, 119.7, 124.5, 129.4, 132.6, 135.3, 136.1, 141.4, 146.6, 160.4, 165.7, 167.3. TOF MS ES+ m/z: calc for $C_{36}H_{30}N_2O_4U$ 856.2510 found 856.2510.

4'-(dimethylamino)-[1,1'-biphenyl]-2-ol (K). (73% yield) 4-(dimethylamino)phenyl)boronic acid (300 mg, 1.8 mmol), 2-iodophenol (360 mg, 1.6 mmol), potassium carbonate (678 mg, 4.9 mmol), palladium diacetate (14.7 mg, 0.065 mmol) were put in a mixture of 5 mL of DMF and 5 mL of water. The solution was stirred overnight at room temperature. The mixture was diluted with ethyl acetate and washed with water to remove DMF and metal impurities; washed with brine, dried over Na_2SO_4 and concentrated. The residue was purified by column chromatography on silica gel, using petroleum ether:$CHCl_3$ 8:2 as eluent, to yield **K** (73%). ^{1}H-NMR (300 MHz in $CDCl_3$), δ (ppm): 7.39-7.36 (m, 2H, ArH), 7.26-7.21 (m, 2H, ArH), 7.01-6.99 (m, 2H, ArH), 6.87 (m, 2H, ArH), 5.46 (b, 1H, OH), 3.03 (s, 6H, N(CH$_3$)$_2$). ^{13}C-NMR (300 MHz in $CDCl_3$), δ (ppm): 152.7, 150.1, 130.2, 129.8, 128.4, 128.3, 124.4, 120.7, 115.5, 113.1, 40.5. MS (m/z): [M + H+] 214.1

4'-(dimethylamino)-2-hydroxy-[1,1'-biphenyl]-3-carbaldehyde (L). (37% yield) Compound **K** (200 mg, 0.94 mmol), freshly distilled triethylamine (0.5 mL, 4.3 mmol) and magnesium chloride $MgCl_2$ (365 mg, 3.7 mmol) were added to 5 mL of freshly distilled dry THF. After 20 min solid paraformaldehyde (564 mg, 18.7 mmol) was added. The reaction was stirred overnight at 77°C under Ar atmosphere. The bright yellow reaction mixture was diluted with ethyl acetate and washed with water (pH = 7-8), and with brine; dried over Na_2SO_4. The crude product was purified by silica column chromatography, using petroleum ether:$CHCl_3$ (7:3) as eluent to yield **L** (37%). ^{1}H-NMR (300 MHz in $CDCl_3$), δ (ppm): 11.51 (s, 1H, OH), 9.94 (s, 1H, CHO), 7.60 (dd, 1H, ArH, Jorto=7.5, Jmeta=1.5), 7.52-7.47 (m, 3H, ArH), 7.07 (t, 1H, ArH, J=7.5), 6.80 (m, 2H, ArH), 3.00 (s, 6H, N(CH$_3$)$_2$). ^{13}C-NMR (300 MHz in $CDCl_3$), δ (ppm): 196.8, 159.1, 150.0, 137.1, 129.9, 124.4, 121.1, 119.8, 112.1, 40.4. MS (m/z): [M + H+] 242.1

Uranyl-salophen 1e. (28% yield) Salicylaldehyde **L** (0.3 mmol, 1 equiv), monoimine **K** (0.3 mmol, 1 equiv.) and $UO_2(OAc)_2 \cdot 2H_2O$ (0.396 mmol, 1.2 equiv.) were solubilized in methanol (2.5 mL). The red solid obtained at the end of the reaction was purified by silica column chromatography using dichloromethane as eluent, to yield **1e** (28%). ^{1}H-NMR (300 MHz in DMSO-d6), δ (ppm): 9.68 (s, 1H, CH=N), 9.60 (s, 1H, CH=N), 7.91-6.89 (m, 2H, ArH), 7.80-7.67 (m, 8H, ArH), 7.00-6.68 (m, 3H, ArH), 6.76-6.68 (m, 2H, ArH), 3.01 (s, 6H, N(CH$_3$)$_2$).

^{13}C-NMR (300 MHz in Acetone-d6), δ (ppm): 170.6, 167.8, 167.0, 166.3, 149.7, 147.2, 147.0, 136.0, 135.9, 135.8, 134.6, 132.7, 130.4, 128.82, 128.80, 127.7, 125.0, 124.4, 120.9, 120.0, 119.9, 117.3, 116.9, 112.1, 39.9. MS (m/z): [M + H+] 704.2.

4'-methoxy-[1,1'-biphenyl]-2-ol (M). (94% yield) (4-methoxyphenyl)boronic acid (500 mg, 3.3 mmol), 2-iodophenol (658 mg, 3.0 mmol), potassium carbonate (1.24 g, 9.0 mmol), palladium diacetate (29 mg, 0.1 mmol) were put in a mixture of 9 mL of DMF and 9 mL of water. This compound was prepared following the same procedure previously described for **K.** The residue was purified by column chromatography on silica gel, using petroleum hexane:CH$_2$Cl$_2$ 8:2 as eluent, to yield **M** (94%). 1H-NMR (300 MHz in CDCl$_3$), δ (ppm): 7.41-7.39 (m, 2H, ArH), 7.24-7.21 (m, 2H, ArH), 7.00-6.96 (m, 4H, ArH), 5.22 (s, 1H, OH), 3.87 (s, 3H, OCH$_3$). ^{13}C-NMR (300 MHz in CDCl$_3$), δ: 159.3, 152.5, 130.3, 130.2, 129.2, 128.8, 127.8, 120.8, 115.6, 114.7, 55.4. MS (m/z): [M+H+] 201.1

2-hydroxy-4'-methoxy-[1,1'-biphenyl]-3-carbaldehyde (N). (36% yield) Compound **M** (490 mg, 2.5 mmol), freshly distilled triethylamine (1.4 mL, 10 mmol) and magnesium chloride MgCl$_2$ (931 mg, 9.8 mmol) were added to 12 mL of freshly distilled dry THF. After 20 min solid paraformaldehyde (1.48 g, 49.0 mmol) was added. The reaction was stirred overnight at 77°C under Ar atmosphere. The bright yellow reaction mixture was diluted with ethyl acetate and washed with HCl 1M solution, water, and with brine; dried over Na$_2$SO$_4$. The crude product was purified by silica column chromatography, using hexane:CH$_2$Cl$_2$ (7:3) as eluent to yield **N** (36%). ^{1}H-NMR (300 MHz in CDCl$_3$), δ (ppm): 11.53 (s, 1H, OH), 9.95 (s, 1H, CHO), 7.61-7.52 (m, 4H, ArH) 7,09 (t, 1H, J = 7.5 Hz, ArH), 7.11-6.97 (m, 2H, ArH), 3.86 (s, 3H, OCH$_3$). ^{13}C-NMR (300 MHz in CDCl$_3$), δ (ppm): 196.9, 159.2, 158.9, 137.5, 132.7, 130.4, 130.1, 128.6, 120.8, 119.9, 113.8, 55.3. MS (m/z): [M - H+] 227.2

Uranyl-salophen 1f. (17% yield) Salicylaldehyde **N** (0.5 mmol, 1 equiv), monoimine **K** (0.5 mmol, 1 equiv.) and UO$_2$(OAc)$_2$·2H$_2$O (0.6 mmol, 1.2 equiv.) were solubilized in methanol (2.5 mL). The red solid obtained at the end of the reaction was purified by silica column chromatography using dichloromethane as eluent, to yield **1f** (17%). ^{1}H-NMR (300 MHz in Acetone-d6), δ (ppm): 9.68 (s, 1H, CH=N), 9.61 (s, 1H, CH=N), 7.85-7.68 (m, 6H, ArH), 7.66 (d, 1H, ArH, J=7.5 Hz), 7.58-7.55 (m, 3H, ArH), 7.09-6.98 (m, 2H, ArH), 6.91 (d, 1H, ArH, J=7.5 Hz), 6.81(t, 1H, ArH, J= 7.5 Hz), 6.70 (t, 1H, ArH, J=7.5 Hz), 3.91 (s, 3H, OCH$_3$).^{13}C-NMR (300 MHz in DMSO-d6), δ (ppm): 170.1, 167.5, 167.0, 158.6, 147.2, 147.1, 136.4, 136.3,

136.2, 135.6, 131.6, 131.3, 129.1,125.3, 125.2, 124.6, 121.0, 120.7, 120.6, 117.4, 117.1, 113.8, 55.5. ESI-MS (m/z): [M + Na+] calculated for $C_{27}H_{20}N_2NaO_5U$ 717.1778, found 713.1763.

4'-bromo-[1,1'-biphenyl]-2-ol (O). (12% yield) (4-bromophenyl)boronic acid (720 mg, 3.6 mmol), 2-iodophenol (704 mg, 3.2 mmol), potassium carbonate (1.35 g, 10 mmol), palladium diacetate (29.4 mg, 0.13 mmol) were put in a mixture of 10 mL of DMF and 10 mL of water. This compound was prepared following the same procedure previously described for **K**. The residue was purified by column chromatography on silica gel, using petroleum ether:CHCl3 8:2 as eluent, to yield **O** (12%). ^{1}H-NMR (300 MHz in CDCl3), δ (ppm): 7.62-7.29 (m, 4H, ArH), 7.26-7.21 (m, 2H, ArH), 7.02-6.94 (m, 2H, ArH), 5.03 (b, 1H, OH). ^{13}C-NMR (300 MHz in CDCl3), δ (ppm): 152.3, 151.2, 136.2, 132.1, 130.8, 130.2, 129.4, 127.0, 121.9, 121.0, 116.0. MS (m/z): [M - H+] 247.0.

4'-bromo-2-hydroxy-[1,1'-biphenyl]-3-carbaldehyde (P). (32% yield) Compound **O** (90 mg, 0.3 mmol), freshly distilled triethylamine (0.17 mL, 1.2 mmol) and magnesium chloride MgCl2 (952 mg, 10 mmol) were added to 5 mL of freshly distilled dry THF. After 20 min solid paraformaldehyde (180 mg, 6.0 mmol) was added. This compound was prepared following the same procedure previously described for **N**. The crude product was purified by silica column chromatography, using hexane:CH2Cl2 (7:3) as eluent to yield **P** (32%). ^{1}H-NMR (300 MHz in CDCl3), δ (ppm): 11.55 (s, 1H, OH), 9.93 (s, 1H, CHO), 7.58-7.54 (m, 4H, ArH) 7,47 (d, 2H, ArH, J = 7.5 Hz), 7.09 (t, 1H, ArH, J = 7.5 Hz). ^{13}C-NMR (300 MHz in CDCl3), δ (ppm): 196.7, 137.4, 135.1, 137.5, 133.5, 131.8, 129.1, 121.8, 120.8, 119.9. MS (m/z): [M - H+] 275.0

Uranyl-salophen 1g. (30% yield) Salicylaldehyde **P** (0.01 mmol, 1 equiv), monoimine **K** (0.01 mmol, 1 equiv.) and UO2(OAc)2·2H2O (0.012 mmol, 1.2 equiv.) were solubilized in methanol (1 mL). The red solid obtained at the end of the reaction was purified by silica column chromatography using dichloromethane as eluent, to yield **1g** (30%). ^{1}H-NMR (300 MHz in DMSO-d6), δ (ppm): 9.68 (s, 1H, CH=N), 9.61 (s, 1H, CH=N), 7.96 (d, 2H, ArH), 7.80-7.72 (m, 7H, ArH), 7.61-7.51 (m, 2H, ArH), 6.98 (d, 1H, ArH, J= 7.5 Hz), 6.80 (t, 1H, ArH, J=7.5 Hz), 6.70 (t, 1H, ArH, J=7.5 Hz). ^{13}C-NMR (300 MHz in DMSO-d6), δ (ppm): 169.9, 167.4, 167.1, 147.0, 138.5, 136.5, 136.4, 136.3, 132.3, 131.2, 130.5, 129.2, 125.3, 124.6, 120.9, 120.7, 120.2, 117.4, 117.2. ESI-MS (m/z): [M+Na$^+$] calculated for $C_{26}H_{17}BrN_2NaO_4U$ 761.0777, found 761.1124.

4'-nitro-[1,1'-biphenyl]-2-ol (Q). (83% yield) (4-nitrophenyl)boronic acid (500 mg, 3.0 mmol), 2-iodophenol (600 mg, 2.7 mmol), potassium carbonate (1.13 g, 8.2 mmol), palladium

diacetate (25 mg, 0.1 mmol) were put in a mixture of 8 mL of DMF and 8 mL of water. This compound was prepared following the same procedure previously described for **K**. The residue was dissolved in boiling ethanol and filtered with celite to yield **Q** (83%). ^{1}H-NMR (300 MHz in CDCl$_3$), δ (ppm): 8.32-8.29 (m, 2H, ArH, AA'), 7.74-7.71 (m, 2H, ArH, XX'), 7.33-7.28 (m, 2H, ArH), 7.05 (t, 1H, ArH, J= 7.5 Hz), 6.95 (dd, 1H, ArH, J$_{orto}$=8, J$_{meta}$=1), 5.19 (b, 1H, OH). ^{13}C-NMR (300 MHz in CDCl$_3$), δ (ppm): 152.4, 146.9, 144.6, 130.5, 130.3, 130.1, 126.2, 123.8, 121.5, 116.5. MS (m/z): [M − H+] 214.0.

2-hydroxy-4'-nitro-[1,1'-biphenyl]-3-carbaldehyde (R). (40% yield) Compound **Q** (552 mg, 2.57 mmol), freshly distilled triethylamine (1.5 mL, 10.7 mmol) and magnesium chloride MgCl$_2$ (976 mg, 10.3 mmol) were added to 12 mL of freshly distilled dry THF. After 20 min solid paraformaldehyde (1.55 g, 51 mmol) was added. This compound was prepared following the same procedure previously described for **N**. The crude product was purified by silica column chromatography, using hexane:CH$_2$Cl$_2$ (7:3) as eluent to yield **R** (40%). ^{1}H-NMR (300 MHz in CDCl$_3$), δ: 11.67 (s, 1H, OH), 9.99 (s, 1H, CHO), 8.38-8.29 (m, 2H, ArH), 7.80-7.77 (m, 2H, ArH,), 7.67-7.65 (m, 2H, ArH), 7.17 (t, 1H, ArH, J=7.5 Hz). ^{13}C-NMR (300 MHz in CDCl$_3$), δ: 196.8, 158.8, 143.0, 137.5, 134.6, 130.1, 128.3, 128.0, 124.4, 123.5, 121.0, 120.2. MS (m/z): [M − H+] 241.9.

Uranyl-salophen 1h. (27% yield) Salicylaldehyde **R** (0.6 mmol, 1 equiv), monoimine **K** (0.6 mmol, 1 equiv.) and UO$_2$(OAc)$_2$·2H$_2$O (0.7 mmol, 1.2 equiv.) were solubilized in methanol (2.5 mL). The red solid obtained at the end of the reaction was purified by silica column chromatography using chloroform as eluent, to yield **1h** (27%). ^{1}H-NMR (300 MHz in Acetone-d6), δ (ppm): 9.71 (s, 1H, CH=N), 9.64 (s, 1H, CH=N), 8.41-8.38 (m, 2H, ArH, AA'), 8.27-8.24 (m, 2H, ArH, XX'), 8.00-7.77 (m, 5H, ArH), 7.59-756 (m, 3H, ArH), 6.95-6.89 (m, 2H, ArH), 6.71 (t, 1H, ArH, J=7.2). ^{13}C-NMR (300 MHz in DMSO-d6), δ (ppm): 167.5, 167.4, 167.2, 147.0, 146.4, 137.8, 136.8, 136.5, 136.4, 131.2, 129.5, 129.4, 129.2, 125.6, 124.6, 123.5, 120.9, 120.8, 117.6, 117.3. MS-ESI (m/z): [M+K$^+$] calculated for C$_{26}$H$_{17}$N$_3$O$_6$KU 744.1262, found 744.1225.

1.5 Bibliography

1. P. Bauduin, A. Renocourt, D. Touraud, W. Kunz, B. W. Ninham, *Curr. Opin. Colloid Interface Sci.* **2004**, 9, 43.

2. F. M. Ashcroft, Ion Channels and Disease, *Academic Press, San Diego*, **2000**.

3. N. Busschaert, C. Caltagirone, W.Van Rossom, P. A. Gale, *Chem. Soc. Rev.* **2015**, 115, 8038.

4. P. D. Beer, P. A. Gale, *Angew. Chem.*, **2001**, 113,502.

5. R. D. Shannon, *Acta Crystallogr. Sect. A* **1976**, 32, 751.

6. B. L. Brandi, H. T. Chifotides and K. R. Dunbar, *Chem. Soc. Rev.*, **2008**, 37, 68.

7. a) W. Liu, Q.-Q.Wang, Y.Wang, Z.-T. Huang, D.-X. Wang, *RSC Adv.,* **2014**, 4 , 9339; b) Y. Chen, D.-X. Wang, Z.-T. Huang, M.-X. Wang, *Chem. Commun.,* **2011**, 47, 8112.

8. N. Chuard, K. Fujisawa, P. Morelli, J. Saarbach, N. Winssinger, P. Metrangolo, G. Resnati, N. Sakai, S. Matile, *J. Am. Chem. Soc.* **2016**, 138, 11264.

9. a)Y. Zhao, Y. Cotelle, L. Liu, J. Lopez-Andarias, A. Bornhof, M. Akamatsu, N. Sakai, and S. Matile, *Acc. Chem. Res.* **2018**, 51, 9, 2255; b) L. Liu, Y. Cotelle, A. J. Avestro, N. Sakai, S. Matile, *J. Am. Chem. Soc.* **2016**, 138, 7876.

10. S. Marsili, R. Chelli, V. Schettino and P. Procacci, *Phys. Chem. Chem. Phys.,* **2008**, 10, 2673.

11. D. A. Dougherty, *Acc. Chem. Res*., **2013**, 46, 885.

12. C. Garau, A. Frontera, D. Quinonero, P. Ballester, A. Costa and P. M. Deya, *ChemPhysChem*, **2003**, 4, 1344.

13. C. Garau, D. Quinonero, A. Frontera, P. Ballester, A. Costa and P. M. Deya, *Org. Lett.*, **2003**, 5, 2227.

14. (a) P. S. Lakshminarayanan, I. Ravikumar, E. Suresh and P. Ghosh, *Inorg. Chem.,* **2007**, 46, 4769; (b) I. Ravikumar, P. S. Lakshminarayanan, M. Arunachalam, E. Suresh and P. Ghosh, *Dalton Trans*., **2009**, 4160. (c) O. B. Berryman, F. Hof, M. J. Hynes and D. W. Johnson, *Chem. Commun.,* **2006**, 506; (d) H. Maeda, Y. Ishikawa, T. Matsuda, A. Osuka and H. Furuta, *J. Am. Chem. Soc.,* **2003**, 125, 11822; (e) H. Schneider, K. M. Vogelhuber, F. Schinle and J. M. Weber, J. *Am. Chem. Soc.,* **2007**, 129, 13022.

15. A. Dalla Cort, P. De Bernardin, G. Forte and F. Yafteh Mihan, *Chem. Soc. Rev.* **2010**, 39, 3863.

16. K. Takao and Y. Ikeda, *Inorg. Chem.,* **2007**, 46 , 1550.

17. Kruppa, M.; König, B. *Chem. Rev.* **2006**, 106, 3520.

18. M. S. Bharara, K. Heflin, S. Tonks, K. L. Strawbridge and A. E. V. Gorden, *Dalton Trans.* **2008**, 2966.

19. M. Cametti, A. Dalla Cort, L. Mandolini, M. Nissinen and K. Rissanen, *New. J. Chem.,* **2008**, 32, 1113.

20. M. Giese, M. Albrecht, K. Rissanen, *Chem. Rev.* **2015**, 115, 8867.

21. T. Korenaga, T. Kosaki, R. Fukumura, T. Ema, and T. Sakai, *Org. Lett.,* **2005**, 7, 4915.

22. V. van Axel Castelli, A. Dalla Cort, L. Mandolini, V. Pinto, D. N. Reinhoudt, F. Ribaudo, C. Sanna, L. Schiaffino, B. H.M. Snellink-Ruël, *Supramol. Chem.* **2002**, 14, 211.

23. M. Giese, M. Albrecht, C. Bannwarth, G. Raabe, A. Valkonen and K. Rissanen, *Chem. Comm.,* **2011**, 47, 8542.

24. O. B. Berryman, F. Hof, M. J. Hynesc, D. W. Johnson, *Chem. Commun.* **2006**, 506.

25. A. Dalla Cort, L. Mandolini, C. Pasquini, L. Schiaffino, *J. Org. Chem.* **2005**,70, 9814.

26. M. Cametti, M. Nissinen, A. Dalla Cort, L. Mandolini, and K. Rissanen, *J. Am. Chem. Soc.,* **2007**, 129 , 3641.

27. R. S. Macomber, *Journal Of Chemical Education*, 69, 375.

28. a) P. Gamez, *Inorg. Chem. Front.,* **2014**, 1, 35-43; b) C. Garau, D. Quinonero, A. Frontera, P. Ballester, A. Costa and P. M. Deya, *New J. Chem.*, **2003**, 27, 211.

29. P. Ballester, *Acc. Chem. Res.* **2013**, 46, 874.

30. L. Adriaenssens, G. Gil-Ramirez, A. Frontera, D. Quinonero, E. C. Escudero-Adàn, P. Ballester, *J. Am. Chem. Soc.* **2014**, 136, 3208.

31. S. E. Wheeler, *Accounts of chemical research*, **2013**, 46, 1029.

32. A. F. Danil de Namor and M. Shehab, *J. Phys. Chem. B,* **2003**, 107, 6462.

33. M. Bühl, N. Sieffert, A. Chaumont and G. Wipff, *Inorg. Chem.*, **2011**, 50, 299.

34. L. Adriaenssens, C. Estarellas, A. V. Jentzsch, M. M. Belmonte, S. Matile, P. Ballester, *J. Am. Chem. Soc.* **2013**, 135, 8324.

35. a) H. Yi, M. Albrecht, A. Valkonen, K. Rissanen*, New J. Chem.,* **2015**, 39, 746; b) M. Giese, M. Albrecht, A. Valkonen, K. Rissanen, *Chem. Sci.,* **2015**, 6, 354; c) M. Giese, M. Albrecht, K. Rissanen*, Chem. Rev.* **2015,** 115, 8867.

36. a) C. J. van Staveren, E. F. Fenton, D. N. Reinhoudt, J. van Eerden, S. J. Harkema, *J Am. Chem. Soc.* **1987**, 109, 3456; b) D.M. Rudkevich, W.P.R.V. Stauthamer, W. Verboom, J.F.J. Engbersen, S. Harkema, D.N. Reinhoudt, *J. Am. Chem. Soc.* **1992**, 114, 9671.

37. Dielectric constant ε = 4.81 at 20ºC.

38. Dielectric constant ε = 36.64 at 20ºC.

39. K. Inamoto, J. Kadokawa, Y. Kondo, *Org. Lett.,* **2013**, 15, 3962; see Supporting Informations.

40. U. N. Hofsløkken, L. Skattebøl, *Acta Chem. Scand*., **1999**, 53, 2582.

41. C. Hansch, A. Leo and R. W. Taft, Chem. Rev., **1991**, 91, 165.

42. G. Gil-Ramìrez, E. C. Escudero-Adàn, J. Benet-Buchholz, and P. Ballester, *Angew. Chem. Int. Ed.* **2008**, 47, 4114.

43. L. Leoni, R. Puttreddy, O. Jurcek, A. Mele, I. Giannicchi, F. Yafteh Mihan, K. Rissanen and A. Dalla Cort, *Chem. Eur.J.* **2016**, 22, 18714. See Supporting Informations.

44. L. Portscheller, H.C. Malinakova, *Org. Lett*., **2002**, 4, 3679-3681.

45. H. Mu, W. Ye, D. Song and Y. Li*, Organometallics*, **2010**, 29, 6282.

46. R. Lebeuf, F. Robert, and Y. Landais, *Org. Lett.,* **2005**, 7, 4557.

Chapter 2. Mechanochemical Synthesis of Salophen Ligands and the corresponding Zn, Ni, and Pd Complexes

The use of grinding to promote reactions between solid reactants or between solids and liquids (kneading) is becoming increasingly an appealing topic for the chemical community.[1] This new approach, for getting a variety of molecular or supramolecular compounds using reactions activated mechanically, is called mechanochemistry.

The classical equipment used for solid state mechanosynthesis are either the well-known mortar and pestle or mixer mills. The last ones allow us to perform reactions in a shorter amount of time and with high energy input, see Figure 2.1.

Figure 2.1. The mixer mill MM 200 is a laboratory "all-rounder". It has been developed specially for dry grinding of small amounts of sample. It can mix and homogenize a wide range of materials in only a few seconds.

The most important advantages are the relative large quantity of starting materials used (quantity of millimols), optimum conversions, time saved, environmental issues and the elimination of volatile products.

Some experimental proofs suggest that it is advantageous for some reactions to add a few drops of solvent to the solid mixture leading to liquid-assisted grinding (LAG). In any case, it is a limited amount of solvent (a few drops of solvent) with respect to the classical reactions performed in solution.

The mechanosynthesized powder product can be characterized by NMR techniques or through X-Ray diffraction analysis.[2] In some cases, a subsequent simple purification step can be necessary to remove the unreacted compounds.

This kind of protocol can become a valid opportunity for ligand preparation as well as for the corresponding metal-complexes.[3] In the context of our research we decided to apply mechanochemistry protocol to the synthesis of salophens [(*N,N*-phenylene-bis(salicylimine)] type ligands and metal-salophen complexes[4] through a one-pot approach under ball milling condition. The synthesis, when carried out in the presence of metal salts, leads directly to the isolation of the corresponding metal complexes. Herein, we report the one-pot mechanochemical synthesis of a series of salophen ligands **1-3** and of the corresponding metal complexes **1M-3M** (M = Zn^{+2}, Ni^{+2}, Pd^{+2}), as a convenient, quick, solvent free alternative to the "classical" procedure. See Figure 2.2.
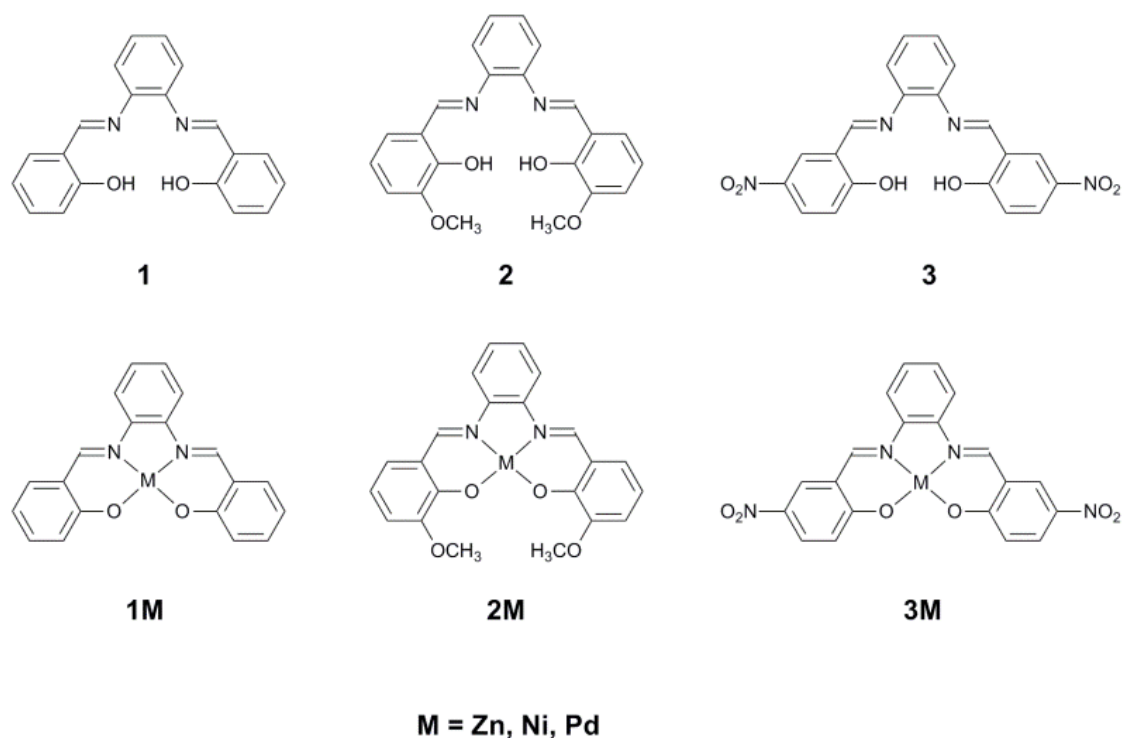
Figure 2.2. Chemical structures of the salophen ligands and of the corresponding metal complexes.

For the synthesis of ligands, **1-3**, we started from *o*-phenylendiamine, salicyladehyde, *o*-vanillin and 5,5'-dinitrosalicylaldehyde, respectively. The solid mixture was ground to obtain the corresponding ligands. To get metal-salophen complexes, **1M-3M** we added to the previous mixture zinc(II) or nickel(II) acetate, $Zn(OAc)_2$, $Ni(OAc)_2$, or palladium(II)-2,4-pentanedionate, $C_{10}H_{16}O_4Pd$.

We report here the procedures and characterizations of the isolated products.

After milling a washing step for the mechano-synthesized compound was required. The as-synthesized products were washed with 3 mL of MeOH and 1 mL of EtOH to remove completely the unreacted compounds.

The salophen ligand **1** (yield 70%) was prepared by kneading 1 mmol of *o*-phenylenediamine and 2 mmol of salicylaldehyde. A yellow powder was obtained. ^{1}H-NMR confirmed the formation of the pure product. Crystal structure of the salophen ligand **1** was retrieved from the

Cambridge Structural Database (CSD), CSD refcode: EKEYEA.[5] The PXRD pattern of the isolated product matches the simulated powder pattern of EKEYEA as shown in Figure 2.3.
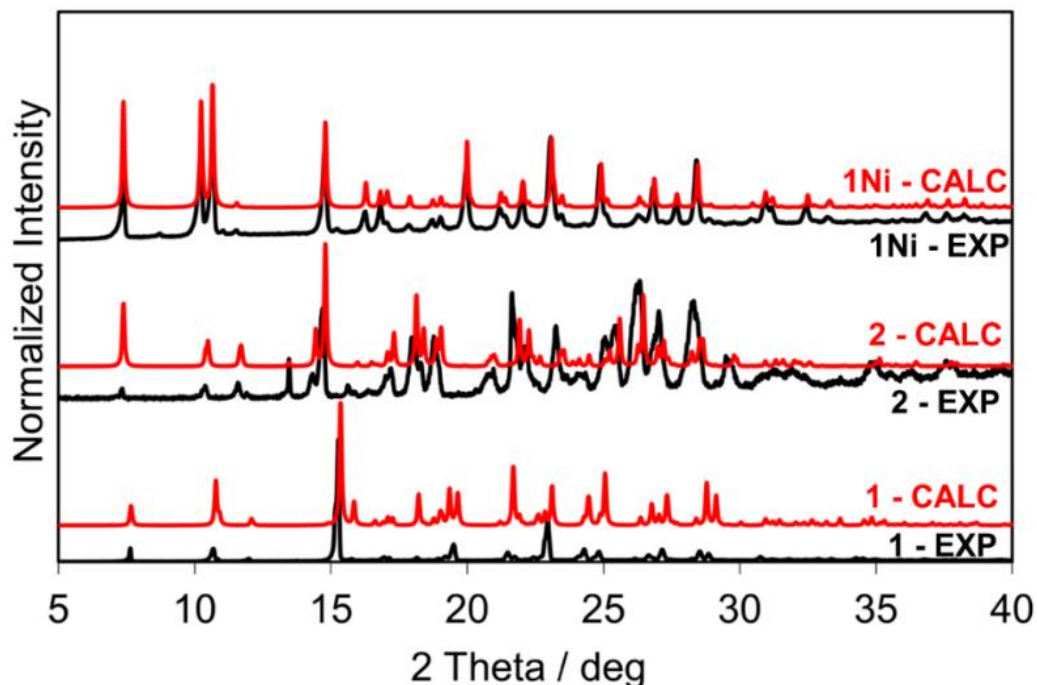

Figure 2.3. From top to bottom: PXRD patterns of **1Ni**, **2**, and **1** (calculated powder patterns in red, experimental powder patterns in black).

Definitive evidences about the formation of such compound in the solid state was obtained by solid state NMR (SSNMR) spectroscopy. Indeed, the ^{13}C cross-polarisation (CP-MAS) spectrum reported in Figure 2.4 shows sharp signals, as expected for the high grade of crystallinity and purity of the compound **1**.
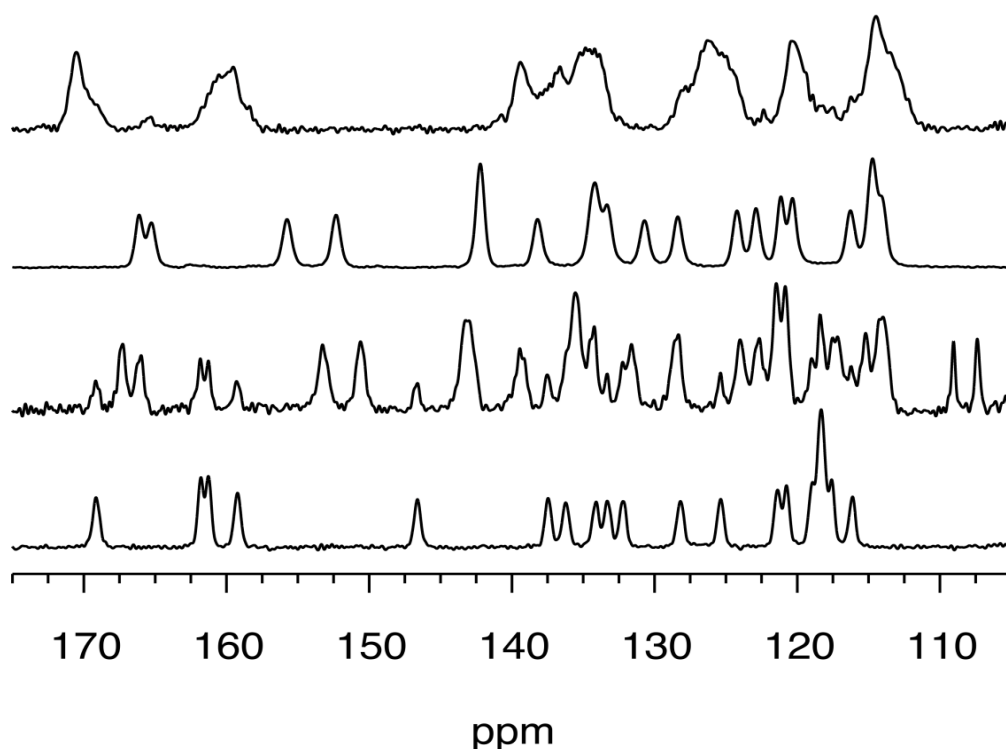
Figure 2.4. SSNMR spectra recorded at 11.7 T and room temperature of mechansynthesized metal-salophens (From top to bottom**: 1Zn**, **1Ni**, **1Pd** and compound **1**).

Compound **2** (yield 60%) was synthesized by LAG (four drops of MeOH were added) from 1 mmol of o-phenylenediamine and 2 mmol of *o*-vanillin. The obtained powder product was orange. Solution state ^{1}H-NMR and SSNMR showed that **2** was formed mechanochemically. The measured X-ray powder diffraction pattern of **2** (Figure 2.3) matches the one simulated from the single-crystal structure, CSD entry MEPWUA.[6]

Attempts to mechanosynthesize by LAG or dry grinding the symmetric salophen ligand **3** from 1 mmol of *o*-phenylenediamine and 2 mmol of 2-hydroxy-5-nitrobenzaldehyde were unsuccessful and led to an unintelligible mixture of compounds.

For the metal-salophen complexes, we noticed that the success of such solid-state synthesis is strictly dependent upon the choice of the counteranion of the transition metal salts. The salts that gave the best results were Zn(OAc)$_2$, Ni(OAc)$_2$ and Pd(II) (2,4-pentanedionate). Chloride salts of Zn(II), Ni(II), Pd(II) led to a physical mixture of the reactants. This could be ascribed to the lower basicity of the counter anion. Indeed, together with the two molecules of water

originate in the condensation reaction, for the coordination of the metal, two protons H$^+$ (of the OH functions) of the salophen ligand must be released.[7] This represents the driving force for the metal coordination in the solid state synthesis.

Compound **1Zn** was prepared (yield 62%) by kneading from 1 mmol of *o*-phenylenediamine, 2 mmol of salicylaldehyde and 1.2 mmol of Zn(OAc)$_2$. ^{1}H-NMR revealed a spectrum consistent with the expected compound. No comparison of the powder pattern of **1Zn** was possible given that its single-crystal structure is not reported in the CSD. Any attempt to get crystals suitable for X-ray analysis was so far unsuccessful. The SSNMR spectra provided in Figure 2.4 shown the absence of peaks of the salophen ligand **1**. The resonance lines of **1Zn** are broader than those of the respective ligand, as expected for a compound characterized by lower crystallinity.

Compound **1Ni** was synthesized by kneading from 1 mmol of o-phenylenediamine, 2 mmol of salicylaldehyde and 1.2 mmol of Ni(OAc)$_2$ (yield 68%). The recovered product showed a red clay-like coloration. ^{1}H-NMR confirmed the purity of the compound. Experimental powder pattern of this one-pot reaction matches the one calculated from single-crystal data (CSD refcode: ZZZTZI02,[8] see Figure 2.3). SSNMR in Figure 2.4 corroborates this aspect, considering that peaks of **1** are no more observed.

Compound **1Pd** was prepared by kneading from 1 mmol of *o*-phenylenediamine, 2 mmol of salicylaldehyde and 1.2 mmol of Pd(II) 2,4-pentanedionate. From SSNMR data in Figure 2.4, it was observed that the reaction is not complete and both peaks of the ligand **1** and the starting product are still detected. Interestingly, peaks and chemical shift values of the resonance lines observed in the SSNMR spectrum of **1Pd** are similar to those of **1Ni** (with small shifts, Figure 2.4). This suggests that the **1Pd** phase recovered after the grinding process is relative to the orthorhombic anhydrous Pd-salophen whose structure is reported in the CSD as PYSALP. PYSALP31 (**1Pd**) and ZZZTZI02 (**1Ni**) are found to be isostructural on the basis of their cell parameters. Purification of **1Pd** was not possible by using the washing procedure reported so far for **1Ni** and **1Zn**. However, **1Pd** can be obtained (in the form of DMSO solvate) in a pure form by recrystallization from DMSO saturated solutions. ^{1}H-NMR spectra of the pure crystallized compound in DMSO-d6 was performed. Orange crystals of the DMSO solvate suitable for X-ray structure determination were obtained.

Compound **2Zn** was synthesized by dry grinding from 1 mmol of *o*-phenylenediamine, 2 mmol of *o*-vanillin and 1.2 mmol of Zn(OAc)$_2$ (yield 64%). ^{1}H-NMR revealed a spectrum consistent with the expected compound. SSNMR spectrum of **2Zn** shows the disappearing of peaks

relative to the ligand **2** as in Figure 2.5. No single crystals suitable for SCXRD have been obtained.
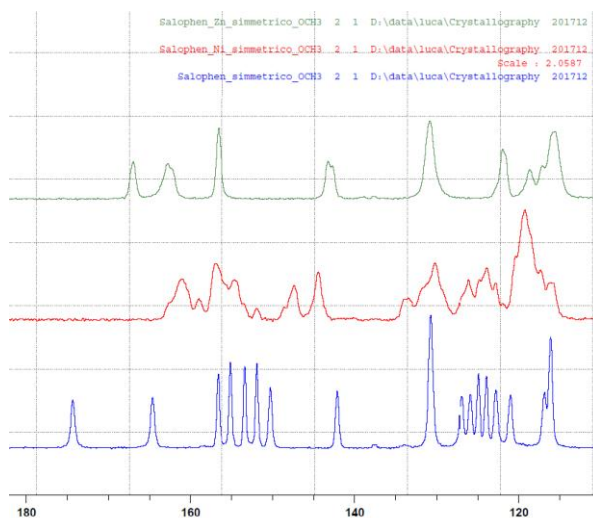

Figure 2.5. SSNMR spectra recorded at 11.7 T and room temperature of mechansynthesized salophen and metal-salophens (From top to bottom: **2Zn**, **2Ni**, and compound **2**).

Compound **2Ni** was synthesized by dry grinding from 1 mmol of *o*-phenylenediamine, 2 mmol of *o*-vanillin and 1.2 mmol of $Ni(OAc)_2$ (yield 65%). ^{1}H-NMR confirmed the formation of the pure product. Analysis by PXRD showed that compound 2Ni is crystalline. Single-crystals of the DMSO solvate suitable for structure determination by SCXRD have been obtained in DMSO after four days. SSNMR spectra of **2Ni** and of the corresponding ligand are provided in Figure 2.5.

Compound **2Pd** was synthesized by LAG from 1 mmol of *o*-phenylenediamine, 2 mmol of *o*-vanillin and 1.2 mmol of Palladium(II) 2,4-pentanedionate. Analogously to what observed for compound **1Pd**, synthesis of **2Pd** is not complete. The solid phase obtained is relative to the **2Pd** tetra-hydrate compound, the structure of which is reported in the CSD with the refcode AVAVUP.[9] Pure crystalline **2Pd** (DMSO solvate) was obtained by recrystallization in DMSO. Crystal structure of **2Pd** is provided in the structural section. Solution state proton and carbon NMR spectra of **2Pd** crystallized confirmed the formation of the pure product.

Compound **3Zn** was synthesized by liquid assisted grinding (four drops of MeOH were added) from 1 mmol of *o*-phenylenediamine, 2 mmol of 2-hydroxy-5-nitrobenzaldehyde and 1.2 mmol

of Zn(OAc)$_2$ (yield 85%). **3Zn** was characterized by ^{1}H-NMR. The as-synthesized product showed only low crystallinity when studied by PXRD. However, yellow needle-like single crystals, suitable for SCXRD, were obtained by slow evaporation from a saturated solution in DMSO. Their analysis led to the crystal structure of a DMSO solvate of the compound. SSNMR spectra of **3Zn** is shown in Figure 2.6.
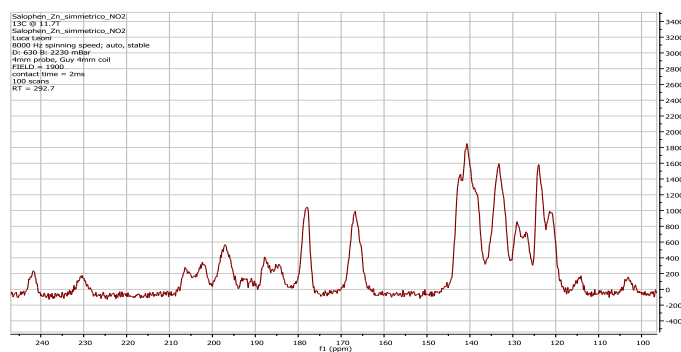

Figure 2.6. SSNMR spectra recorded at 11.7 T and room temperature of compound **3Zn**.

All as-synthesized powder products were crystallized from DMSO saturated solutions by slow evaporation technique. Crystal structures corroborates other identification techniques. All solid obtained are DMSO solvates.
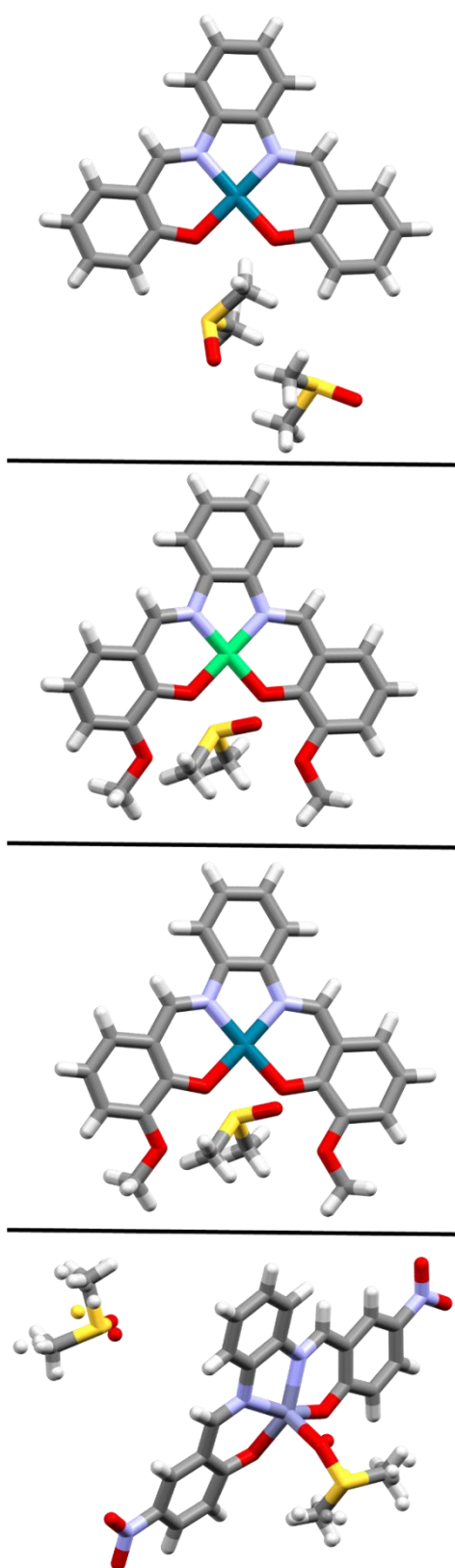
Figure 2.7. Asymmetric unit of **1Pd**, **2Ni**, **2Pd** and **3Zn** (from top to bottom) obtained as DMSO solvates and adducts (shown in capped sticks representation).
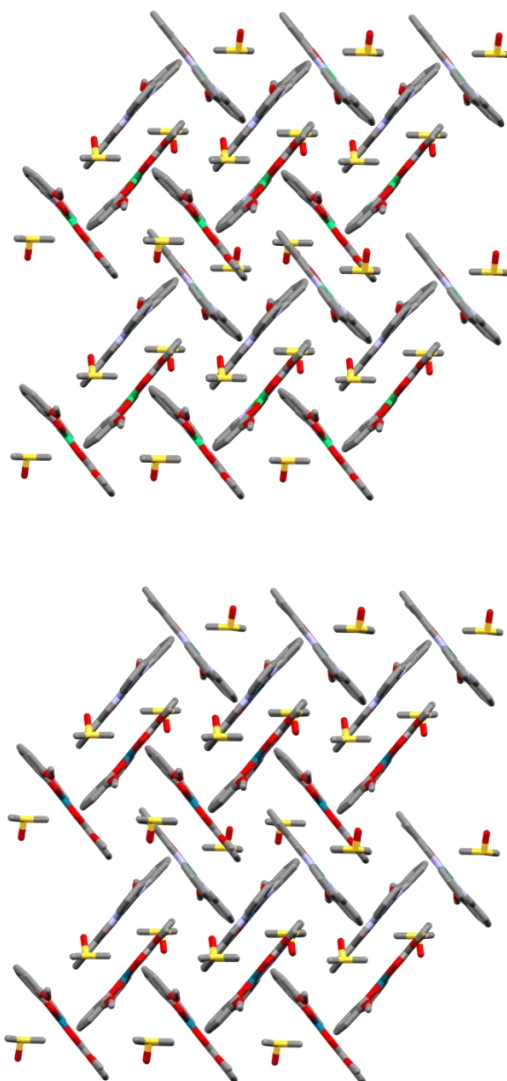
Figure 2.8. Isostructurality between **2Ni.(DMSO)**, top, and **2Pd.(DMSO)**, bottom.

Solid **1Pd·2(DMSO)**. Orange plates were obtained from a saturated DMSO solution after 4 days. A DMSO solvate is obtained crystallizing in the P21/n space group with a 1:2 stoichiometry. The overall packing assumes a herringbone aspect.

Solid **2Ni·(DMSO)**. Dark red plates were obtained in DMSO after 4 days. Crystals belong to the monoclinic P21/c space group. Molecule has a planar conformation. Molecules of salophen complex are assembled in centrosymmetric dimers, which are staked in parallel displaced fashion over a half of the molecule. This way, the remaining half molecule is available for

edge-to-face interactions with a second centrosymmetric dimer. The resulting packing assumes, then, a herringbone-like structure (Figure 2.8).

Solid **2Pd·(DMSO)**. Red blocks were obtained in DMSO after 4 days. Crystals belong to the monoclinic P21/c space group. Molecule has a planar conformation. Structure of **2Pd·(DMSO)** is isostructural (Figure 2.8) to the one of **2Ni.(DMSO)** as seen by comparison of cell parameters and by their comparison of their powder X-ray patterns.

Solid **3Zn@DMSO·(DMSO)**. Yellow plates were obtained in DMSO after 4 days. Crystals belong to the monoclinic P21/c space group. One molecule of **3Zn** is present in the asymmetric unit along with 2 molecules of DMSO. Interestingly one molecules is localized in a void area in the solid and interacts with **3Zn** by non-covalent interactions. The second molecule of DMSO is, instead, coordinated by the O-atom to the Zinc of the salophen. Therefore the metal center in Zn-salophen complexes acts as a receptor. In the CSD various examples of water, pyridine, acetate and DMF adducts of Zn-salophens are reported.[10] Compound **3Zn** has biological properties and its biological activity has been analyzed in a previous investigation.[11] In vitro studies show that there is a strong interaction with free plasmid DNA and cellular uptake and cytotoxicity studies show that they enter the cells but are not cytotoxic.

To conclude, libraries of compounds with different steric and electronic variations (salophen ligands and metal-salophen complexes) were mechanosynthesized in a quick and quantitative way, by (liquid-assisted) grinding. We demonstrated that, when *o*-phenylenediamine, benzaldehyde or its derivatives, and a divalent Zn/Ni/Pd salt are milled together, the one-pot mechanochemical synthesis of metal-salophen complexes is achieved. Compounds were fully characterized by NMR spectroscopy and characterized by powder X-ray diffraction (PXRD) analysis and single-crystals X-ray diffraction analysis whenever possible. Formation of metal-salophen complexes during the ball milling process has been convincingly proved with different techniques (PXRD and SSNMR). The success of the solid state synthesis of the metal salophens is strictly dependent upon the choice of the counter-anion of the transition metal salts. We achieved good yields by using $Zn(OAc)_2$, $Ni(OAc)_2$ and Pd(II) 2,4-pentanedionate. Instead, salts like $ZnCl_2$, $NiCl_2$, $PdCl_2$ showed to be less reactive and led to a mixture of compounds. Pt-salophen complexes were not obtained despite many attempts with different reaction conditions and Pt salts.

2.1 Experimental section

All reactants were purchased from Sigma–Aldrich and used as received. Solvents used for the washing step and crystallization (EtOH, MeOH, DMSO) are commercially available and were used without further purification.

All compounds were synthesized by mechanosynthesis. Dry- and liquid-assisted grinding (LAG, in methanol) were performed by means of a Retsch MM 400 Mixer Mill in 2 mL Eppendorf tubes (8–10 stainless-steel grinding balls of 1 mm diameter for each sample). The operating frequency was set at 30 Hz and reactants were milled for 60 minutes. After milling a washing step for the compounds was required. The as-synthesized products were washed with 3 mL of MeOH and 1 mL of EtOH.

X-ray powder patterns were collected in the 2θ range 5-40° using a Panalytical X'Pert PRO diffractometer (Bragg-Brentano geometry, Cu Kα radiation, X'Celerator linear detector, step size 0.017°; 45 mA, 30 kV). The program Mercury was used for calculation of X-ray powder patterns from single-crystal data.

Single-crystal X-ray diffraction (SCXRD) data were collected at 100 K for **1Pd·2(DMSO)**, **2Ni·DMSO** and **2Pd·DMSO**, and at 295 K for **3Zn@DMSO·(DMSO)** on an Oxford Diffraction Gemini Ultra R system (4-circle kappa platform, Ruby CCD detector) using Mo Kα ($\lambda = 0.71073$ Å) radiation for **1Pd·2(DMSO)**, **2Ni·DMSO** and **2Pd·DMSO** and Cu Kα ($\lambda = 1.54184$ Å) for **3Zn@DMSO·(DMSO)**. The structures were solved by SHELXT[12] and then refined by full-matrix least square refinement of $|F|^2$ using SHELXL-2016.[13] Non-hydrogen atoms were refined anisotropically. Hydrogen atoms were located from difference Fourier map. Hydrogen atoms were refined in the riding mode with isotropic temperature factors fixed at $1.2U_{eq}$ of the parent atoms ($1.5U_{eq}$ for methyl group).

Liquid NMR spectra were collected at 25°C on a JEOL ECA spectrometer operating at 9.4 T (400 MHz) using DMSO-d6 as solvent. The ^{1}H chemical shift scale was calibrated using the residual signal of DMSO (2.50 ppm). Compound **1** (yield = 70%) ^{1}H NMR δH (400 MHz, DMSO-d6), 12.93 (2 H, s, OH), 8.91 (2H, s, CH), 7.64 (2 H, d, CH, J = 8Hz), 7.45-7.36 (6 H, m, CH), 6.96-6.92 (4 H, m, CH). ^{13}C NMR δC (100 MHz, DMSO-d6), 164.1, 160.4, 142.3, 133.5, 132.5, 127.8, 119.8, 119.5, 119.1, 116.7. Compound **2**. (yield = 60%) ^{1}H NMR δH (400 MHz, DMSO-d6), 12.99 (2 H, s, OH), 8.89 (2H, s, CH), 7.45-7.36 (4 H, m, CH), 7.22 (2 H, d,

CH, J = 8 Hz), 7.10 (2 H, d, CH, J = 8 Hz), 6.88 (2 H, t, CH, J = 8 Hz), 3.78 (6 H, s, OCH3). ^{13}C NMR δC (100 MHz, DMSO-d6), 164.9, 151.1, 148.4, 142.6, 128.3, 124.3, 120.3, 119.9, 119.1, 116.0, 56.2). Compound **1Zn** (yield = 62%). ^{1}H NMR δH (400 MHz, DMSO-d6), 8.99 (2H, s, CH), 7.88-7.86 (2 H, m, CH), 7.40-7.35 (4 H, m, CH), 7.21 (2 H, t, CH, J = 8 Hz), 6.68 (2 H, d, CH, J = 8 Hz), 6.48 (2 H, t, CH, J = 8 Hz). ^{13}C NMR δC (100 MHz, DMSO-d6) 172.3, 162.9, 139.4, 136.2, 134.3, 127.3, 123.1, 119.4, 116.5, 112.9). Compound **1Ni** (yield of 68%) ^{1}H NMR δH (400 MHz, DMSO-d6), 8.86 (2H, s, CH), 8.13-8.11 (2 H, m, CH), 7.57 (2 H, d, CH, J = 8Hz), 7.32-7.27 (4 H, m, CH), 6.85 (2 H, d, CH, J = 8Hz), 6.64 (2 H, t, CH, J = 8 Hz). ^{13}C NMR δC (100 MHz, DMSO-d6) 165.8, 157.1, 142.9, 135.7, 134.8, 128.2, 120.8, 120.7, 116.7, 115.8). Compound **1Pd** ^{1}H NMR δH (400 MHz, DMSO-d6), 9.17 (2H, s, CH), 8.34-8.30 (2 H, m, CH), 7.71 (2 H, d, CH, J = 8Hz), 7.43-7.42 (4 H, m, CH), 6.99 (2 H, d, CH, J = 8Hz), 6.69 (2 H, t, CH, J = 8 Hz). ^{13}C NMR δC (100 MHz, DMSO-d6) 166.6, 155.5, 143.7, 136.8, 136.7, 128.7, 121.4, 121.2, 117.7, 115.8). Compound **2Zn** (yield = 64%) ^{1}H NMR δH (400 MHz, DMSO-d6), 8.98 (2H, s, CH), 7.87-7.85 (2 H, m, CH), 7.35-7.33 (2 H, m, CH), 6.99 (2 H, d, CH, J = 8 Hz), 6.83 (2 H, d, CH, J = 8 Hz), 6.40 (2 H, t, CH, J = 8 Hz), 3.73(6 H, s, OCH$_3$). ^{13}C NMR δC (100 MHz, DMSO-d6) 164.2, 163.3, 153.0, 139.9, 127.9, 127.6, 119.2, 116.9, 114.3, 112.3, 55.7). Compound **2Ni** (yield = 65%) ^{1}H NMR δH (400 MHz, DMSO-d6), 8.87 (2H, s, CH), 8.12-8.10 (2 H, m, CH), 7.30-7.29 (2 H, m, CH), 7.17 (2 H, d, CH, J = 8Hz), 6.85 (2 H, d, CH, J = 8Hz), 6.54 (2 H, t, CH, J = 8 Hz), 3.72 (6H, s, OCH$_3$). ^{13}C NMR δC (100 MHz, DMSO-d6) 157.6, 156.9, 151.2, 142.8, 128.0, 125.9, 120.7, 116.7, 115.5, 115.1, 56.2). Compound **2Pd**. ^{1}H NMR δH (400 MHz, DMSO-d6), 9.14 (2H, s, CH), 8.33-8.32 (2 H, m, CH), 7.41-7.39 (2 H, m, CH), 7.29 (2 H, d, CH, J = 8Hz), 6.98 (2 H, d, CH, J = 8Hz), 6.60 (2 H, t, CH, J = 8 Hz), 3.78 (6H, s, OCH$_3$). ^{13}C NMR δC (100 MHz, DMSO-d6) 157.8, 154.9, 150.9, 143.1, 128.0, 127.1, 120.5, 117.2, 114.9, 114.4, 55.3). Compound **3Zn**. (yield = 85%) ^{1}H NMR δH (400 MHz, DMSO-d6), 9.18 (2H, s, CH), 8.57 (2 H, d, CH, J = 3Hz), 8.05 (2 H, dd, CH, J$_1$ = 8Hz, J$_2$ = 3Hz), 7.94 (2 H, m, CH), 7.45 (2 H, m, CH), 6.74 (2 H, d, CH, J = 8 Hz). ^{13}C NMR δC (100 MHz, DMSO-d6) 177.2, 163.2, 139.5, 134.9, 134.6, 129.1, 129.0, 124.3, 119.1, 117.8.

^{13}C SSNMR spectra were collected at room temperature on a Bruker Avance 500 spectrometer operating at 11.7 T (125 MHz for ^{13}C) using a 4mm CP-MAS probe and a spinning frequency of 10 kHz. All the spectra were recorded using 512 averaged transients, a recycle delay of 5 s nad contact time of 2 ms. The chemical shift scale was referenced externally to solid adamantane (38.48 ppm and 29.45 ppm)[14] with respect to TMS.

2.2 Bibliography

1. S. L. James, C. J. Adams, C. Bolm, D. Braga, P. Collier, et al. *Chem. Soc. Rev.,* **2012**, 41, 413.

2. J. Dubois, M. Colaço and J. Wouters, CHEMIE NOUVELLE n°117-décembre **2014**.

3. a) J.-L. Do, T. Friščić *ACS Cent. Sci.* **2017**, 3, 13–19. b) F. Fischer, N. Fendel, S. Greiser, K. Rademann, F. Emmerling, *Org. Process Res. Dev.,* **2017**, 21, 655. c) A. A. L. Michalchuk, I. A. Tumanov, E. V. Boldyreva, *J. Mater. Sci.*, **2018**, 1. d) T. Stolar, L. Batzdorf, S. Lukin, D. Žilić, C. Motillo, T. Friščić, F. Emmerling, I. Halasz, K. Užarević, *Inorg. Chem.,* **2017**, 56, 6599.

4. L. Leoni and A. Dalla Cort *Inorganics* **2018**, 6, 42.

5. P. E. Reyes-Gutiérrez, T. Kapal, B. Klepetářová, D. Šaman, R. Pohl, Z. Zawada, E. Kužmová, M. Hájek, F. Teplý, *Sci. Rep.* **2016**, 6, 23499.

6. W.-K. Lo, W.-K. Wong, W.-Y. Wong, J. Guo, K.-T. Yeung, Y.-K. Cheng, X. Yang, R. A. Jones, *Inorg. Chem.,* **2006**, 45, 9315.

7. A. Dalla Cort, P. De Bernardin, G. Forte, F. Yafteh Mihan, *Chem. Soc. Rev.*, **2010**, 39, 3863.

8. J. Wang, F.-L. Bei, X.-Y. Xu, X.-J. Yang, X. Wang, *J. Chem. Crystallogr,.* **2003**, 33, 845.

9. L. Ding, Z. Chu, L. Chen, X. Lü, B. Yan, J. Song, D. Fan, F. Bao, *Inorg. Chem. Commun.* **2011**, 14, 573.

10. E. C. Escudero-Adán, M. M. Belmonte, E. Martin, G. Salassa, J. Benet-Buchholz, A. W. Kleij, *J. Org. Chem.,* **2011**, 76, 5404. E. S. Aazam, S. W. Ng, E. R. T. Tiekink, IUCr, *Acta Crystallogr. Sect. E Struct. Reports Online*, **2011**, 67, m314. N. E. Eltayeb, S. G. Teoh, S. Chantrapromma, H.-K. Fun, K. Ibrahim, *IUCr, Acta Crystallogr. Sect. E Struct. Reports Online* **2007**, 63, m1633. K. Ouari, A. Ourari, J. Weiss, *J. Chem. Crystallogr.* **2010**, 40, 831. H.-C. Lin, C.-C. Huang, C.-H. Shi, Y.-H. Liao, C.-C. Chen, Y.-C. Lin, Y.-H. Liu, *Dalt. Trans.* **2007**, 0, 781.

11. I. Giannicchi, R. Brissos, D. Ramos, J. de Lapuente, J. C. Lima, A. D. Cort, L. Rodríguez, *Inorg. Chem.* **2013**, 52, 9245.

12. G. M. Sheldrick, IUCr, *Acta Crystallogr. Sect. A Found. Adv.,* **2015**, 71, 3.

13. G. M. Sheldrick, IUCr, *Acta Crystallogr. Sect. C Struct. Chem.* **2015**, 71, 3.

14. Chemical shift referencing in MAS solid state NMR; C.R. Morcombe and K.W. Zilm, *Journal of Magnetic Resonance*, **2003**, 162, 479.

Chapter 3.   A New Water Soluble Zn-salophen Derivative

Non-covalent and highly specific molecular interactions are involved in the successful execution of vital processes, i.e. the crucial role of the hydrogen bonding between adjacent complementary residuals in the association of the two polynucleotidic strands of DNA through Watson–Crick interactions.
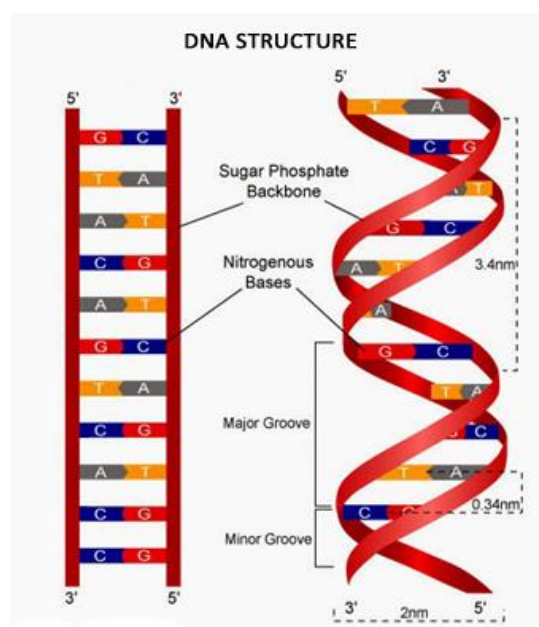

Figure 3.1. Schematic representations of the assembly of the double helix of DNA thanks to the rule exerted by hydrogen bonding. (A = adenine, T = tymine, C = Cytosine, G = guanine).

Non-Watson–Crick interactions between bases and non-canonical nucleic acids structures have also importance in biology and the study of these structures is considerably increasing. For example, many researchers are studying hydrogen-bonded helices based on the assembly of tetrameric units, i.e guanine (G)-quartets. A G-quartet is formed by four G bases arranged in a square planar cyclic hydrogen-bonding pattern, where each guanine is both the donor and

acceptor of two hydrogen bonds, providing a central site where the oxygen lone pair of the carbonyl groups can coordinate with metal cations (Figure 3.2A). Several G-quartets can stack upon each other by means of π–π interactions, to form a 3D structure, called a G-quadruplex (Figure 3.2B).
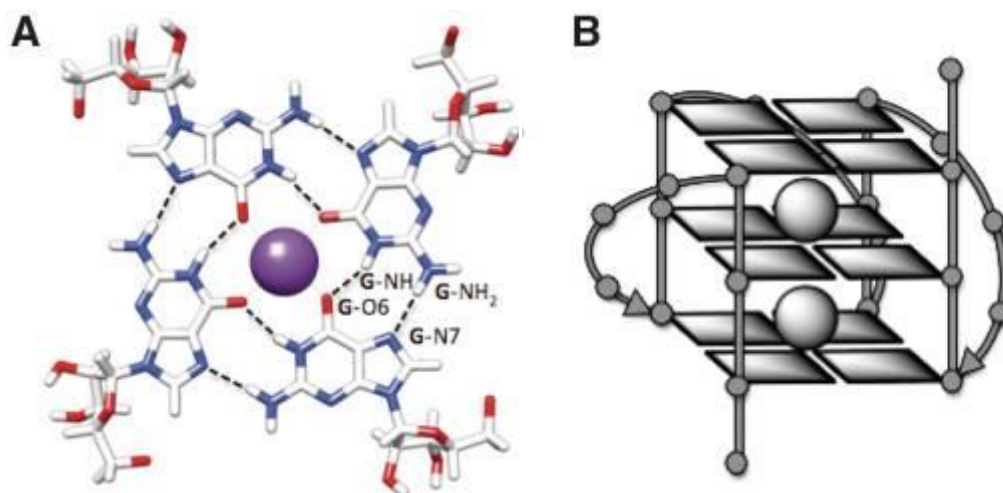

Figure 3.2. Schematic representations of (A) a G-quartet arrangement, (B) a G-quadruplex nucleic acids structure.

Quadruplex DNA presents a target of considerable current interest in DNA-directed drug design. [1] The initial interest in quadruplexes emerged from their taking part in telomeres and in the regulation of telomerase activity. Indeed, telomerase is expressed in over 90% of tumor cell lines and thus, telomerase inhibition represents a potentially highly selective target for anticancer drug design.[2] There are quite a number of G-quadruplex-interactive compounds including anthraquinones,[3] cationic porphyrins,[4] perylenes,[5] ethidium derivatives,[6] quinolones,[7] piperazines,[8] pentacyclicacridinium salts,[9] and fluoroquinophenoxazines,[10] which inhibit telomerase. For example, telomestatin, Figure 3.3, is a natural product isolated from Streptomyces anulatus 3533-SV4; it is a very potent telomerase inhibitor.[11] Therefore, the common structural feature of G-quadruplex ligands is an extended planar chromophore that can stack on, or intercalate, the G-tetrads.
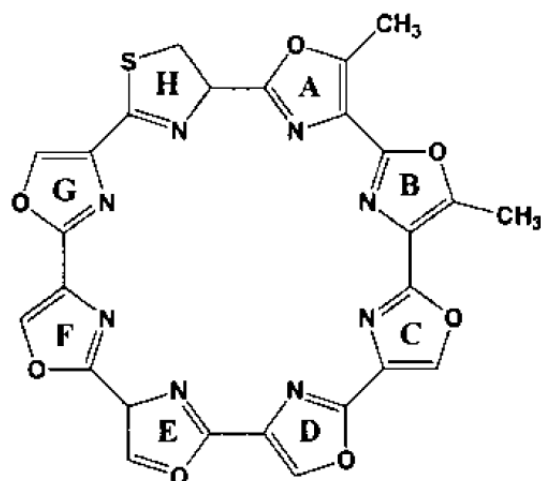
Figure 3.3. Structures of telomestatin.

Recently, non macrocyclic planar metal complexes have also been extensively studied as potential quadruplex stabilizers.[1] Metal salophen compounds bearing amine-based side arms (protonated under physiological conditions), are very good candidate for these type of studies (Figure 3.4).[1] Their strong absorption band in the region of about 280-500 nm (depending on the substitution on the salophen ligand and the metal center) render them excellent candidates as chemosensors. The basic pendant arms in Figure 3.4 allow favorable electrostatic interactions with the loops and grooves of the phosphate backbone of quadruplex DNA. [12]
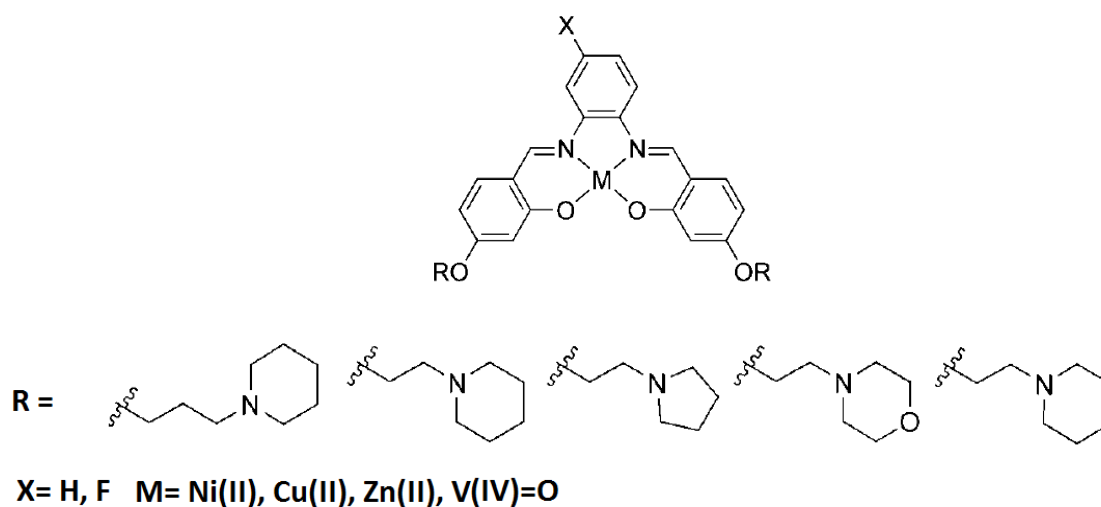

R =

X= H, F   M= Ni(II), Cu(II), Zn(II), V(IV)=O

Figure 3.4. Metal salphen complexes with cyclic amine side arms.

Also very similar series of Pt(II) complexes of salophen and salen were prepared also.[13]

Since our group has experience in preparing water soluble Zn-salophen complexes[14] and considering the biological rule of zinc that is essential to life, we decided to synthesized a new water soluble Zn-salophen complex as G-quadruplex binder (Figure 3.5) bearing ethyl-piperidine substituents (positively charged at physiological pH) to enhance quadruplex DNA binding properties. We decided to add a third substituent (a carboxyl group that are negatively charged at physiological pH) on the ligand skeleton to increase the water solubility of the salophen complex.
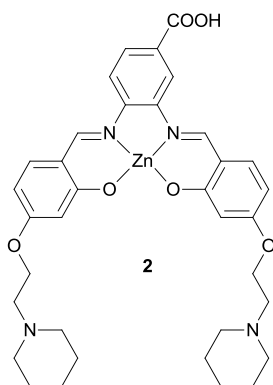

Figure 3.5. New water soluble Zn-salophen complex **2**.

This complex was synthesized as shown in Scheme 3.1 and characterized by spectroscopic and NMR techniques. The synthesis of the alkyl-derivatized salophen complex **2** (Figure 3.5) was accomplished in a two-step approach involving a nucleophilic substitution reaction between 2,4-dihydroxybenzaldehyde and 2-piperidinoethyl hydrochloride in the presence of a base to form the salicylaldehyde derivative **1**, followed by a condensation reaction with 3,4-diaminobenzoic and complexation with Zn^{2+}. To avoid the formation of the zwitterionic monoamine **4**, Scheme 3.2, that prevents the formation of the pure product **2**, we added a slight excess of a base (Et_3N). In this way we obtained the complete deprotonation of 3,4-diaminobenzoic acid **3** without the accumulation of the intermediate **4** during the reaction.
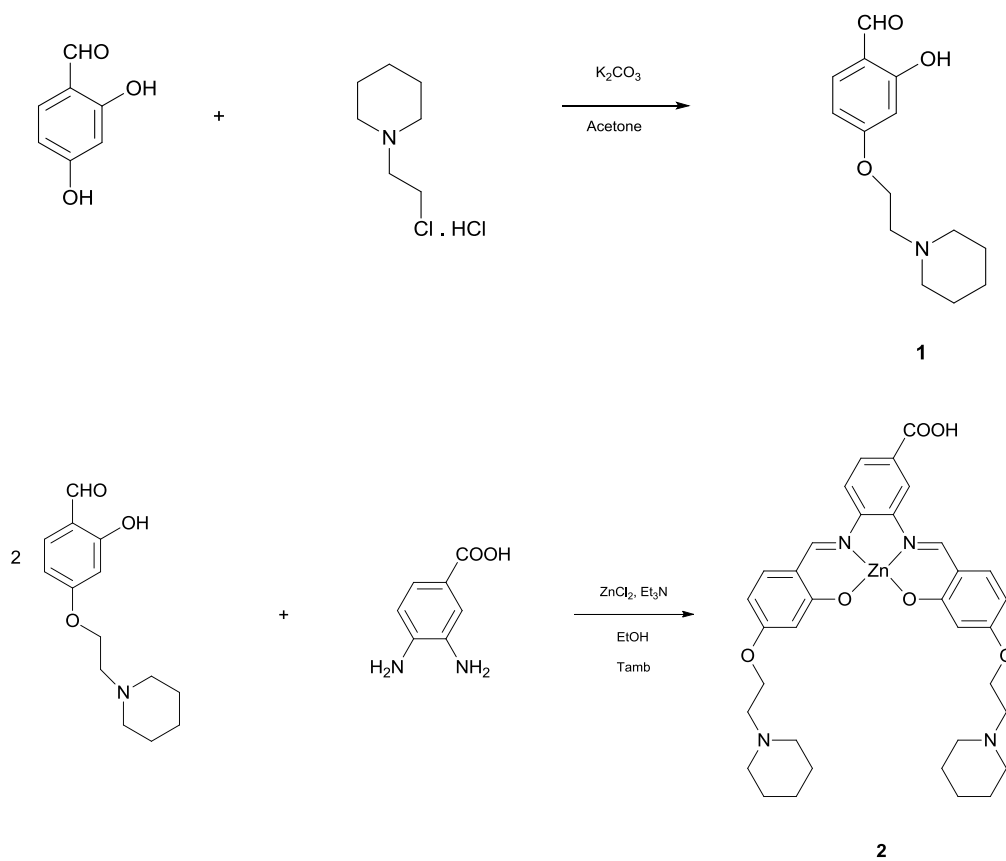
Scheme 3.1. Synthesis of Zn-salophen complex **2**.
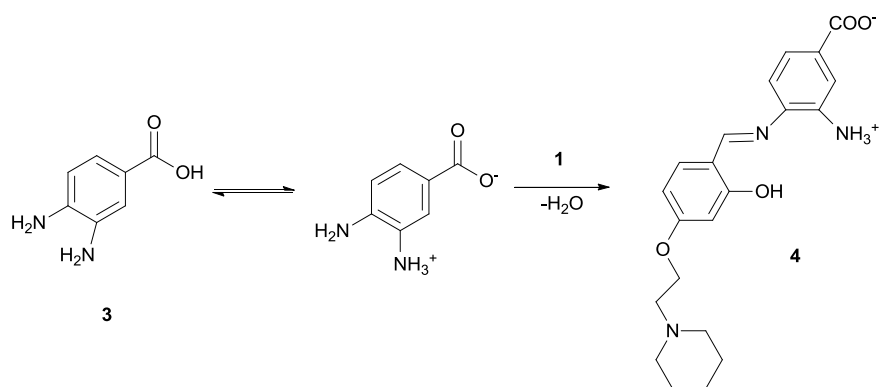
Scheme 3.2. Zwitterionic monoimine.

Absorption spectra at different concentrations of compound **2** were performed in water and DMSO to observe the occurrence of aggregation in solution, if any. Indeed, because of the five-coordinate square pyramidal geometry of the zinc atom, Zn(II)-salophen complexes tend to dimerize in non-coordinating solvents[15] (chloroform, dichloromethane, toluene, etc.) in the absence of a donor guest or by hydrophobic effects in case of water solution. In some cases, for this reason, these compounds self-assemble into nanofiber.[16] The dimerization occurs through the axial coordination of the phenolic oxygen of one molecule with the zinc atom of an adjacent molecule and gives rise to a Zn-O-Zn-O square/ rectangular form (Figure 3.6).[17]
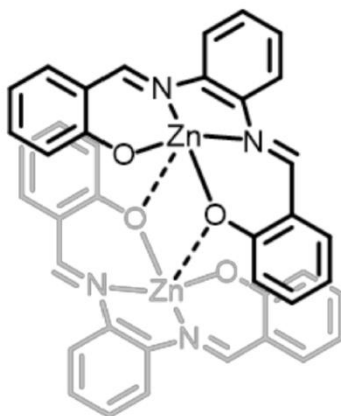

Figure 3.6. Formation of the Zn(II)-salophen dimer mediated by Zn···O interactions.

The absorbance vs. concentration plots for compound **2** (in H_2O left and DMSO right) show adherence to the Lambert–Beer law in the range of the concentration studied (see Figure 3.7). This suggests that no aggregation phenomena occurred at these concentrations in both solvents. In coordinating solvents such as DMSO, compound **2** is monomeric because of the axial coordination of the solvent to the Zn metal center.[18]
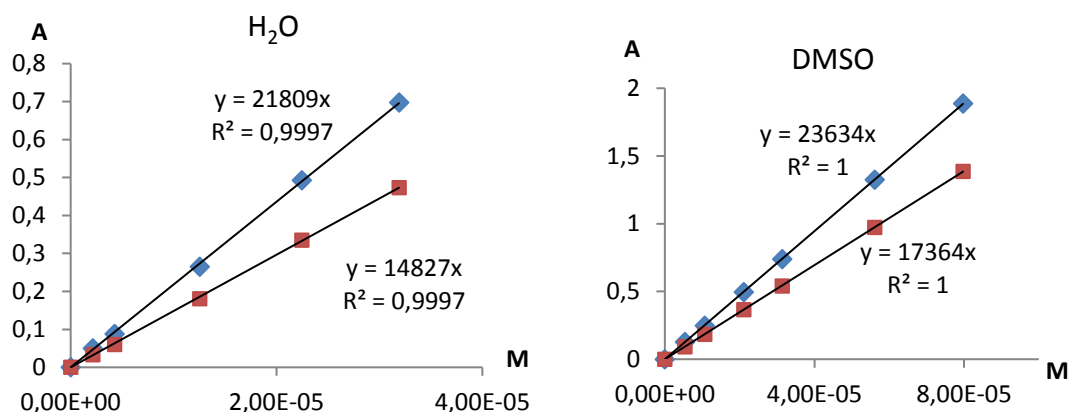
Figure 3.7. Absorbance vs. concentration plots for compound **2** (in H_2O left and DMSO right).

The aqueous diluted solution of **2** is likely characterized by the presence of defined dimer aggregates already at very low concentrations whereas larger oligomeric aggregates are conceivably formed at higher concentrations ($>4 \times 10^{-5}$ M). The experimental evidence of that was the ESI$^+$-TOF spectrum in Figure 3.8 that showed that a dimeric form is already present at the very low concentrations used in these experiments ($<10^{-6}$M).
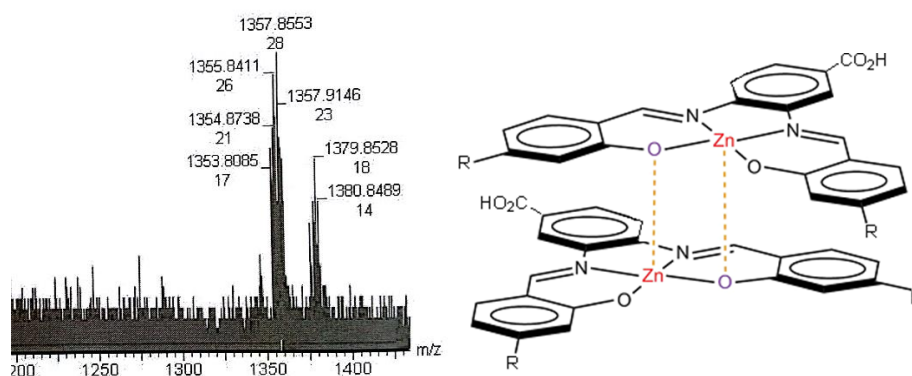

Figure 3.8. Left. Part of ESI$^+$-TOF spectrum in figure that showed the dimeric form already present at a concentration $<10^{-6}$M. Right. Representation of the dimer.

Optical absorption spectra at the same concentration of 4×10^{-5} M of **2** in water and DMSO in Figure 3.9 also indicate the existence of aggregate species in water (formation of dimers), as they are characterized by structureless features, with large bandwidths blue-shifted, compared to monomer one in a coordinating solvent as DMSO. [19]
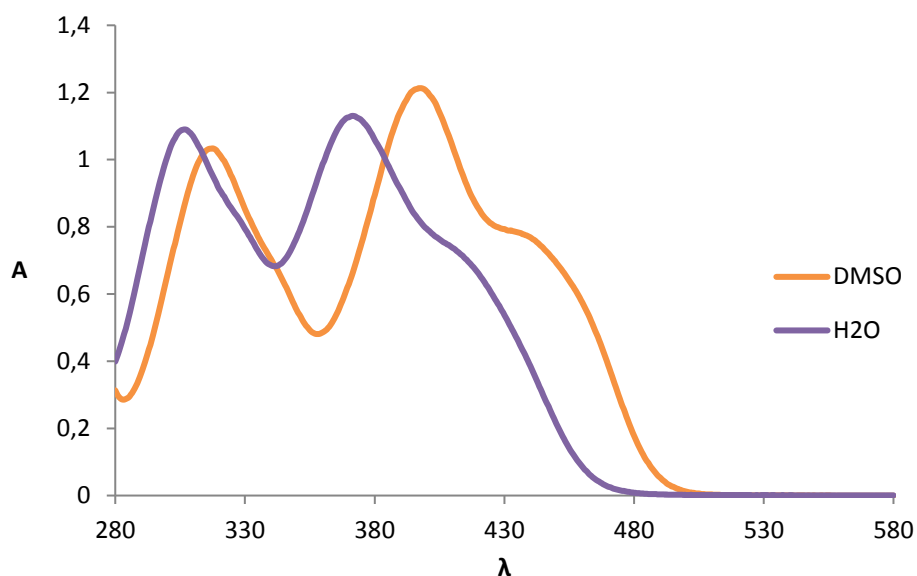
Figure 3.9. Absorption bands blue-shifted (water solution), violet line, compared to monomer one in a coordinating solvent as DMSO, orange line.

Compound **2** is slightly water soluble with maximum concentration at ambient temperature of 3×10^{-4} M (saturated solution). Comparing the water solubility of the same zinc-salophen without the carboxylic group (**5**)[1] with respect of **2** (see Figure 3.10); **5** is not soluble in water already at a concentration $<<10^{-4}$ M. We detected the maximum concentration of **2** by equation (1).

$$\frac{A_x}{A_{stand}} = \frac{\varepsilon \, c_x \, l_x}{\varepsilon \, c_{stand} \, l_{stand}} \qquad (1)$$

Where:

A_{stand}: absorbance of the standard solution of **2**.

A_x: : absorbance of the saturated solution of **2**.

$\mathcal{E}$: molar extinction coefficient of **2**.

l: the path lengths.

c_{stand} e c_x: concentration of the two solutions (standard and unknown concentration of **2**).

The molar extinction coefficient ε was obtained from the Lambert-Beer's law.

$l_x = 0.1\ cm,\ l_{standard} = 1\ cm$. From the equation (1) the concentration of the saturated solution in water was **$3 \cdot 10^{-4}$M.**
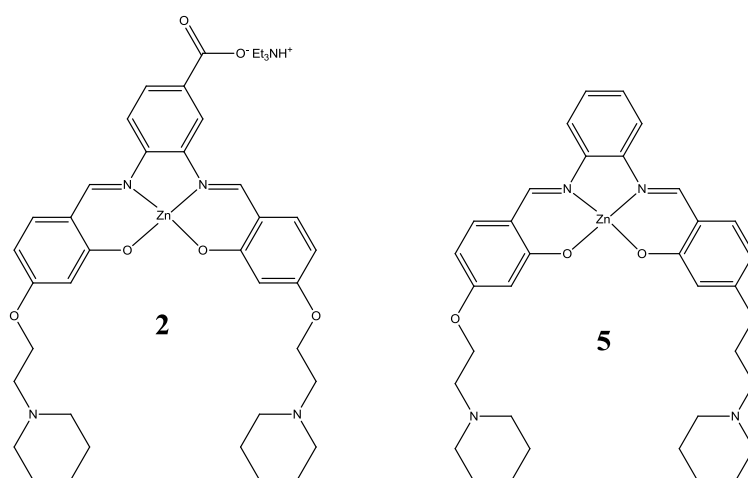

Figure 3.10. Compound **2** and **5**[1], 10^{-4} M in water.

3.1 NMR Studies

Compound **2** was fully characterized by NMR techniques (COSY experiments are not reported herein).

The ^{1}H NMR studies indicate the existence of dimers of **2** in dilute solutions in water. Indeed, the observed broadening and shift of signals (see Figure 3.11 and Table 3.1), on switching from coordinating (DMSO-d_6) to heavy water (D_2O), are in accord with definite aggregate species.[19] The NMR spectra in Figure 3.11 were recorded at a concentration of 10^{-4} M.
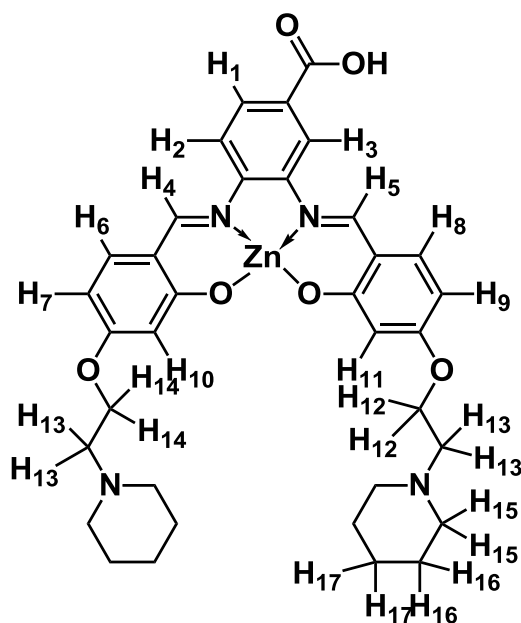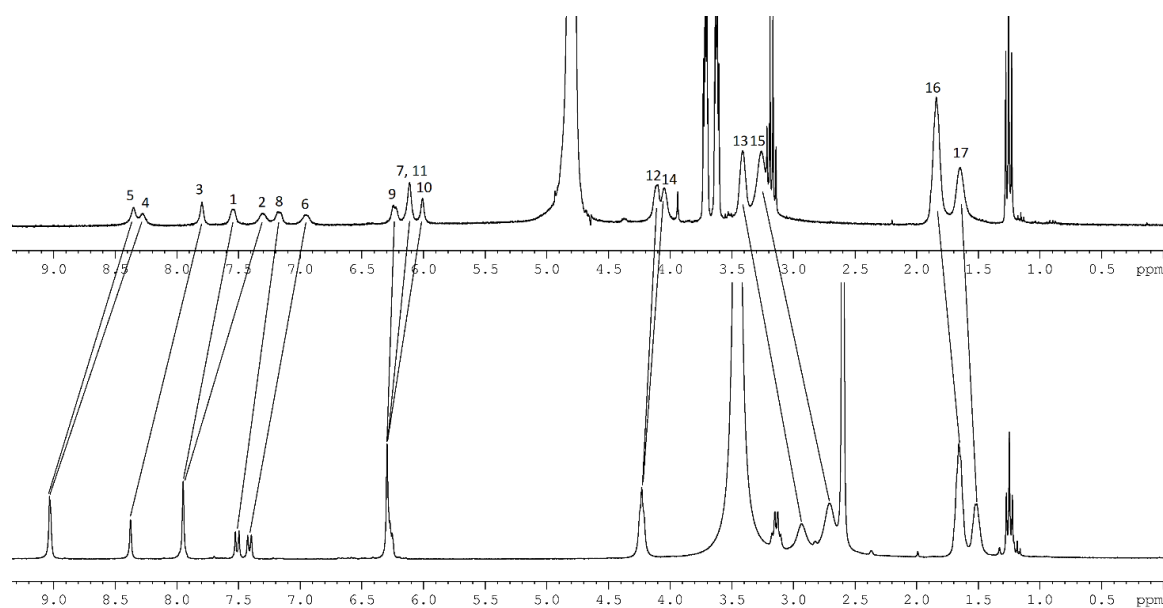
Figure 3.11. ^{1}H-NMR spectra of compound **2** in D$_2$O e DMSO-d_6 (10^{-4} M) and relative shifts.

	H$_1$	H$_2$	H$_3$	H$_4$	H$_5$	H$_6$	H$_7$
δ$_{ppm}$ *DMSO-d_6*	7,95	7,95	8,37	9,03	9,03	7,4	6,27
δ$_{ppm}$ *D$_2$O*	7,54	7,3	7,79	8,28	8,35	6,95	6,11
Δδ$_{DMSOd6-D2O}$	*0,41*	*0,65*	*0,58*	*0,75*	*0,68*	*0,45*	*0,16*

	H$_8$	H$_9$	H$_{10}$	H$_{11}$	H$_{12}$	H$_{13}$	H$_{14}$
δ$_{ppm}$ *DMSO-d_6*	7,51	6,27	6,27	6,27	4,23	2,93	4,23
δ$_{ppm}$ *D$_2$O*	7,17	6,24	6,01	6,11	4,1	3,41	4,05
Δδ$_{DMSOd6-D2O}$	*0,34*	*0,03*	*0,26*	*0,16*	*0,13*	*-0,48*	*0,18*

Table 3.1. δ$_{ppm}$ and Δδ values of compounds **2** from DMSO-d_6 to heavy water.

The 2D-NOESY spectrum in DMSO-d_6 in Figure 3.12, showed intense cross peaks between spatially-close protons as expected from the predicted structure (NOESY spectra in water are not reported herein).
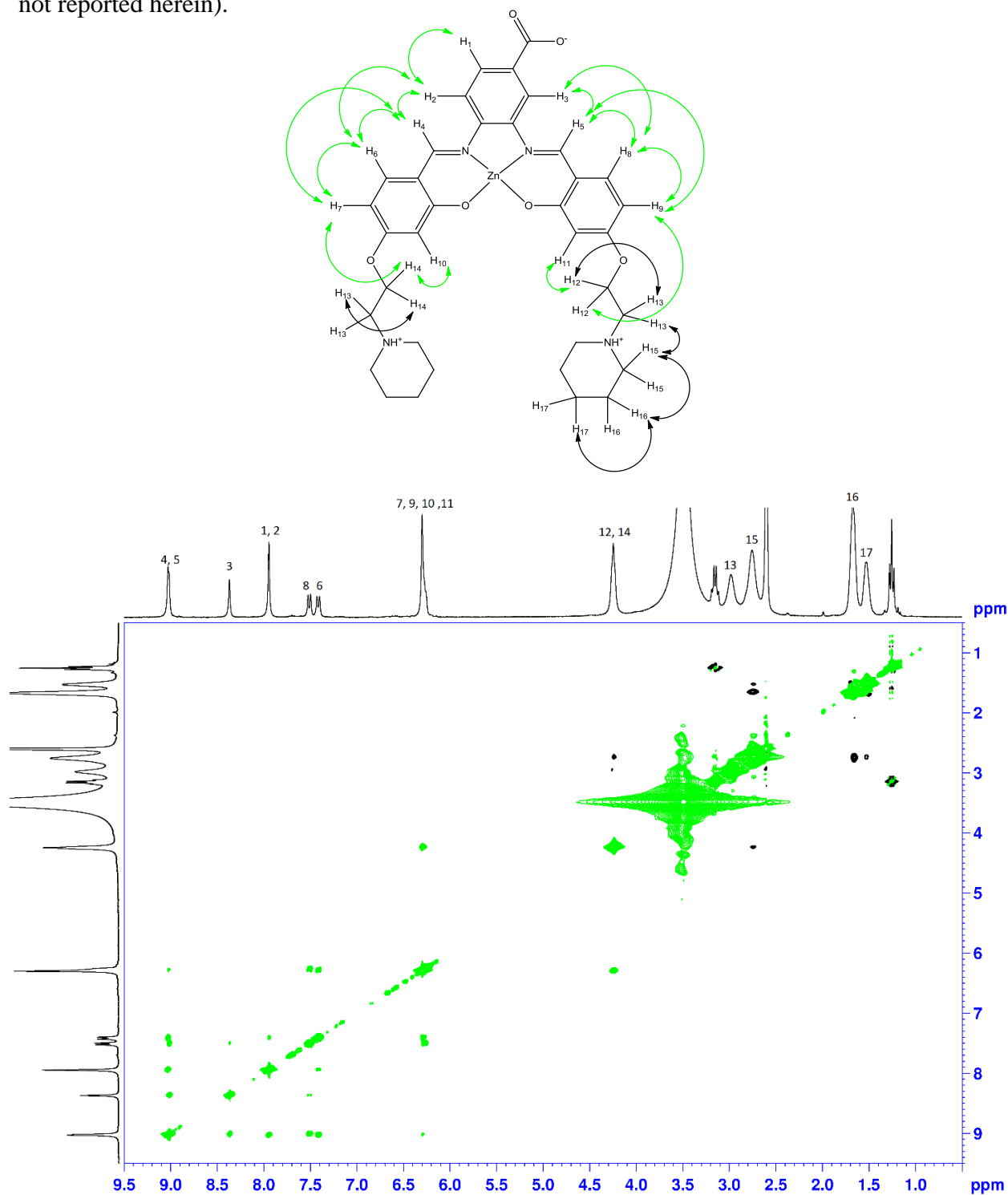

Figure 3.12. 2D NOESY spectrum of **2** in DMSO-d_6 solution.

3.2 Diffusion-Ordered Spectroscopy (DOSY) in water

DOSY has been used as an independent method to estimate the degree of aggregation and the molecular mass of **2**, through the measurement of the diffusion coefficient, D [m^2 s^{-1}]. This technique plays an important role in the identification of supramolecular species in solution owing to the straightforward two-dimensional (2D) representation of the components of the system. Equilibria between the aggregates are usually established in solution and, if the interconversion rate of the compounds is faster than NMR time-scale, a single set of resonances is observed in the DOSY spectrum as in our case. This implies that the average diffusion value obtained from diffusion NMR experiments contains information about the level of aggregation [9a] (see Figure 3.13).

In this experimental condition, the Stokes–Einstein equation is not possible to apply.[20] The molecular mass in solution of the complexes, **m**, was simply estimated using Graham's law of diffusion: $D = K(T/m)^{1/2}$, where the constant K depends on geometric factors. By assuming a constant temperature and K the same for both species in solution, the relative diffusion rate of two general species A and B is given by: $D_A/D_B = (m_B/m_A)^{1/2}$. This allows the calculation of an unknown molecular mass, m_x, by the following eqn:

$m_x = m_A(D_A/D_B)^2$.

Therefore, the diffusion rate values obtained by DOSY can be used to estimate the molecular mass of a species by comparison with the actual D value of a known internal reference (e.g., the solvent: HDO signal at 25 °C, D = 19.02 x10^{-10} m^2 s^{-1}, m_{HDO} = 19,02 Da.[21]

We estimated, by using the eqn below, that the molecular mass of the complexes was between monomer and dimer (see Table 3.2) and it is consistent with the formation of a stabile dimer in water solution.

$$m_{complex} = m_{HDO}(D_{HDO}/D_{complex})^2$$

Concentration (M)	$D_{complex}$ $(\cdot 10^{-10}\ m^2\ s^{-1})$	$D_{solvent}$ $(\cdot 10^{-10}\ m^2\ s^{-1})$	Molecular weight of the compound (Da)	Calculated mass (Da)
$3.5\cdot 10^{-4}M$	2.5	19.02	678	1099

Table 3.2. Estimated molecular mass of the complexes by the eqn : $m_{complex} = m_{HDO}(D_{HDO}/D_{complex})^2$.
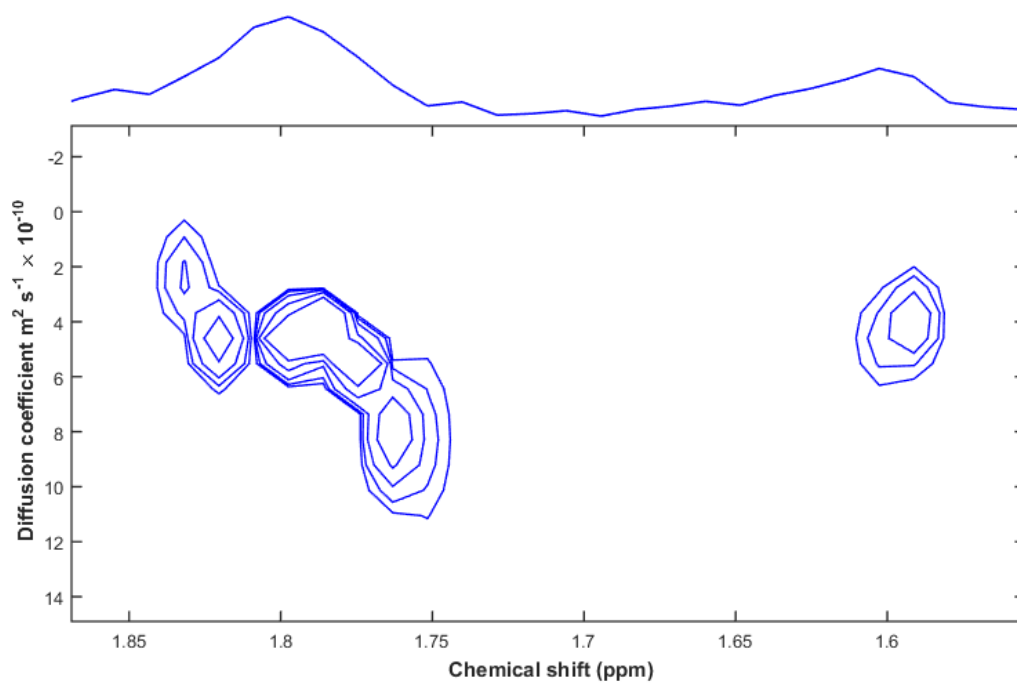

Figure 3.13. Selected area of the DOSY spectrum of **2** in D₂O solution .

3.3 UV-vis titrations

Definitive evidences of the existence of definite aggregate species in water were found by UV-vis studies.

The binding constant between the water soluble Zn-salophen complex **6** in Figure 3.14 measured in a previous investigation showed very high affinity toward the acetate anion with **$K_a > 10^6$ M^{-1}**.[14]
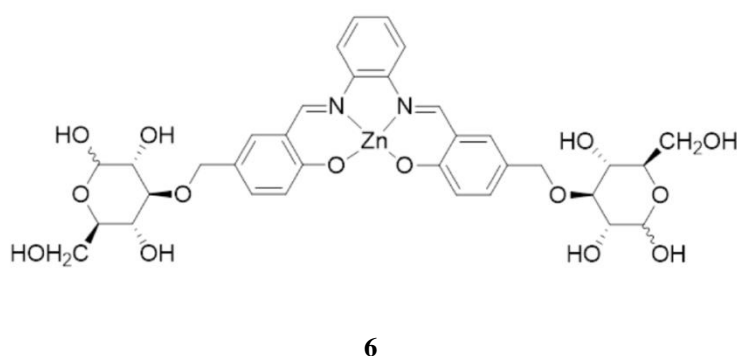

6

Figure 3.14. Structure of compound **6**.

Association constant values, K_a (M^{-1}), for the complexation of tetrabutylammonium acetate TBAOAc with receptor **2** were obtained by UV-vis titrations in DMSO with a **K_a = 11638 ± 1 M^{-1}** and in water with **K_a = 29 ± 3 M^{-1}** at 298 K.

The low binding constant found in water is a further confirmation of the presence of defined dimer aggregates. Indeed, **2** retains its dimeric structure also in presence of a very good guest for Zn-salophen compounds as acetate anion.[14]

3.4 Experimental section

TBAOAc reagents were purchased from Sigma-Aldrich. All the solvents used for reactions and titrations were reagent grade and used as received. Flash column chromatography was performed with Silica gel 40 – 63 μm. NMR spectra were recorded on a Bruker AC300P spectrometer. HRMS Spectra were recorded by a MICROMASS Q-Tof micromass spectrometer. UV–vis measurements were performed on a Perkin Elmer Lambda 18 spectrophotometer. Association constants obtained by UV-vis titrations were calculated using ReactLab[TM] EQUILIBRIA. The association constants (K_a) for the binding processes were determined by averaging the values from at least two titrations using a simple 1:1 binding model. Compound **5** were available from previous investigations.[1] Coumpound **1** were prepared according to previously reported procedures.[13]

Zinc-salophen 2. (97% yield). Salicylaldehyde **1** (0.40 mmol, 100 mg), 3,4-diaminobenzoic (0.68 mmol, 13 mg), $ZnCl_2$ (0.68 mmol, 93 mg) and 1.55 mL of Et_3N were solubilized in ethanol (8 mL) and stirred overnight. The yellow solid obtained after removing the solvent was washed with ethanol, CH_2Cl_2 and diethyl ether to yield **2** (132 mg, 0.19 mmol). ^{1}H-NMR (300 MHz in DMSO-d_6), δ: 9.03 (s, 2H, HC=N), 8.37 (s, 1H, ArH), 7.94 (s, 2H, ArH), 7.50 (d, 1H, ArH), 7.40 (d, 1H, ArH), 6.29-6.25 (m, 4H, ArH), 4.23 (b, 4H, CH_2O), 2.93 (b, 4H, CH_2N), 2.70 (b, 8H, piperidina), 1.65 (b, 8H, piperidina), 1.51 (b, 4H, piperidina). ^{1}H-NMR (300 MHz in D_2O), δ: 8.35 (s, 1H, HC=N), 8.27 (s, 1H, HC=N), 7.79 (s, 1H, ArH), 7.54 (b, 1H, ArH), 7.29 (b, 1H, ArH), 7.18 (b, 1H, ArH), 7.17 (b, 1H, ArH), 6.24 (b, 1H, ArH), 6.11 (b, 2H, ArH), 6.00 (b, 1H, ArH), 4.09 (b, 2H, CH_2O), 4.04 (b, 2H, CH_2O), 3.41 (b, 4H, CH_2N), 3.26 (b, 8H, piperidina), 1.84 (b, 8H, piperidina), 1.64 (b, 4H, piperidina).

ESI-MS (m/z): calculated 676.22 found 677.23 [M+H][+].
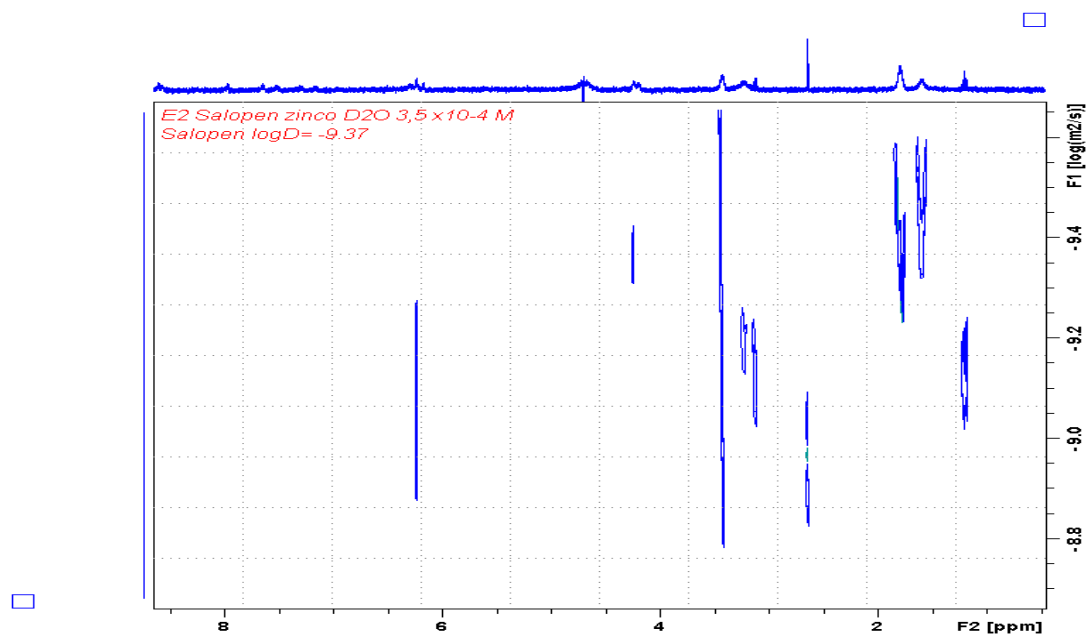
DOSY (400 MHz in D$_2$O) of **2**, C = 3.5·10^{-4} M

3.5 Bibliography

1. S. N. Georgiades, N.H. Abd Karim, K. Suntharalingam, R. Vilar, *Angew. Chem. Int. Ed.* **2010**, 49, 4020–4034.

2. T. de Lange, T. Jacks, *Cell* **1999**, 96, 273-275.

3. (a) D. Sun, B. Thompson, B. E. Cathers, M. Salazar, S. M. Kerwin, J. O. Trent, T. C. Jenkins, S. Neidle, L. H. J. Hurley, *Med. Chem.* **1997**, 40, 2113. (b) P. J. Perry, M. A. Read, R. T. Davies, S. M. Gowan, A. P. Reszka, A. A. Wood, L. R. Kelland, S. Neidle, *J. Med. Chem.* **1999**, 42, 2679. (c) M. A. Read, A. A. Wood, R. J. Harrison, S. M. Gowan, L. R. Kelland, H. S. Dosanjh, S. Neidle, *J. Med. Chem.* **1999**, 42, 4538. (d) M. Read, R. J. Harrison, B. Romagnoli, F. A. Tanious, S. H. Gowan, A. P.Reszka, W. D. Wilson, L. R. Kelland, S. Neidle, *Proc. Natl. Acad. Sci. U.S.A.* **2001**, 98, 4844.

4. (a) R. T. Wheelhouse, D. Sun, H. Han, F. X. Han, L. H. Hurley*, J. Am. Chem. Soc.* **1998**, 120, 3261. (b) F. X. Han, R. T. Wheelhouse, L. H. Hurley, *J. Am. Chem. Soc.* **1999**, 121, 3561. (c) H. Han, A. Rangan, D. R. Langley, L. H. Hurley, *J. Am. Chem. Soc.* **2001**, 123, 8902. (d) D.-F. Shi, R. T. Wheelhouse, D. Sun, L. H. Hurley, *J. Med. Chem.* **2001**, 44, 4509.

5. (a) H. Han, C. L. Cliff, L. H. Hurley, *Biochemistry* **1999**, 38, 6981. (b) O. Yu. Fedoroff, M. Salazar, H. Han, V. V. Chemeris, S. M. Kerwin, L. H. Hurley, *Biochemistry* **1998**, 37, 12367. (c) A. Rangan, O. Yu. Fedoroff, L. H. Hurley, *J. Biol. Chem.* **2001**, 276, 4640.

6. F. Koeppel, J.-F. Riou, A. Laoui, P. Malliet, P. B. Arimondo, D. Labit, O. Petigenet, C. Helene, J.-L. Mergny, *Nucleic Acids Res.* **2001**, 29, 1087.

7. R. J. Harrison, S. M. Gowan, L. R. Kelland, S. Neidle, *Bioorg. Med. Chem. Lett.* **1999**, 9, 2463.

8. J.-F. Riou, P. Mailliet, A. Laoui, E. Renou, O. Petigenet, L. Guittat, J.-L. Mergny, *Proc. Am. Assoc. Cancer Res.* **2001**, 42, 837.

9. S. M. Gowan, L. Brunton, M. Valenti, R. Heald, M. A. Read, J. R. Harrison, M. F. G. Stevens, S. Neidle, L. R. Kelland, *Proc. Am. Assoc. Cancer Res.* **2001**, 42, 86.

10. W. Duan, A. Rangan, H. Vankayalapati,; M.-Y. Kim, Q. Zeng, D. Sun, O. Yu. Fedoroff, D. Nishioka, S. Y. Rha, E. Izbicka, D. D. Von Hoff, L. H. Hurley, *Molecular Cancer Therapeutics* **2001**, 1, 103.

11. M.-Y. Kim, H. Vankayalapati, K. Shin-ya, K. Wierzba, and L. H. Hurley *J. Am. Chem. Soc.*, **2002**, 124, 2098–2099.

12. (a) J. E. Reed, A. A. Arnal, S. Neidle, R. Vilar, *J. Am. Chem. Soc.***2006**, 128, 5992. (b) A. Arola-Arnal, J. Benet-Buchholz, S. Neidle, R. Vilar, *Inorg. Chem.* **2008**, 47, 11910.

13. N. H. Abd Karim, O. Mendoza, A. Shivalingam, A. J. Thompson, S. Ghosh, M.K. Kuimovaa and R. Vilar, *RSC Adv.,* **2014**, 4, 3355–3363.

14. A. Dalla Cort, P. De Bernardin, L. Schiaffino, *CHIRALITY,* **2009,** 21, 104–109.

15. G. Consiglio, S. Failla, P. Finocchiaro, I. P. Oliveri, R. Purrello, S. Di Bella, *Inorg. Chem.* **2010**, 49, 5134-5142.

16. I. P. Oliveri, S. Failla, G. Malandrino, S. Di Bella, *J. Phys. Chem. C* **2013**, 117, 15335-15341.

17. A. W. Kleij, M. Kuil, D. M. Tooke, A. L. Spek, J. N. H. Reek, *Inorg. Chem.* **2007**, 46, 5829-5831.

18. A. Dalla Cort, P. De Bernardin, G. Forte, F. Y. Mihan, Chem. *Soc. Rev.* **2010**, 39, 3863-3874.

19. a) G. Consiglio, S. Failla, P. Finocchiaro, I.P. Oliveri, S. Di Bella, *Dalton Trans.,* **2012**, 41, 387-395. b) Juan Tang, Yuan-Bo Cai, Jing Jing, Jun-Long Zhang, *Chem. Sci.,* **2015**, 6, 2389-2397.

20. A. Macchioni, G. Ciancaleoni, C. Zuccaccia and D. Zuccaccia*, Chem. Soc.Rev.,* **2008**, 37, 479–489.

21. G. Consiglio, S. Failla, P. Finocchiaro, I. P. Oliveri, R. Purrello and S. Di Bella, *Inorg. Chem.*, **2010**, 49, 5134–5142.